QUANTUM ESPRESSO

September 15–20, 2019
Ljubljana, Slovenia

Summer School on Advanced Materials and Molecular Modelling

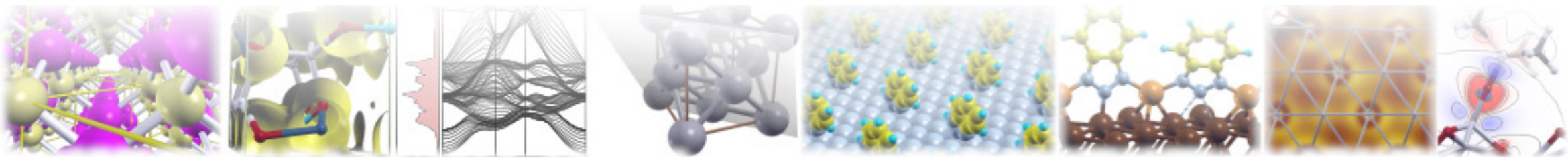

Elevator pitches (part II)

QUANTUM ESPRESSO FOUNDATION

MAX DRIVING THE EXASCALE TRANSITION

Jožef Stefan Institute
Ljubljana, Slovenija

cecam
Centre Européen de Calcul Atomique et Moléculaire

EUROTECH
Imagine. Build. Succeed.

Evidence for a linear coordination of Ag^+ in water: a X-ray absorption spectroscopy, classical and a*b initio* Molecular Dynamics study

Matteo Busato,[a] Andrea Colella,[b] Giordano Mancini,[c] Matteo Peluso,[c] Daniele Veclani,[a] Andrea Melchior,[a] Marilena Tolazzi,[a] Ingmar Persson,[d] Paola D'Angelo[b]

[a]DPIA, Laboratorio di Scienze e Tecnologie Chimiche, Università di Udine, Via del Cotonificio 108, 33100 Udine, Italy
[b]Dipartimento di Chimica, Università di Roma "La Sapienza", P.le A. Moro 5, 00185 Roma, Italy
[c]Scuola Normale Superiore, Piazza dei Cavalieri 7, I-56126 Pisa, Italy
[d]Department of Molecular Sciences, Swedish University of Agricultural Sciences, P.O.Box 7015, SE-750 07 Uppsala, Sweden

Ljubljana, September 16 – 20, 2019

Summer School on Advanced Materials and Molecular Modelling

Ag^+ coordination number (CN) in water: experimental works

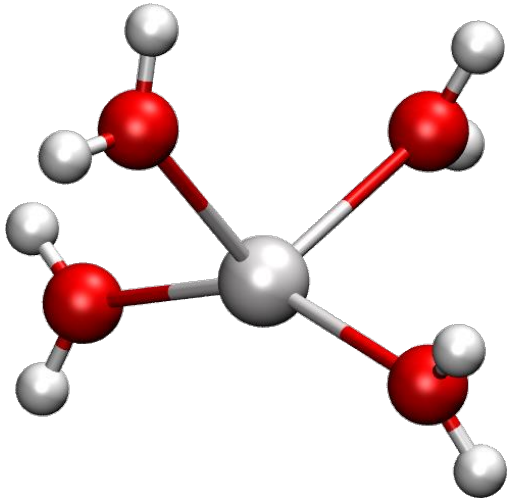

CN = 2 + 2

LAXS and EXAFS[1]

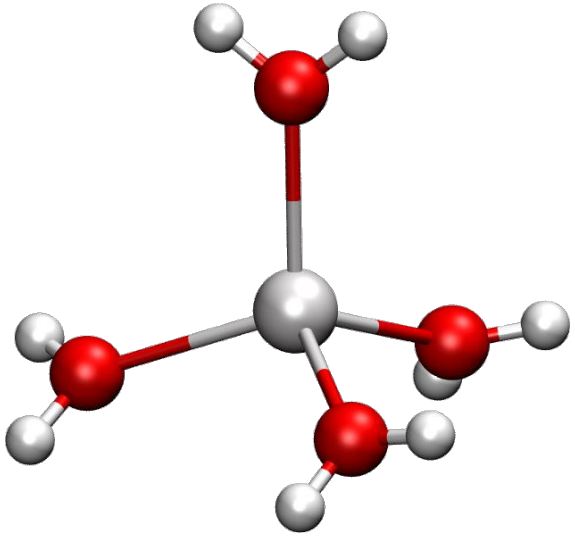

CN = 4

Neutron diffraction[2,3]

EXAFS[4,5]

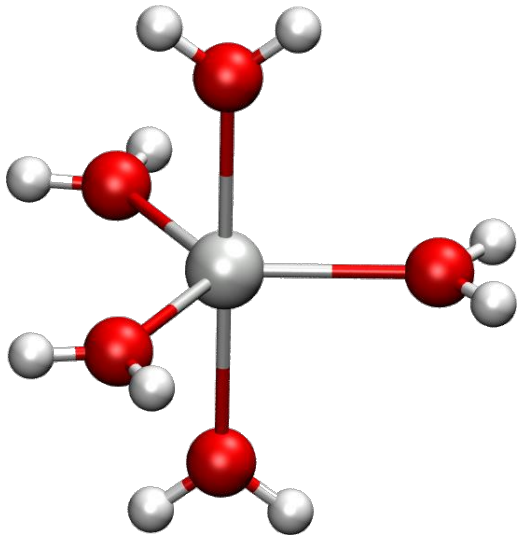

CN = 5

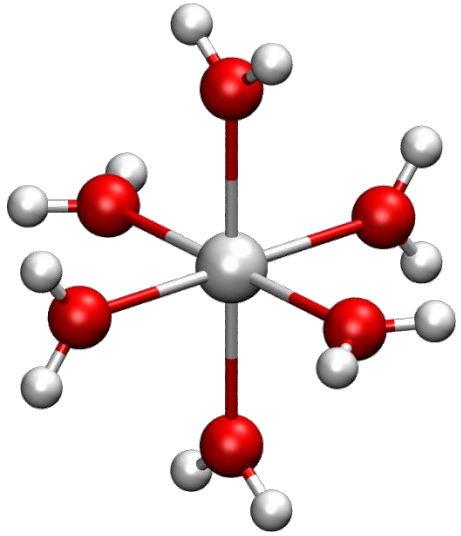

CN = 6

EXAFS[6]

[1] Persson et al. Inorg. Chem. 2006, 45, 7428

[2] Skipper et al. J. of Phys.: Cond. Matter 1989, 1, 4141
[3] Sandstrom et al. J. Phys. C: Solid State Phys. 1985, 18, 1115
[4] Yamaguchi et al. T. Acta Chem. Scand. 1984, 38, 423
[5] Tsutsui et al. J. Phys. Chem. A 1997, 101, 2900

[6] Fulton et al. J. Phys. Chem. A 2009, 113, 13976

Ag^+ coordination number (CN) in water: theoretical works

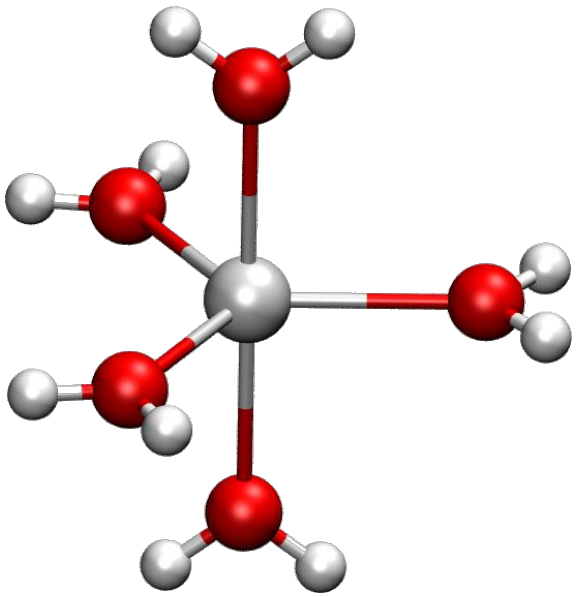

CN = 5

QM/MM[1]
Ab initio MD[2-4]
Classical MD[5]

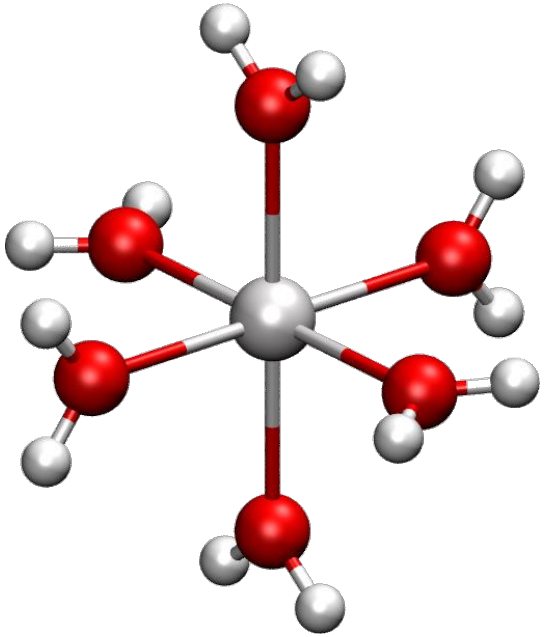

CN = 6

Monte Carlo[6]
Ab initio MD[7,8]
Classical MD[5]

[1] Armunanto et al. J. Phys. Chem. A 2003, 107, 3132
[2] Spezia et al. Phys. Rev. Lett. 2003, 91, 1
[3] Spezia et al. J. Chem. Phys. 2004, 120, 5261
[4] Vuilleumier et al., J. Chem. Phys. 2001, 115, 3454
[5] Li et al., J. Chem. Theor. Comput. 2015, 11, 1645

[6] Dubois et al. J. Phys. Chem. B 2001, 105, 9363
[7] Leung et al., J. Chem. Phys. 2009, 130, 204507
[8] Blauth et al. Chem. Phys. Lett. 2010, 500, 251

Ag^+ coordination number (CN) in water: theoretical works

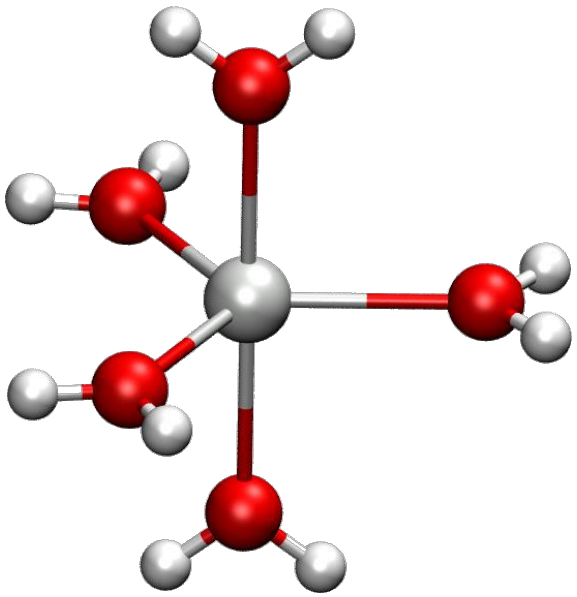

CN = 5

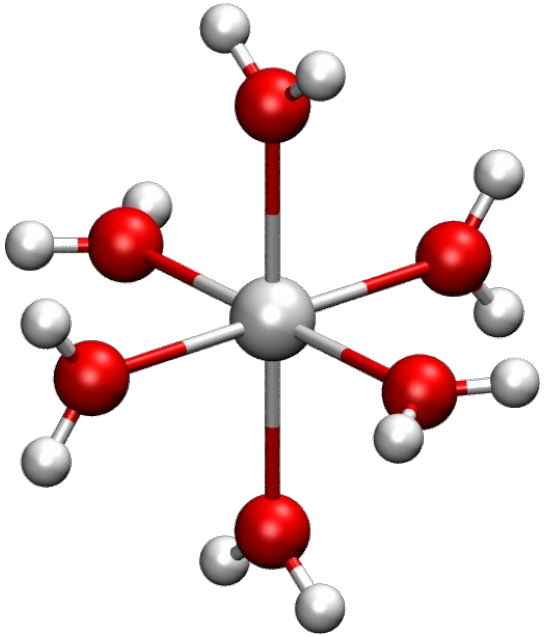

CN = 6

Challenges:
- reproducing CNs ≤ 4 within the experimental bond distance
- reproducing asymmetric coordinations (linear)

X-ray absorption spectroscopy (XAS)

EXAFS data analysis

EXAFS: high-energy part of a XAS spectrum

Results

Fitting for fixed CNs between 1.7 and 6.0:

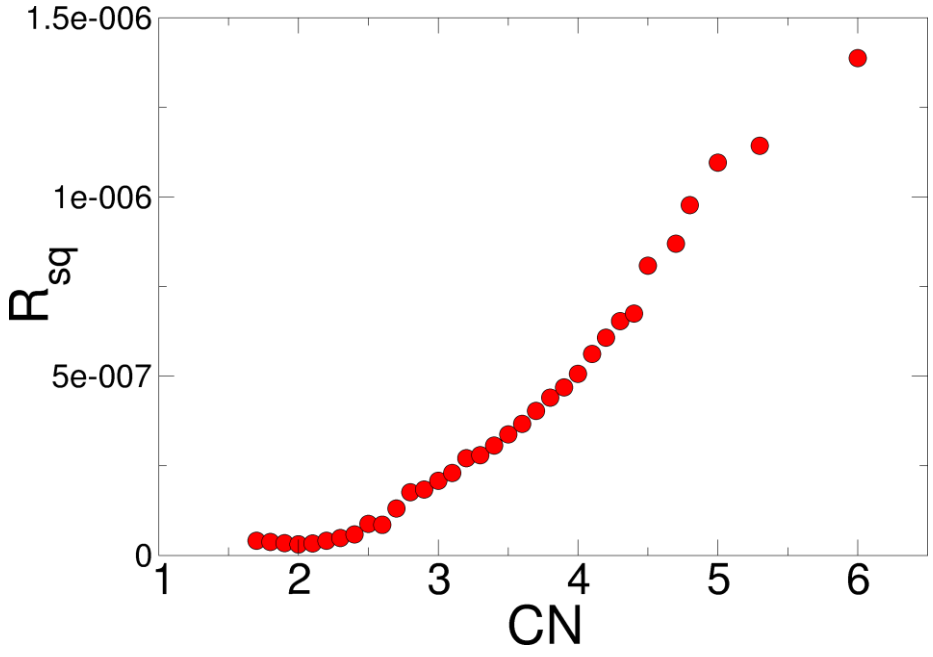

Minimum residue between experimental and fitted spectra for CN = 2.0

X-ray absorption spectroscopy (XAS)

EXAFS data analysis

EXAFS: high-energy part of a XAS spectrum

Results

Fitting for fixed CNs between 1.7 and 6.0:

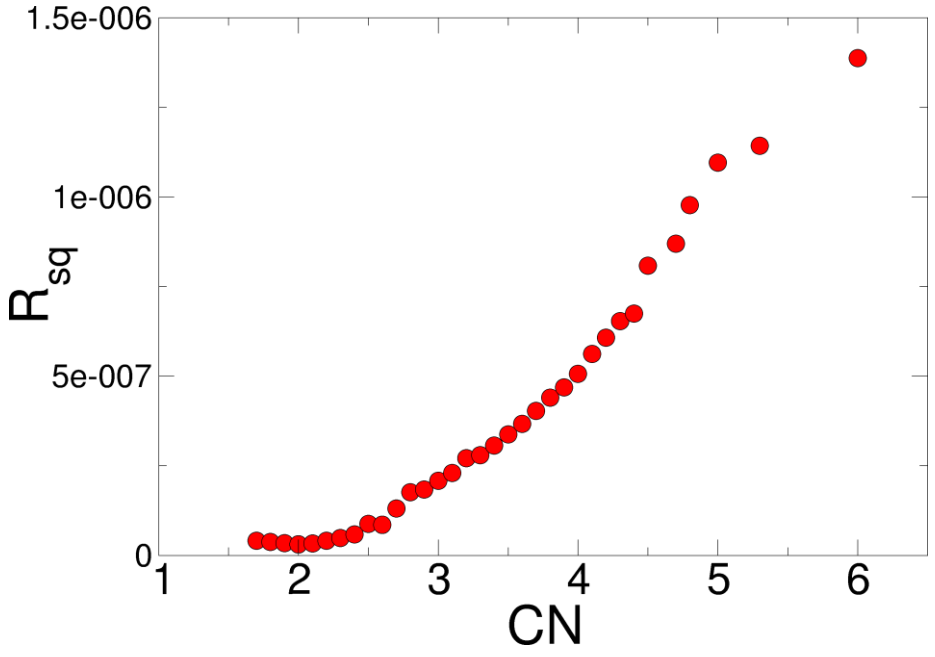

Best-fit results:

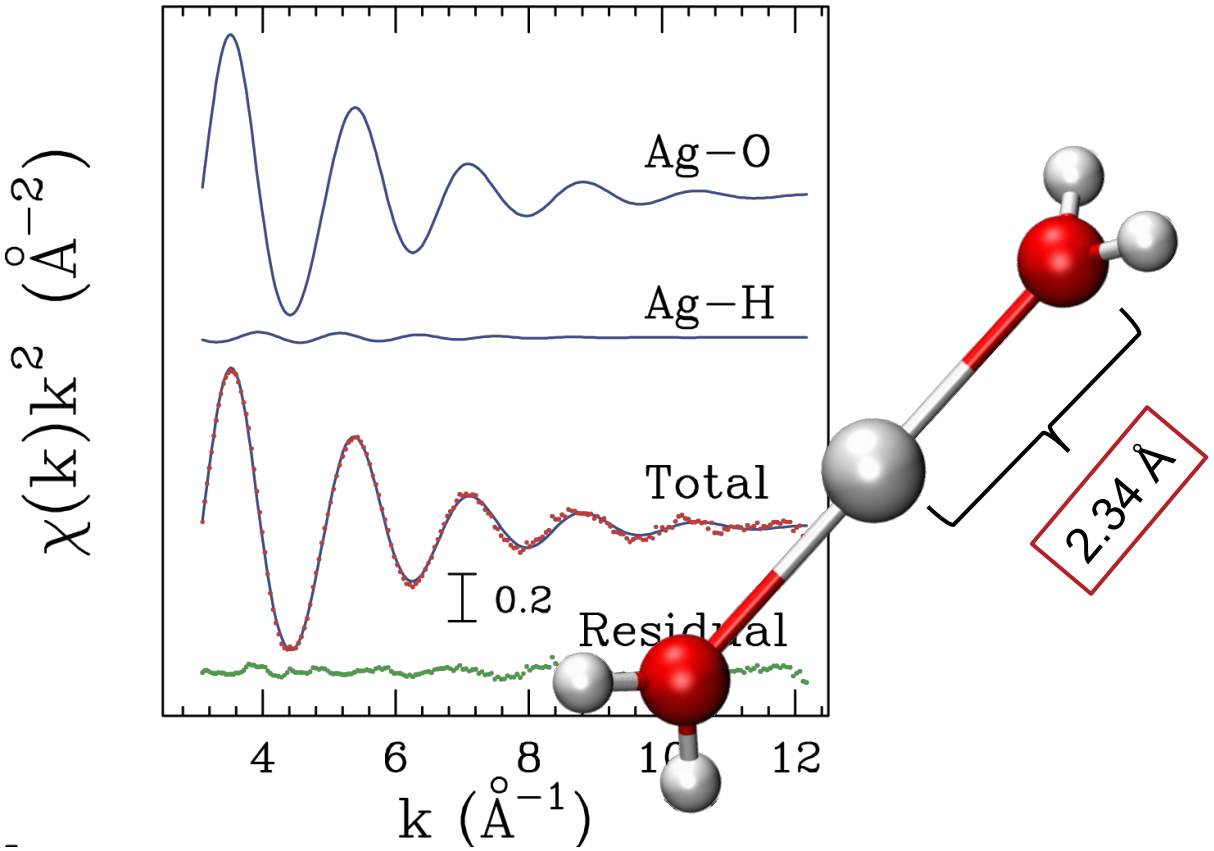

Minimum residue between experimental and fitted spectra for CN = 2.0

X-ray absorption spectroscopy (XAS)

XANES data analysis

Results

XANES: low-energy part of a XAS spectrum.

Sensible to 3D displacement around the metal.

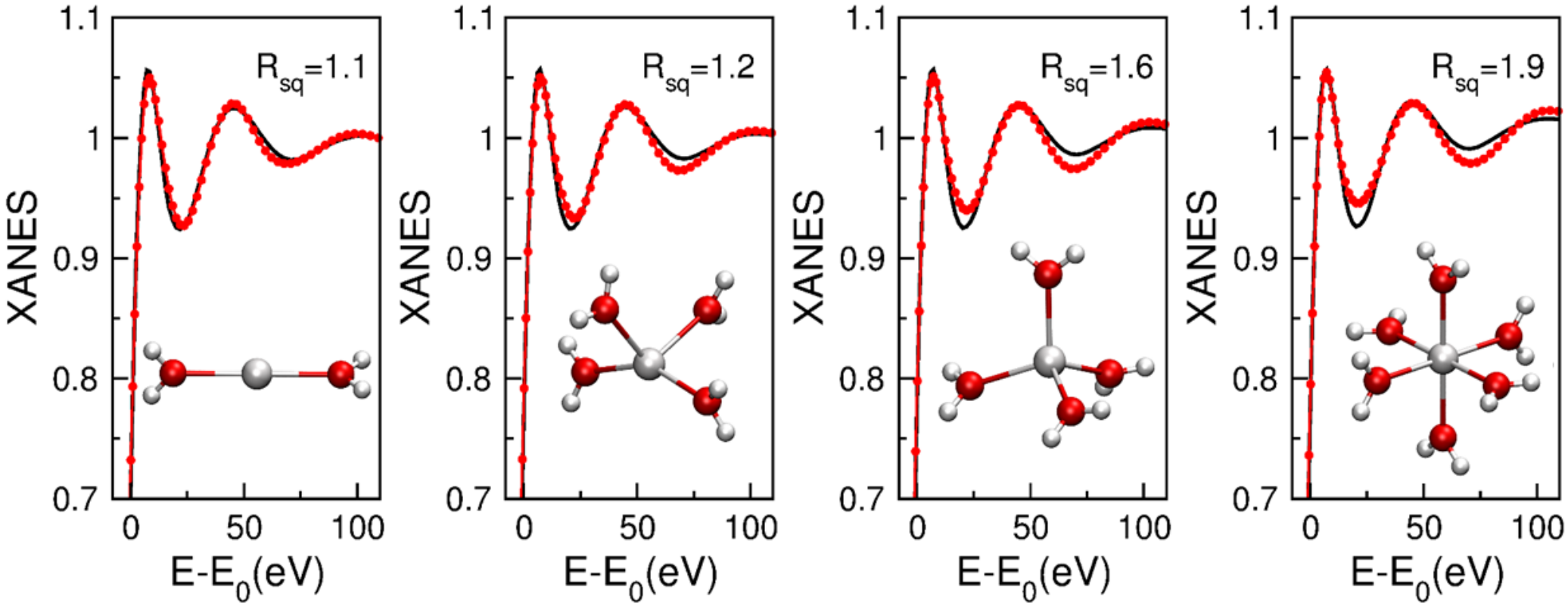

Best-fit for linear coordination

Car-Parrinello MD

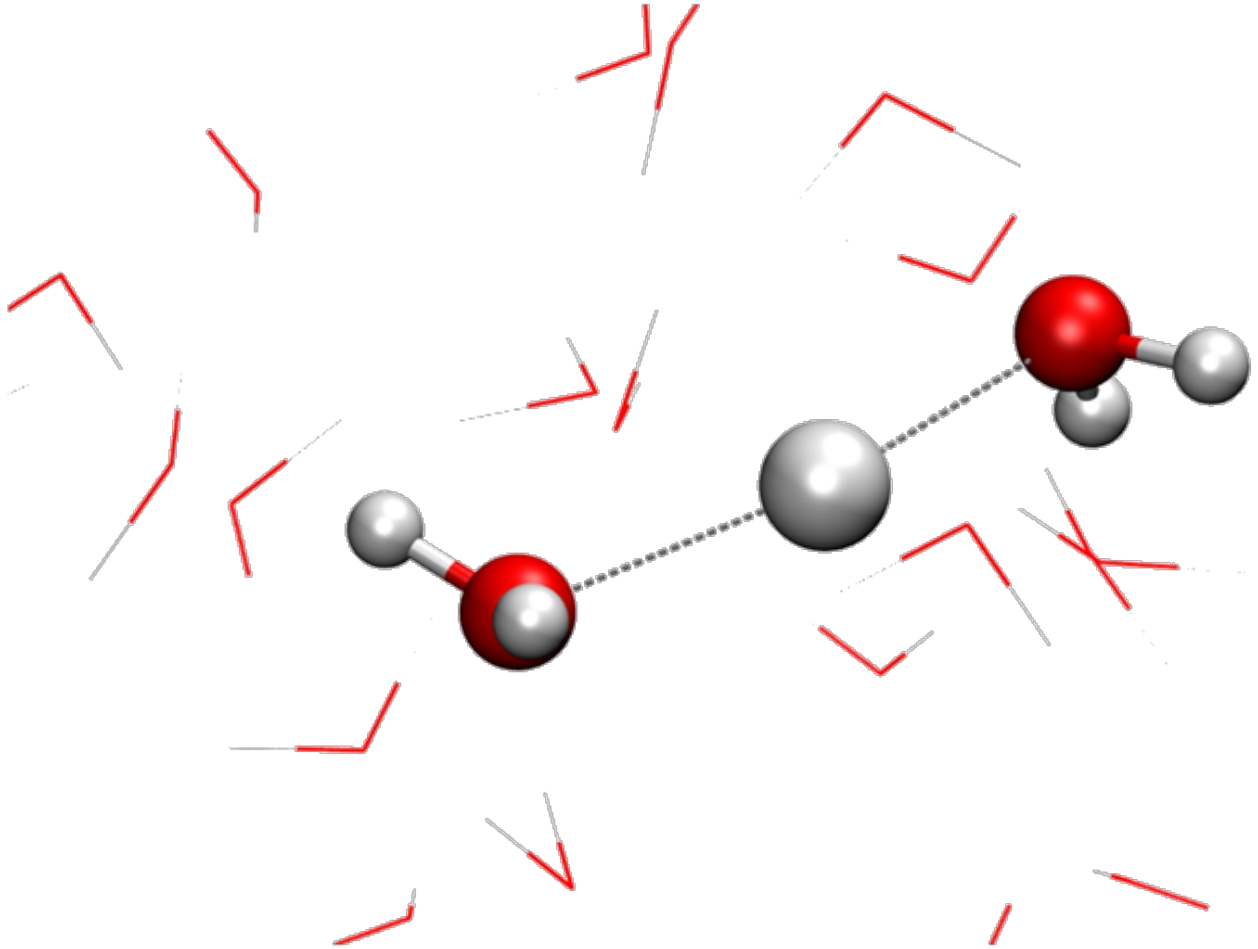

CN	$r_{Ag\text{-}O}$ (Å)
2.0	2.20

CPMD confirms the linear coordination

Classical MD

Results

Three-site model with virtual sites (VS)

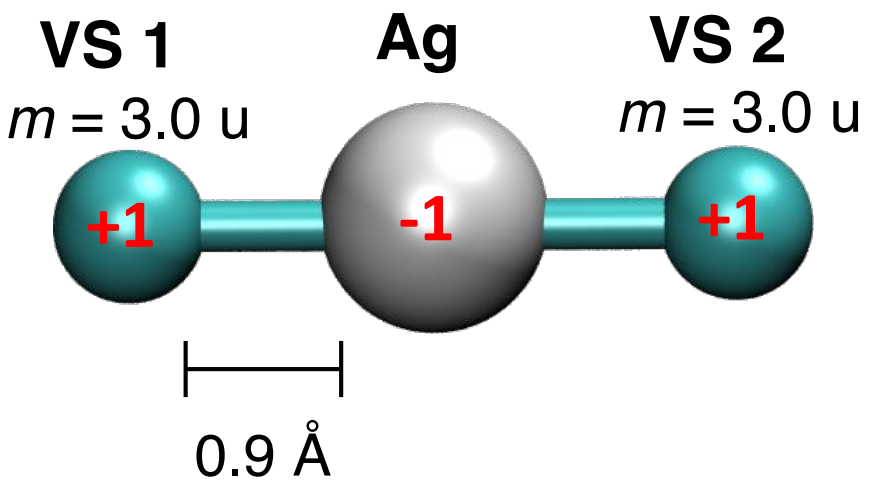

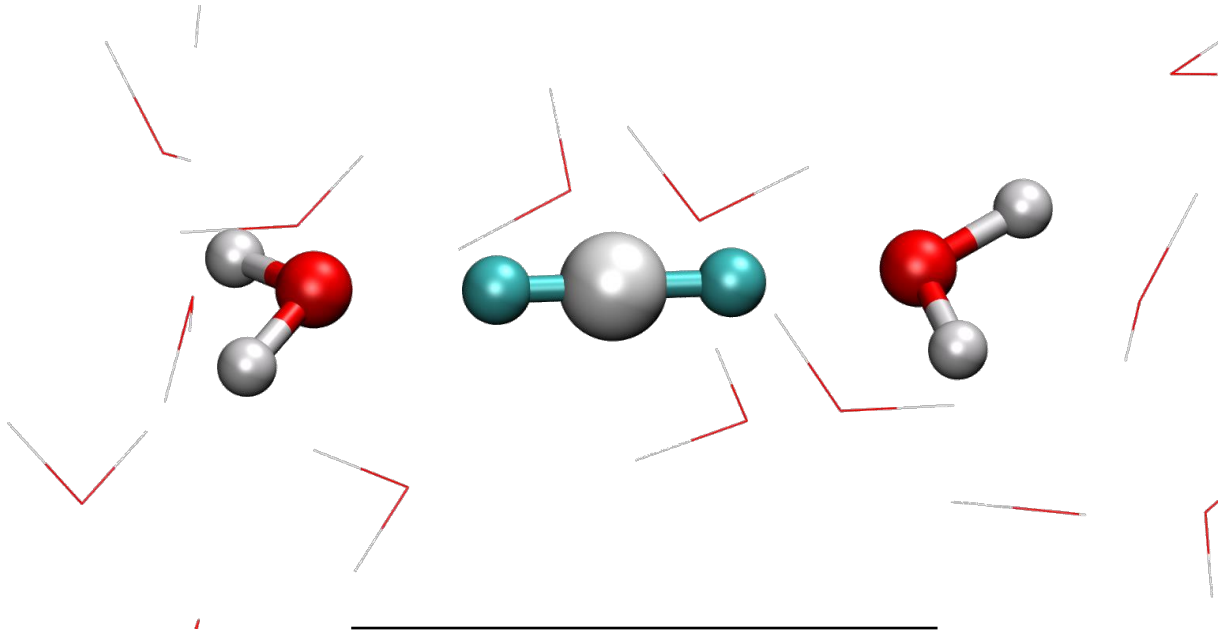

CN	$r_{Ag\text{-}O}$ (Å)
2.0	2.34

VS*s* allow the reproduction of the experimental coordination

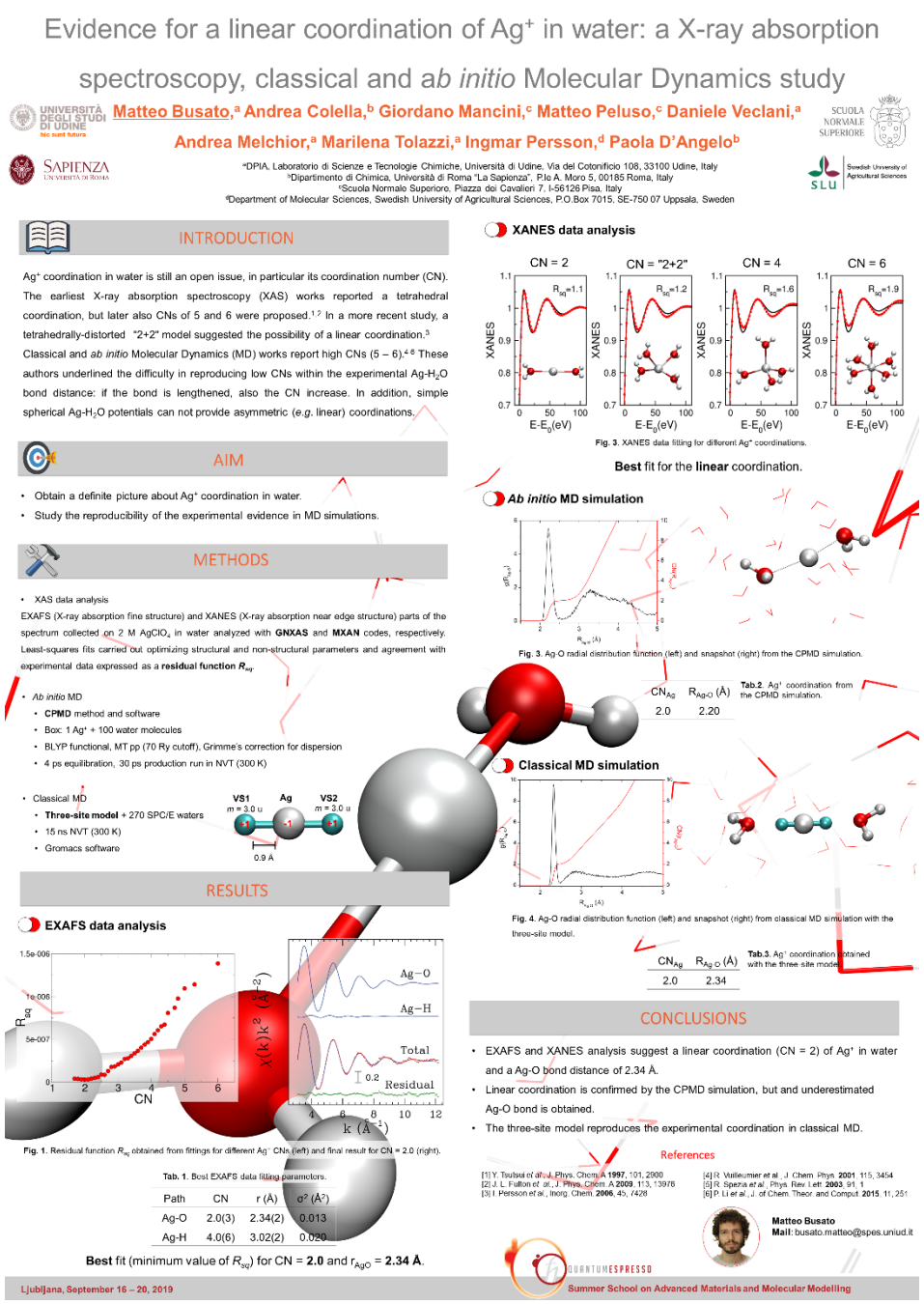

Thank you for your attention

Please come and visit

Quantum ESPRESSO
Summer School on Advanced Materials and Molecular Modelling,
September 16-20, 2019, Ljubljana, Slovenia

HRTEM AND DFT STUDY OF TRANSLATION STATES IN Sb- DOPED ZnO

Vesna RIBIĆ [a], Aleksander REČNIK [b], Anton KOKALJ [b], Matej KOMELJ [b], Zorica BRANKOVIĆ [a] and Goran BRANKOVIĆ [a]

[a] *Institute for Multidisciplinary Research, Belgrade, Serbia*

[b] *Jožef Stefan Institute, Ljubljana, Slovenia*

Inversion boundaries in ZnO

- Inversion boundaries (IBs) are the most common type of planar faults causing inversion of polarity: head-to-head (→|←) or tail-to-tail (←|→)
- they are triggered by the addition of specific IB-forming dopants: In_2O_3, Fe_2O_3, Mn_2O_3, Ga_2O_3, SiO_2, SnO_2, TiO_2 and Sb_2O_3
- IBs predominatly lie in basal planes (b-IB), but with some dopants they occupy pyramidal planes of ZnO structure (p-IB)

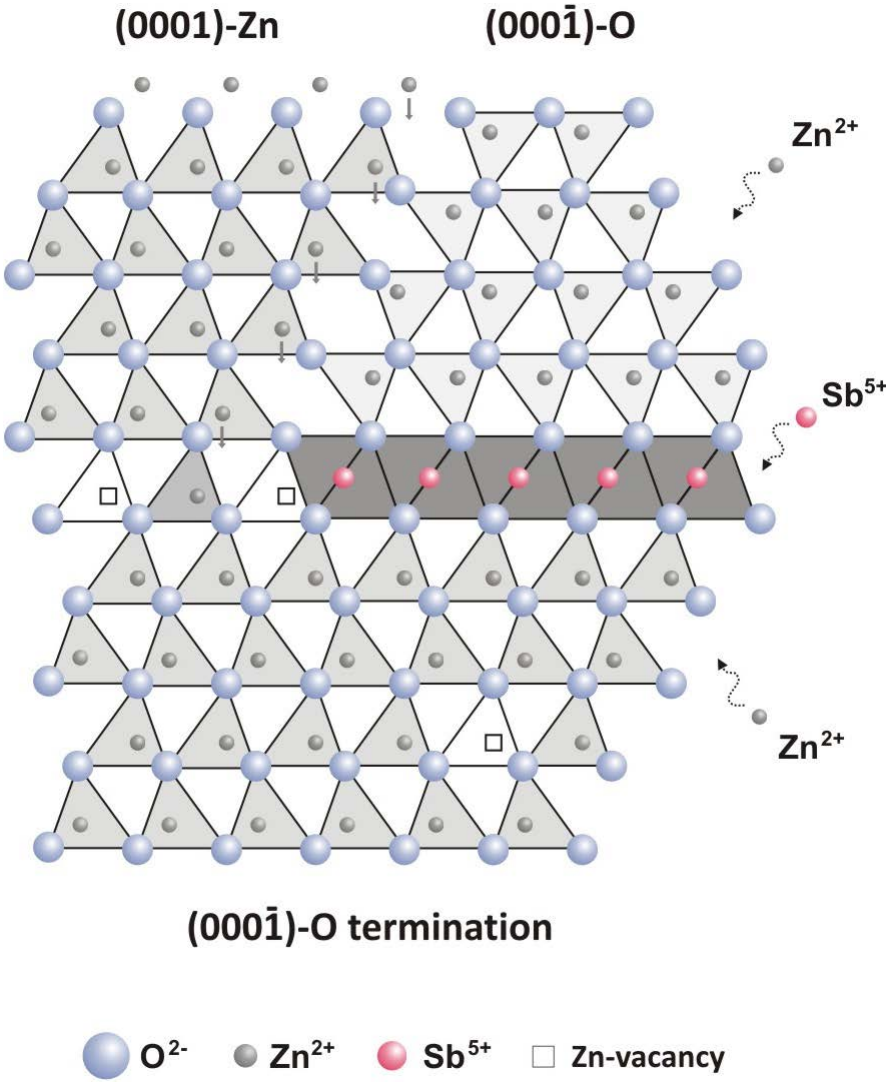

Translations of head-to-head b-IBs

∴ Depending on stacking sequence, there exist three possible translations for basal-plane head-to-head (→|←) IBs:

1 Only inversion of ZnO domain from selected (0001) plane. Determined by Hoemke (2017) for Mn-doped ZnO.

2 Stacking fault followed by inversion of translated domain. First reported by Rečnik (2001) for Sb-doped ZnO.

3 Double stacking fault followed by inversion of displaced domain. Reported by Walther (2006) for Fe-doped ZnO.

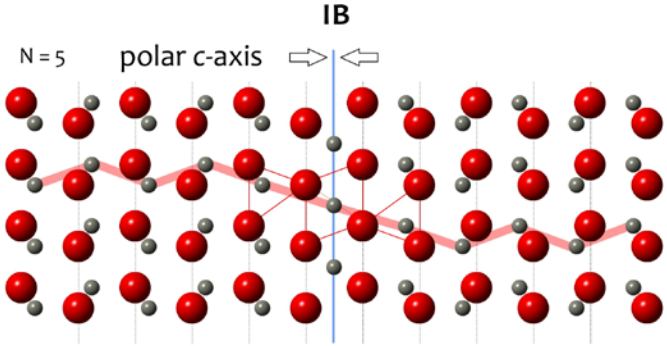

... Aβ–Bα–Aβ–Bα–A-γ-B–βA–αB–βA–αB ...

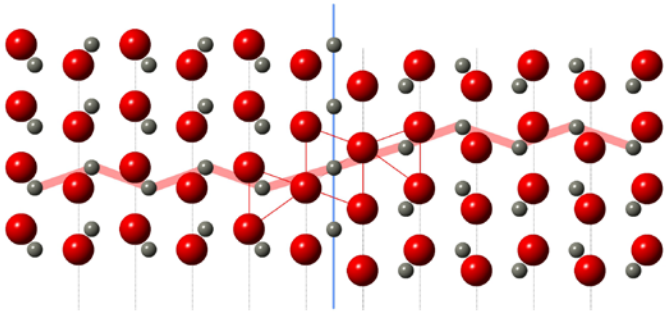

... Aβ–Bα–Aβ–Bα–A-β-C–γA–αC–γA–αC ...

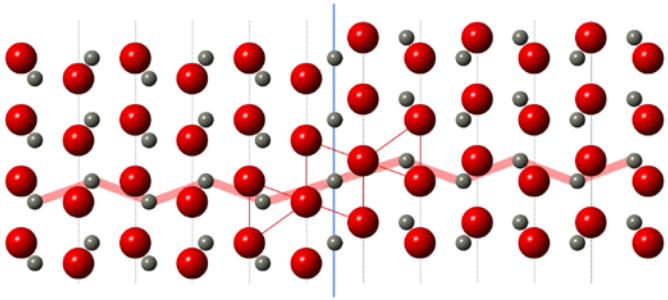

... Aβ–Bα–Aβ–Bα–A-β-C–γB–βC–γB–βC ...

?

DFT

Translations can be followed in the O-sublattice.

Translations of head-to-head b-IBs

∴ They can be produced from pure wurtzite ZnO or through preceeding SFs, followed by inversion.

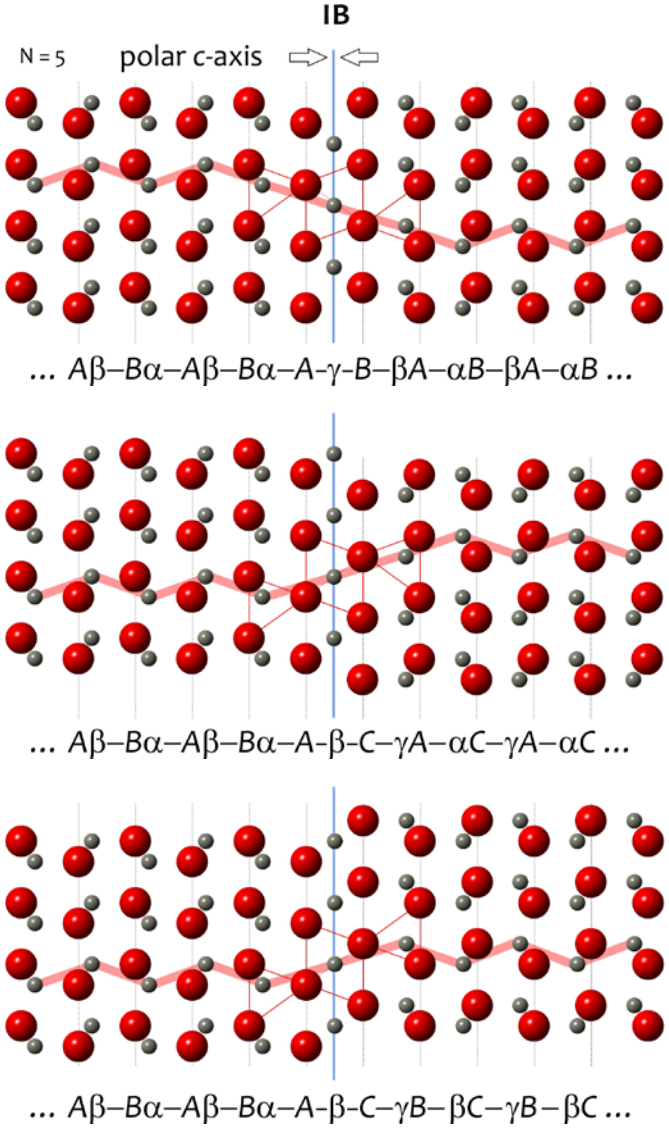

Translations of head-to-head b-IBs

Model 1

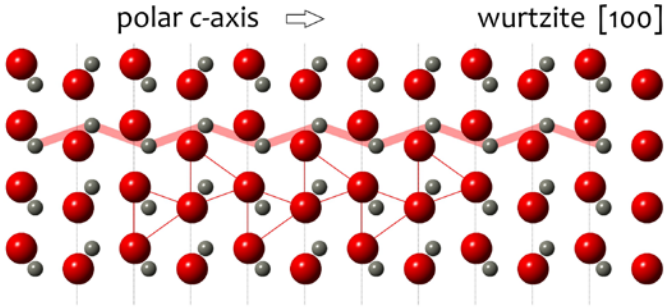

... Aβ–Bα–Aβ–Bα–Aβ–Bα–Aβ–Bα–Aβ–B ...

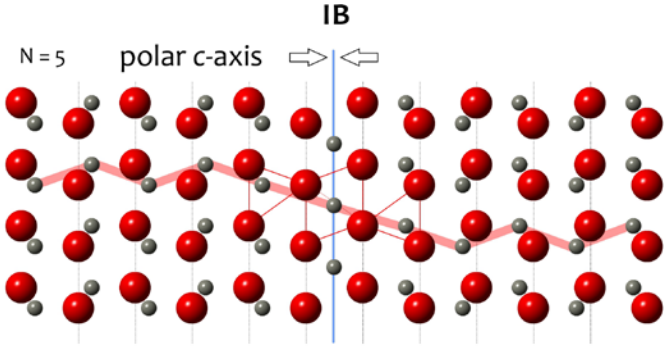

... Aβ–Bα–Aβ–Bα–A-γ-B–βA–αB–βA–αB ...

DFT

Model 2

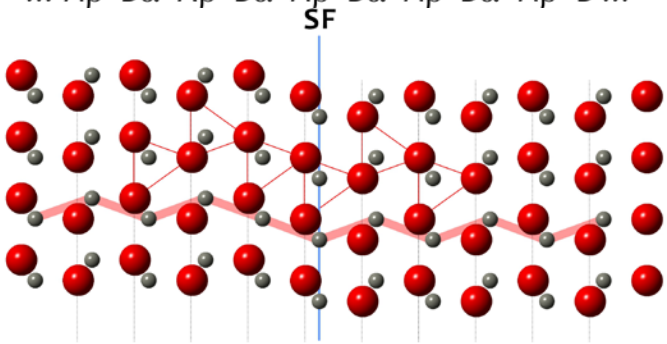

... Aβ–Bα–Aβ–Bα–Aγ–Cα–Aγ–Cα–Aγ–C ...

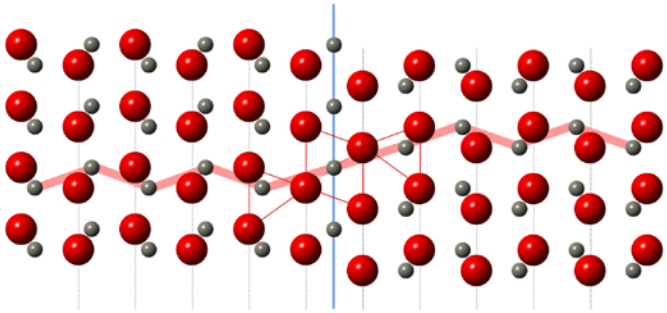

... Aβ–Bα–Aβ–Bα–A-β-C–γA–αC–γA–αC ...

Model 3

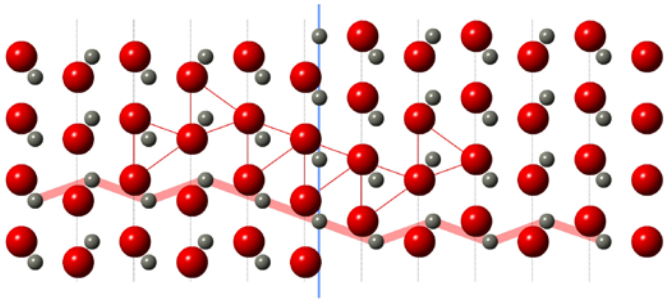

... Aβ–Bα–Aβ–Bα–Aγ–Cβ–Bγ–Cβ–Bγ–C ...

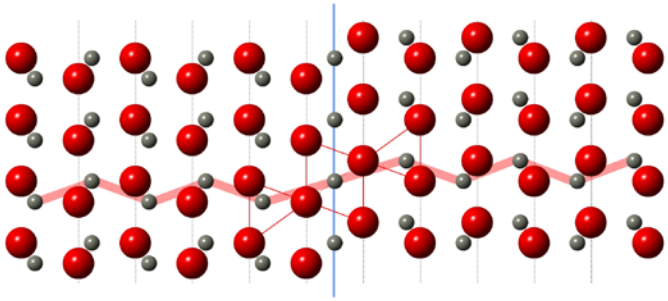

... Aβ–Bα–Aβ–Bα–A-β-C–γB–βC–γB–βC ...

Translations of head-to-head b-IBs

∴ Two more translations have been reported in literature ..

... that would produce two further IB models:

(not yet reported)

Model 4

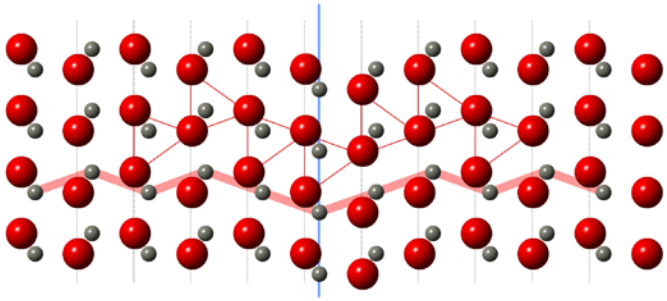

... Aβ–Bα–Aβ–Bα–Aγ–Cα–Aβ–Bα–Aβ–B ...

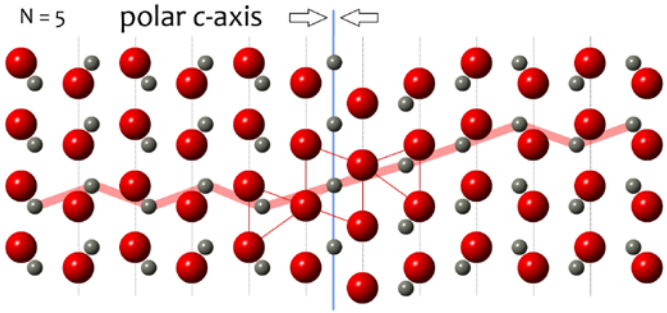

... Aβ–Bα–Aβ–Bα–A-β-C–γA–αB–βA–αB ...

Model 5

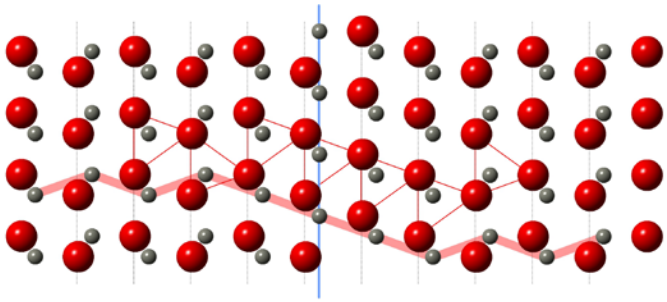

... Aβ–Bα–Aβ–Bα–Aγ–Cβ–Bα–Aβ–Bα–A ...

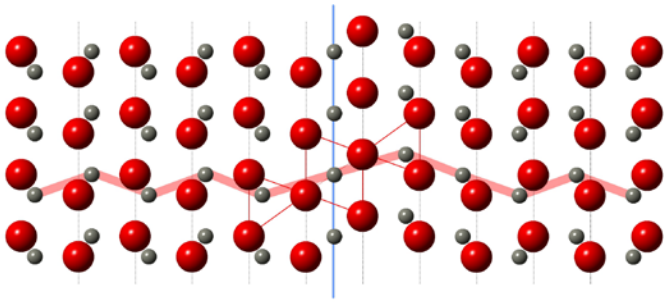

... Aβ–Bα–Aβ–Bα–A-β-C–γB–βA–αB–βA ...

DFT of IB-Sb

- Quantum-Espresso, PBE approximation, Ultrasoft pseudopotentials
- Supercells with 8 atomic layers on both sides of IBs; 216 atoms (6 H atoms)

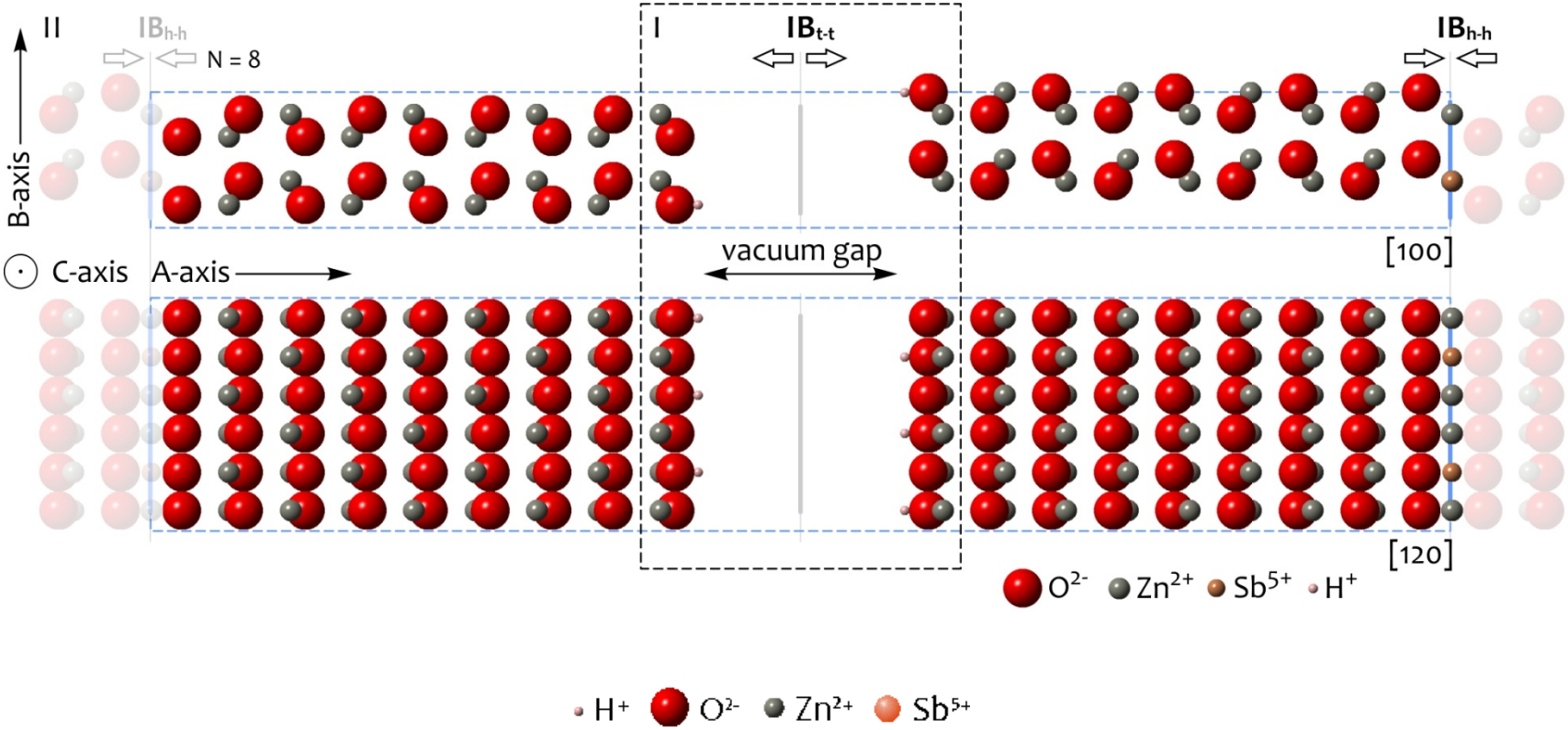

Results IB-Sb

- All calculations converged; structure of ZnO is preserved

Contraction along c-axis in the oxygen sublattice for Model 2	
DFT relaxed	HRTEM, Rečnik et al (2001)
-0.516 ± 0.001 Å	-0.53 ± 0.05 Å
ΔOx = 0.0976 ± 0.0002	ΔOx = 0.102 ± 0.01

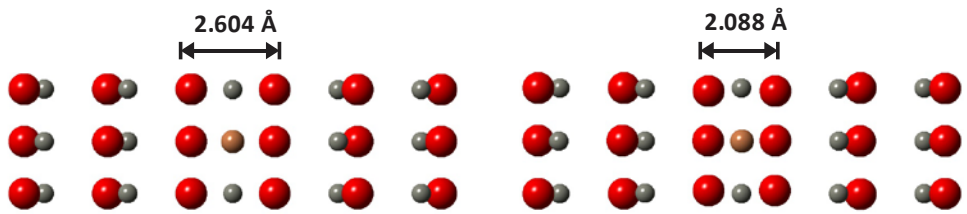

- 3rd translation model turned out to be the most stable one

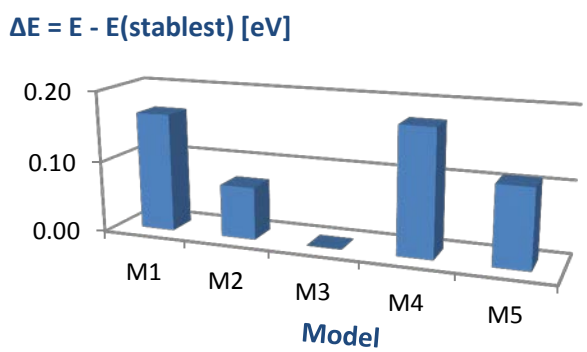

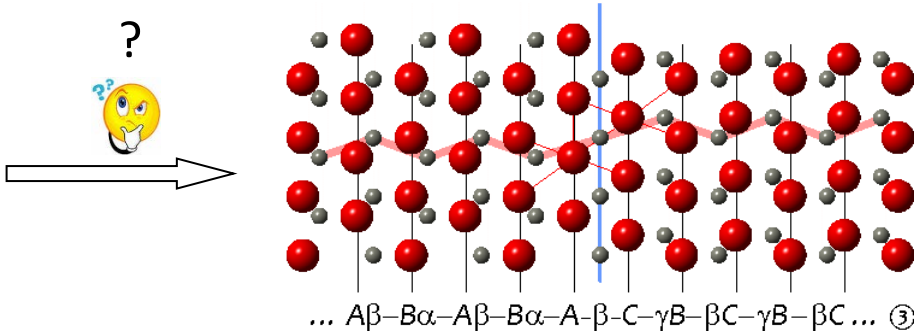

Experimental proof for the DFT result - translations in Sb-IBs

HRTEM images of IB in Sb^{5+}-doped ZnO

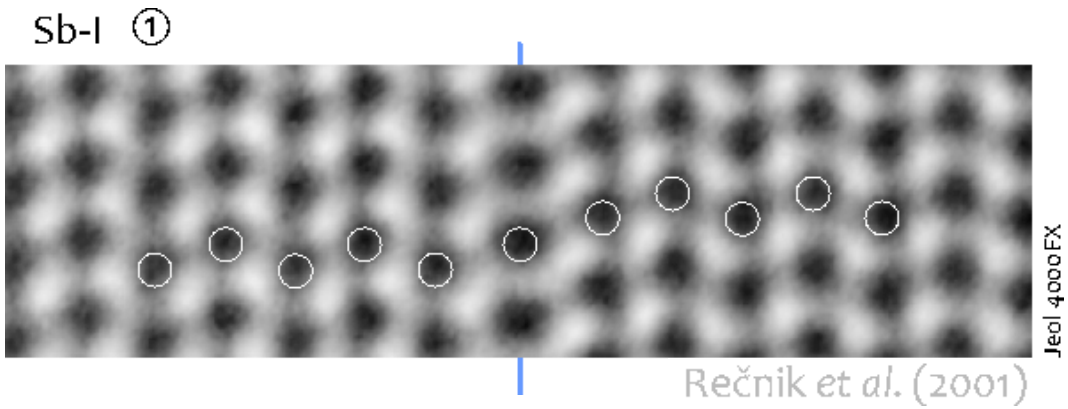

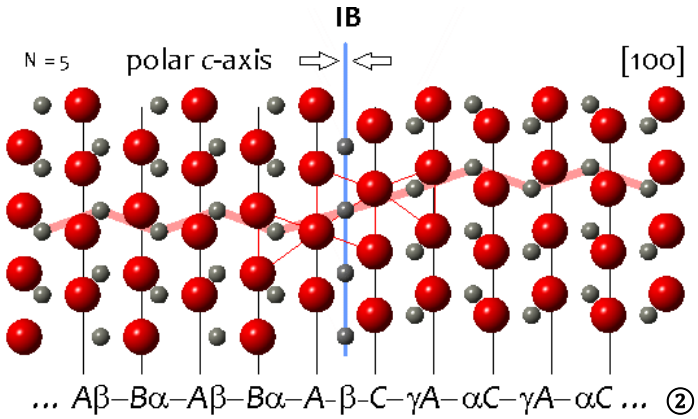

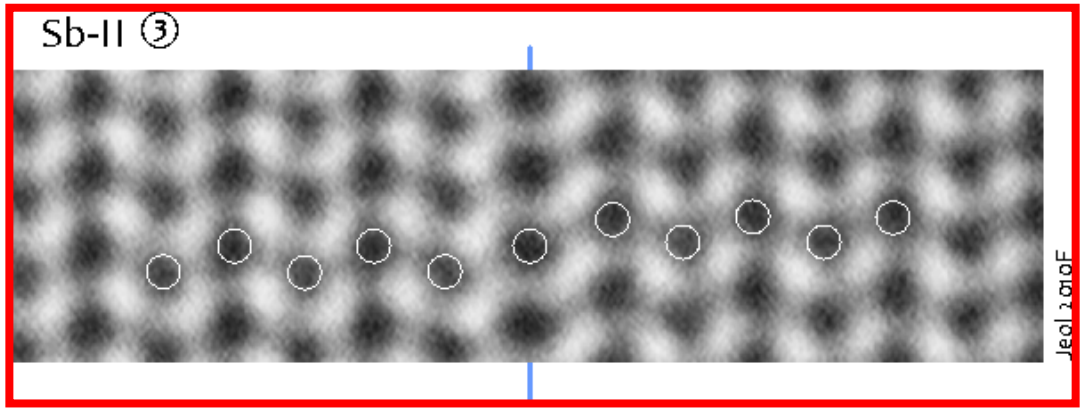

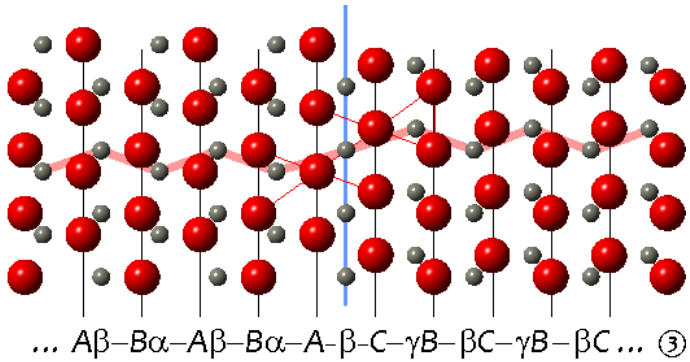

Experimental confirmation of Model 3!

CONCLUSIONS

- ∴ DFT result are in good agreement with experimental ones
- ∴ DFT revealed that the third model was most stable for Sb, which was then experimentally confirmed

Ab-initio study of proton transfer reaction between H_3O^+ ion and volatile organic compounds related to cork-taint in wine

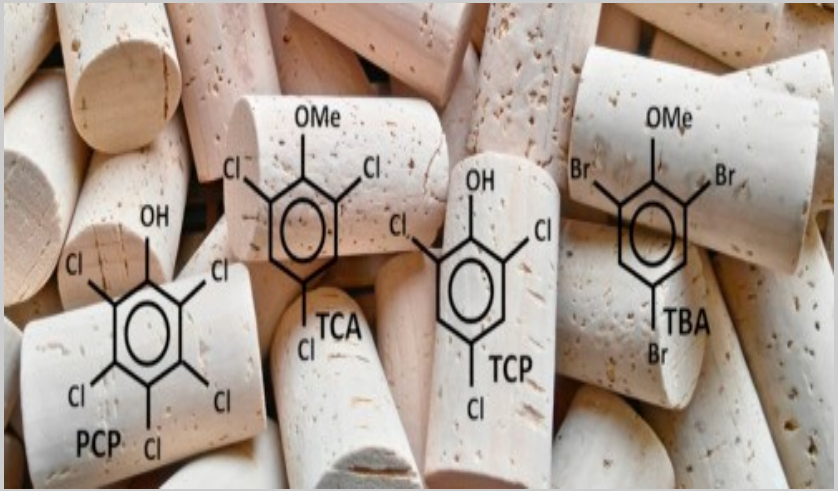

Manjeet Kumar

PhD student
Dept. of Physics
University of Milan

Volatile organic compounds in wine

- Volatile organic compounds (VOC) are the chemicals that easily become vapors or gases.
- VOCs are emitted as gases from certain solids or liquids.
- A set of undesirable smells or tastes found in a bottle of wine is referred to a wine fault.
- VOCs in wine: Chloroanisole, Bromoanisole and Chlorophenols along with many others.
- Detection techniques require to be very fast and detection limit as low as pptv.

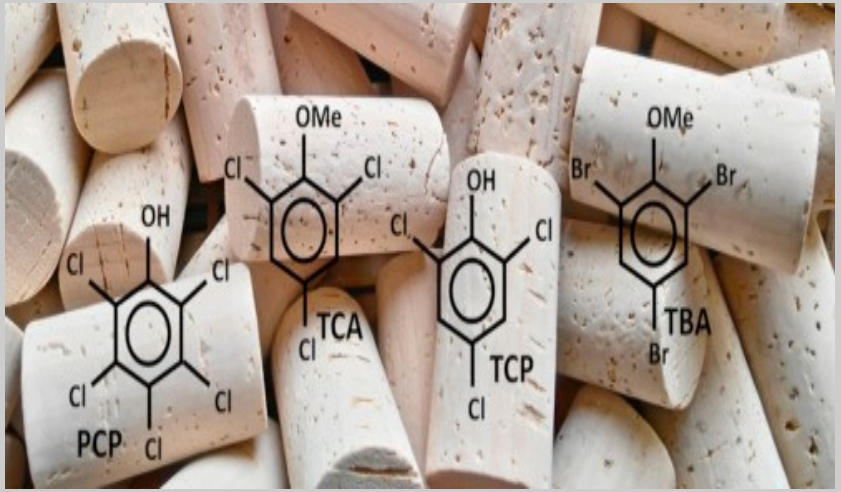

Proton-Transfer Reaction Mass Spectrometry (PTR-MS)

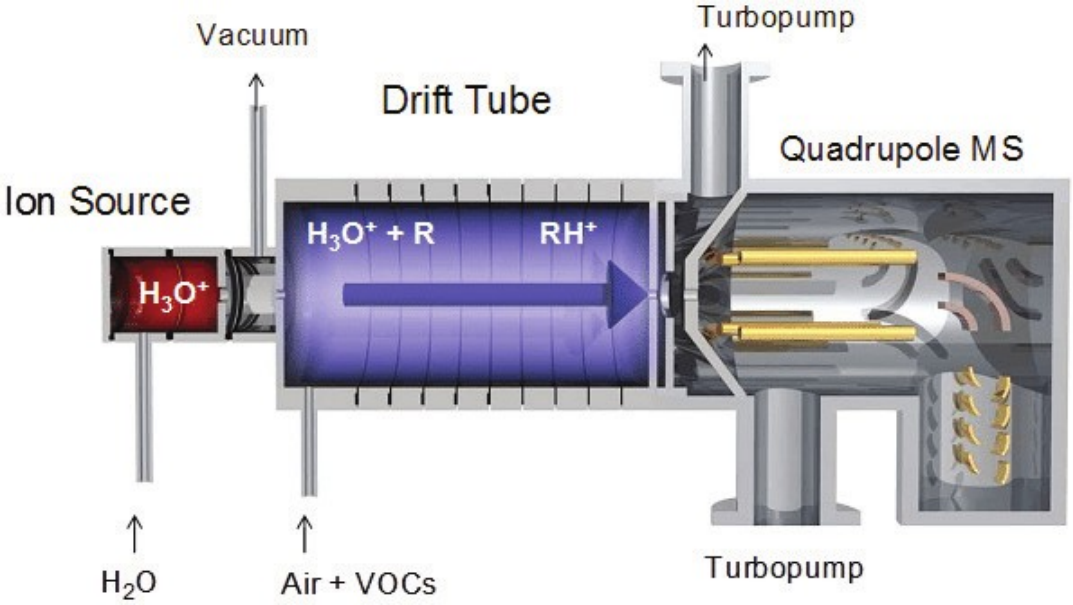

Proton transfer reaction in drift tube :

$$H_3O^+ + M = MH^+ + H_2O$$

$$[MH^+]_t/[H_3O^+] = I_{MH+}/I_{H3O}{}^+ = k[M]t$$

K = rate coefficient, t = reaction time

Theoretical models

Ion-molecule collision:

$$\kappa_L = \sqrt{\frac{\pi \alpha q^2}{\mu \epsilon_0}}$$

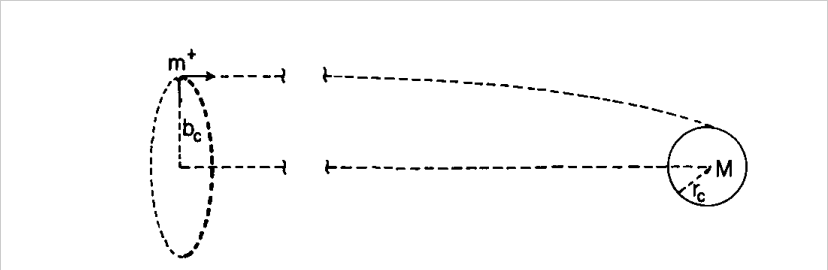

Average dipole orientation:

$$\kappa_{ADO} = \sqrt{\frac{\pi \alpha q^2}{\mu \epsilon_0}} + \frac{C \mu_D q}{\epsilon_0} \sqrt{\frac{1}{2 \pi \mu \kappa_B T}}$$

Capture rate coefficient:

$$\kappa_{cap} = \kappa_L \times \kappa_c(\tau, \epsilon)$$

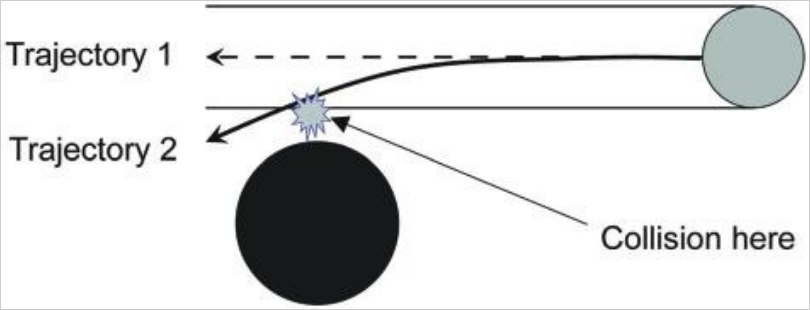

Method and Results :

- Dipole moment and polarizability of the molecules are calculated using Quantum ESPRESSO code.

- DFT functional BLYP and Ultrasoft Pseudopotentials.

- Ion-molecule reaction rate coefficients (Langevin, Average dipole orientation and parametrized Trajectory method) at 300 & 380 K between H_3O^+ and VOC under PTR-MS working conditions.

Compound name	μ_D (Debye)	α (Å^3)	T (K)	$K_{Langevin}$ $10^{-9}cm^3s^{-1}$	K_{ADO} $10^{-9}cm^3s^{-1}$	K_{cap}(com) $10^{-9}cm^3s^{-1}$
2,4,6-TCA	1.41	21.47	300	2.58	3.09	2.73
			380		3.09	2.71
2,4,6-TBA	1.44	25.67	300	2.78	3.26	2.91
			380		3.27	2.89
2,3,4,6-TeCA	1.59	23.58	300	2.70	3.27	2.88
			380		3.27	2.86
2,4-DCA	3.45	19.12	300	2.46	4.19	3.84
			380		4.19	3.72
2,6-DCA	2.17	18.53	300	2.42	3.41	2.89
			380		3.41	2.85
Octen-3-ol	1.57	17.12	300	2.37	3.01	2.61
			380		3.01	2.59
Octen-3-one	3.07	16.43	300	2.33	3.89	3.56
			380		3.89	3.45
MDMP	1.18	16.88	300	2.34	2.70	2.46
			380		2.70	2.45
2-MIB	1.47	20.31	300	2.54	3.09	2.71
			380		3.09	2.70
Geosmin	1.37	22.02	300	2.64	3.14	2.78
			380		3.14	2.76
Guaiacol	3.00	14.84	300	2.21	3.75	3.45
			380		3.75	3.34
PCA	1.38	26.10	300	2.82	3.26	2.94
			380		3.26	2.93

KE_{com} vs Reduced electric field

- Kinetic energy is a function of E/N for collision between H_3O^+ and different molecules.

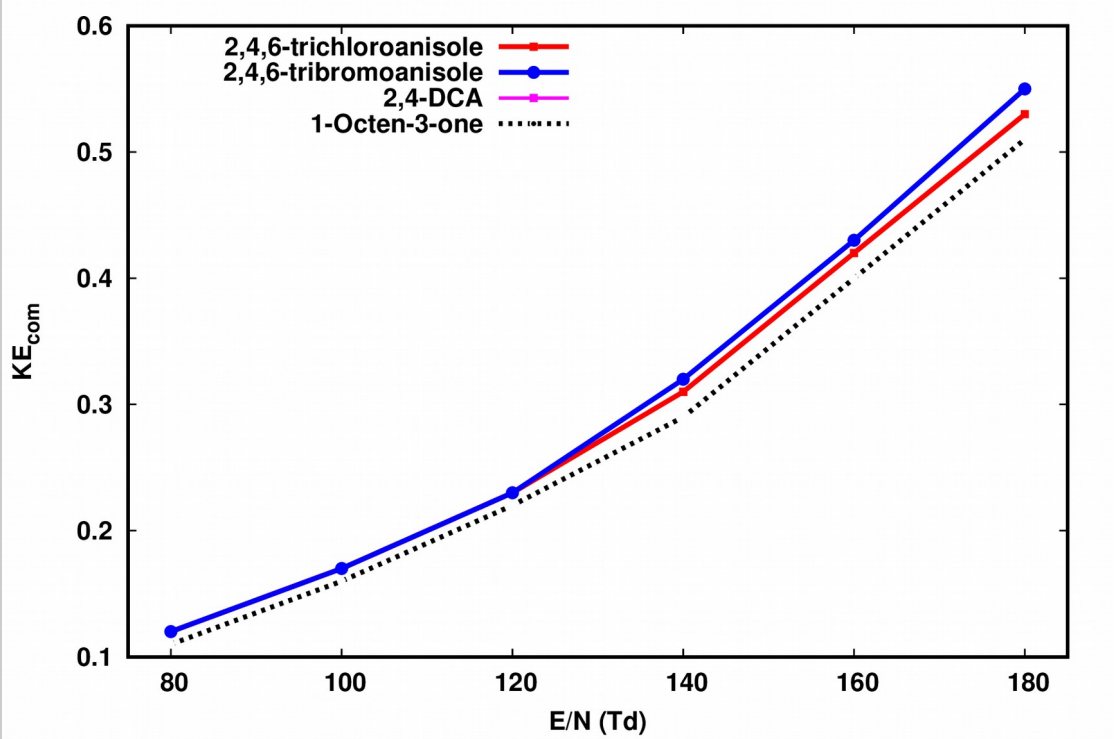

Td = townsend
1 Td = 10^{-17} V. cm^2.

Rate coefficients vs KE_{com}

- Variation of rate coefficients with KE_{com} at different internal temperatures.

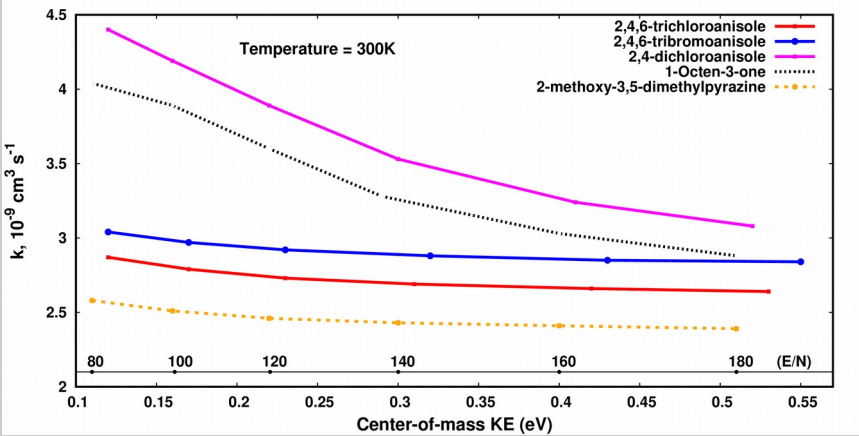

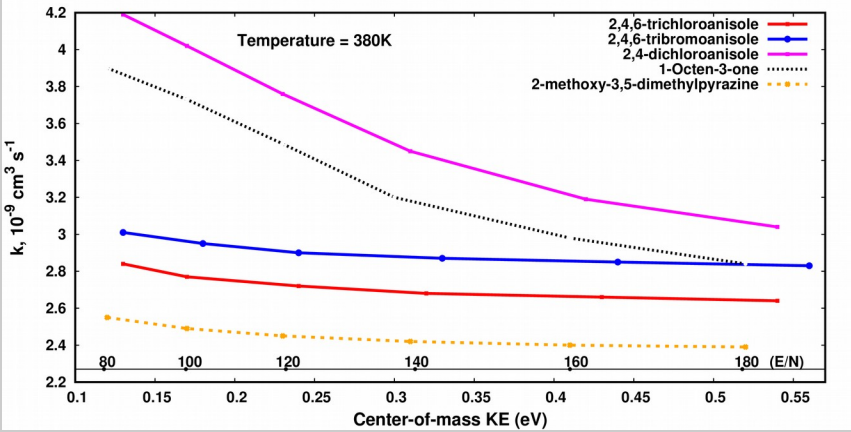

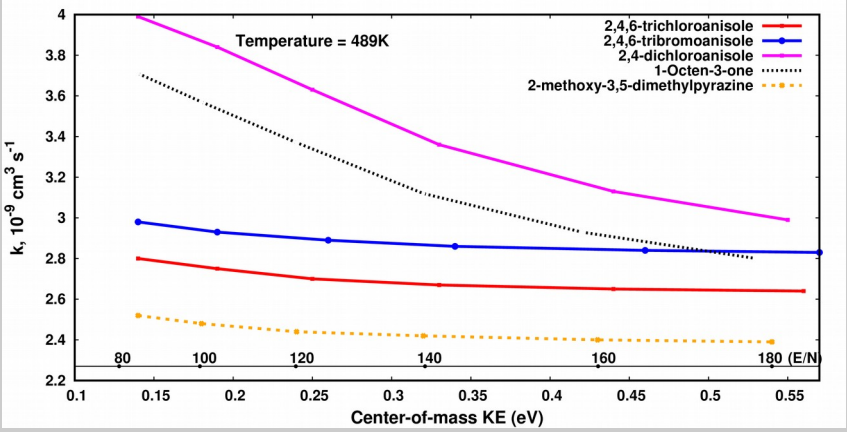

Conclusion :

- The rate coefficients predicted using ADO depend uniquely on the dipole moment and Polarizability and independent of temperature.
- Where as rate coefficients by parameterized trajectory method show small variation with temperature.
- Rate coefficients obtained form parameterized trajectory method remain constant with internal temperature (E/N>120 Td).
- Overall rate coefficient decreases with increasing center-of-mass kinetic energy.

Response of GaN to sequential ion irradiation

J. Hanžek[1], H. Vázquez[2], F. Djurabekova[2], M. Karlušić[1,*]

1 Ruđer Bošković Institute, Bijenička 54, 10000 Zagreb, Croatia

2 Department of Physics, University of Helsinki, P.O. Box 43, 00014, Helsinki, Finland

* Corresponding author: marko karlusic@irb.hr

Track formation with swift heavy ions

[1]

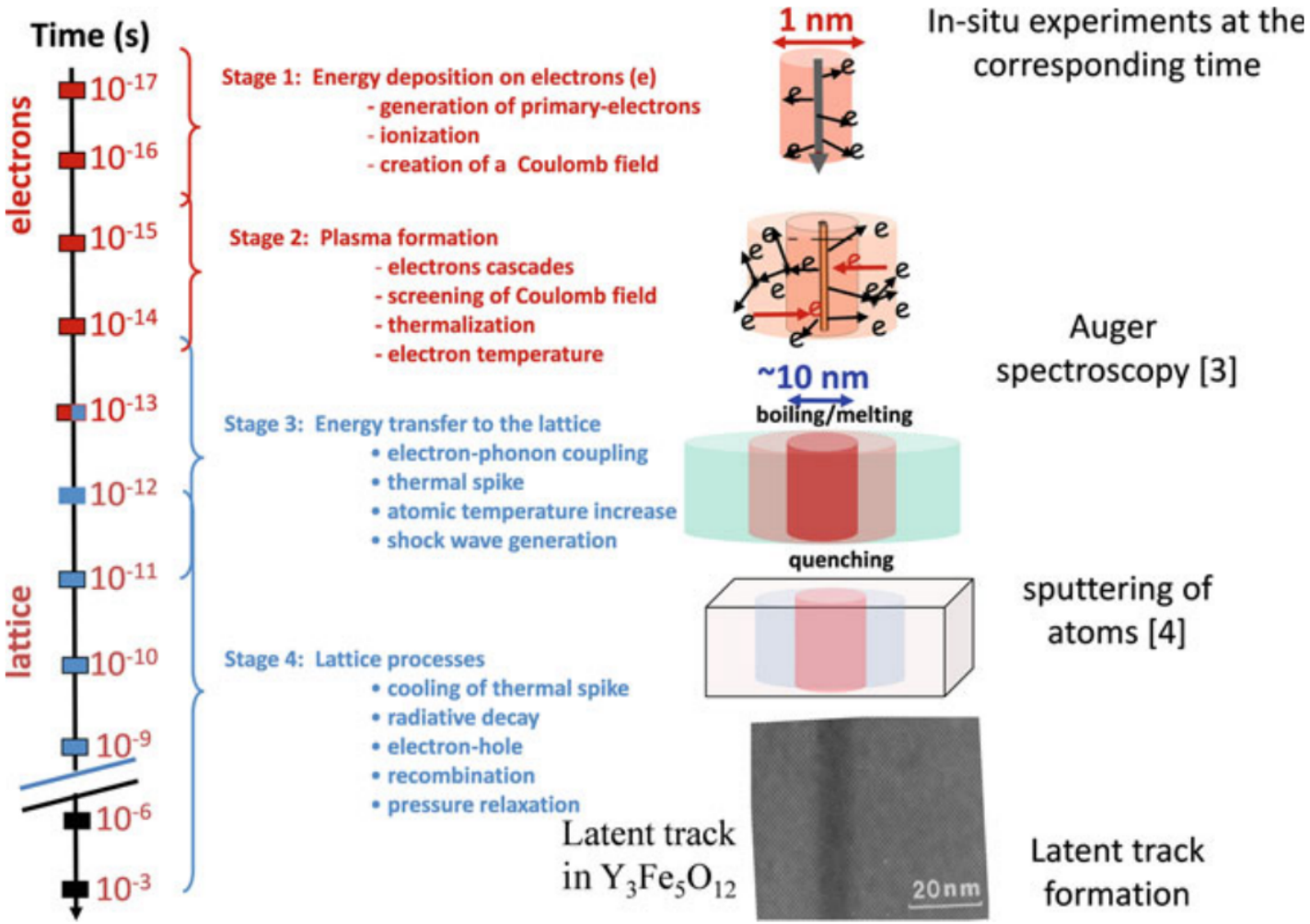

Analytical thermal spike model

thermal wave[2]:

$$\Delta T(r,t) = \frac{Q}{\pi a^2(t)} e^{-\frac{r^2}{a^2(t)}}$$

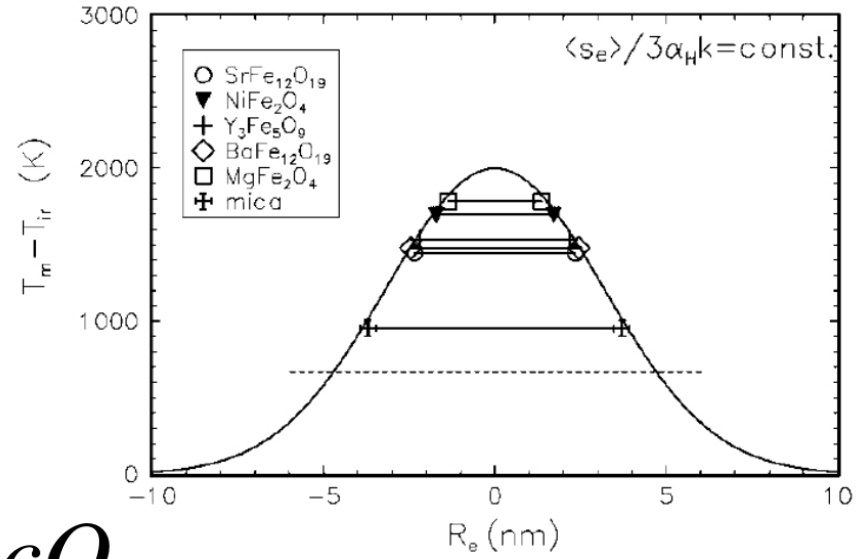

conservation of energy:

$$gS_e = \rho c Q + \rho \pi R^2 L \simeq \rho c Q$$

condition of trace formation:

$$S_{et} = \frac{\rho c \pi a_0^2 \Delta T_m}{g}$$

Molecular dynamic simulation of GaN

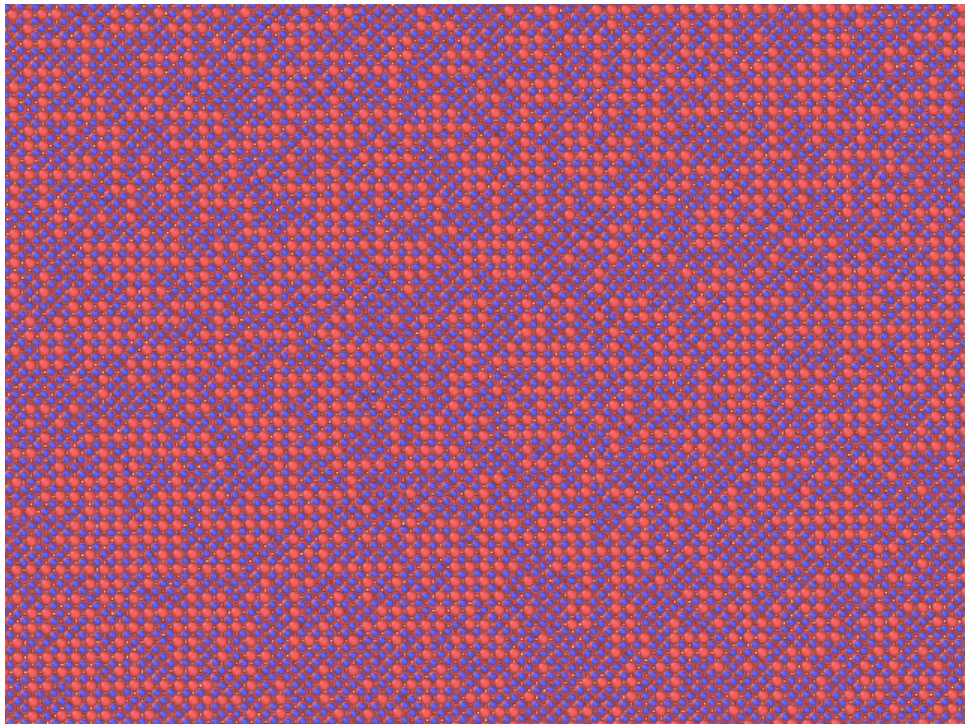

Crystalline GaN.

There is no ion track[3].

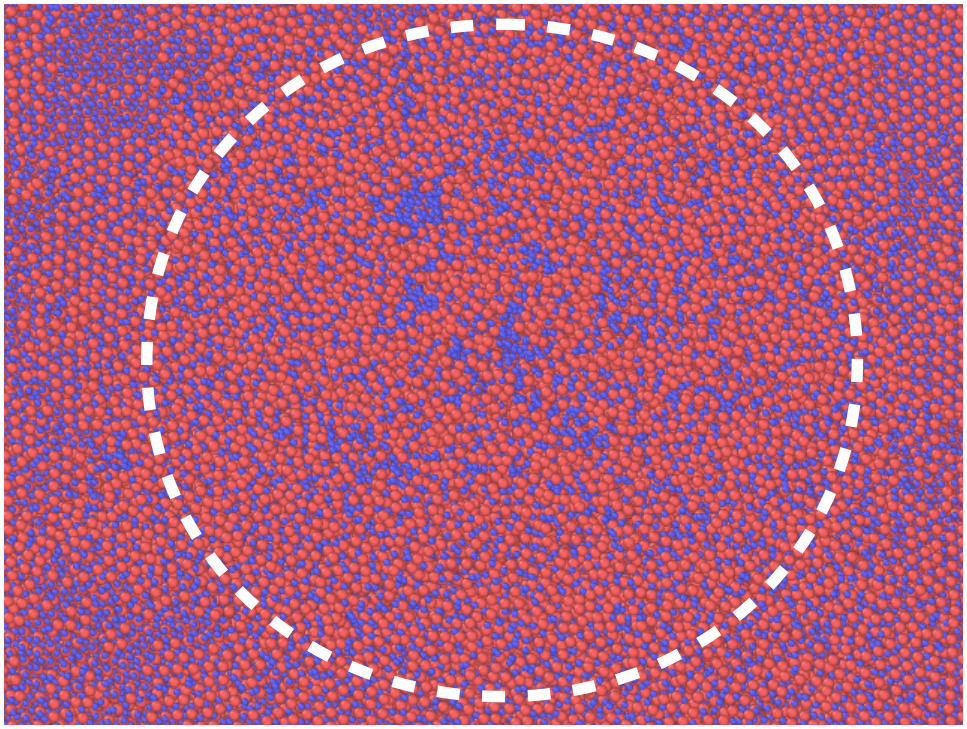

Pre-damaged GaN.

The ion track radius is about 7nm.

Literature

[1] Werner Wesch Elke Wendler; Ion Beam Modification of Solids, Ion-Solid Interaction and Radiation Damage Springer Switzerland 2016

[2] G Szenes; General features of latent track formation in magnetic insulators irradiated with swift heavy ions Physical review. B, Condensed matter 51(13):8026-8029 · May 1995

[3] M Karlušić1, R Kozubek2, H Lebius3, B Ban-d'Etat3, R A Wilhelm4, M Buljan1, Z Siketić1, F Scholz5, T Meisch5, M Jakšić1, S Bernstorff6, M Schleberger2 and B Šantić1; Response of GaN to energetic ion irradiation: conditions for ion track formation J. Phys. D: Appl. Phys. 48 (2015) 325304 (12pp)

DFT study of hydrogen bonding between metal hydroxides and common organic functional groups

Lea Gašparič,[1,2] Matic Poberžnik,[2] Anton Kokalj[2]

[1]Faculty of Chemistry and Chemical Technology, University of Ljubljana, Ljubljana, Slovenia
[2]Department of Physical and Organic Chemistry, Jožef Stefan Institute, Ljubljana, Slovenia

1. Our aim

- Investigation of the hydrogen bond (donor and acceptor abilities)
- Can one approximate molecule–surface hydrogen bonding with small clusters?

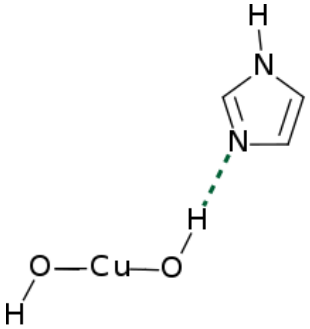

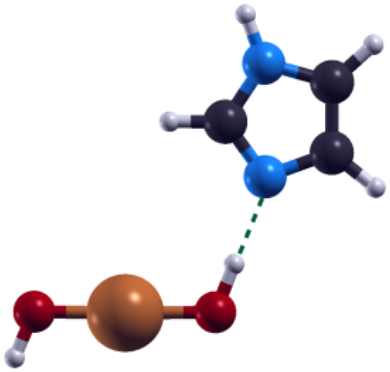

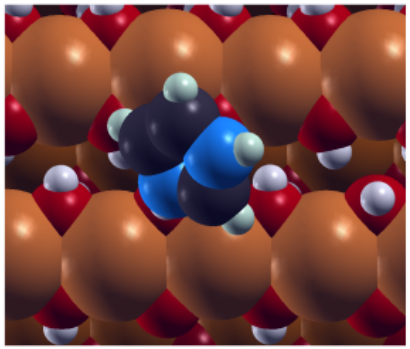

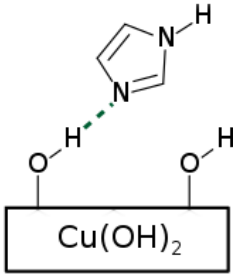

2. Our approach

DFT based calculations:

- Cluster calculations (Gaussian 16)

$Cu(OH)_2$

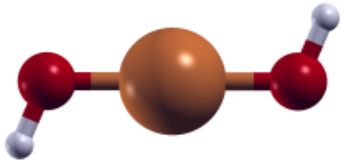

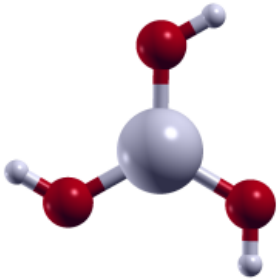

$Al(OH)_3$

- Adsorption calculations

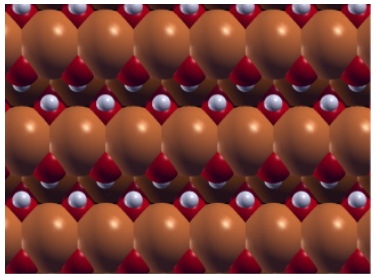

$Cu(OH)_2$ (001)

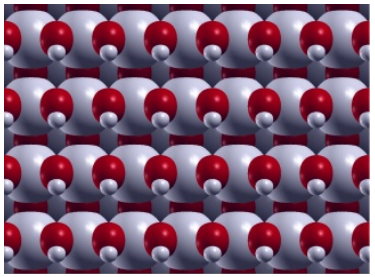

Boehmite - AlOOH (010)

3. The results

- Hydrogen bonds (X···H–Y; X, Y = N, O, S) and adsorption energies
- Donor and acceptor H-bonding strength of common organic functional groups with metal hydroxides

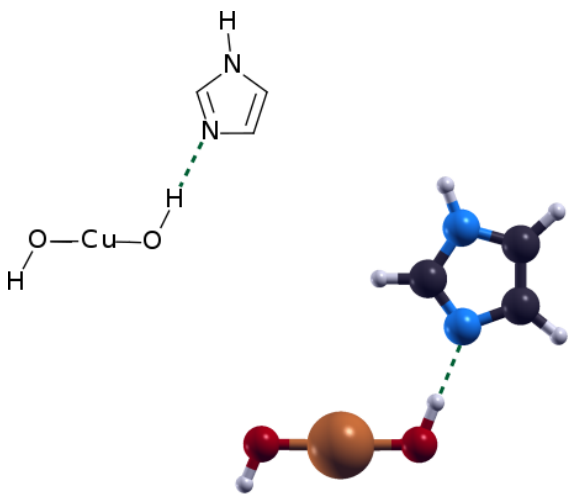

$\Delta E = -0.41$ eV

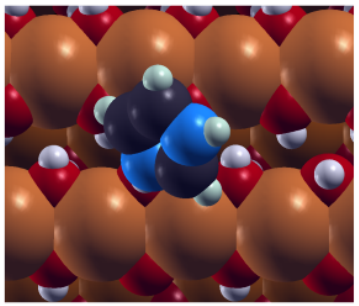

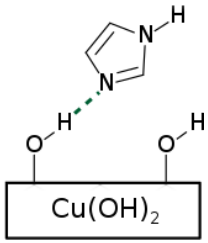

$\Delta E = -0.37$ eV

4. What have we learned?

- Small clusters usually give reasonable H-bond energy

- **BUT**: molecules can form several H-bonds with the surface therefore small clusters cannot account for the correct adsorption geometry and the number of hydrogen bonds

Additional information and questions

For any questions or more detailed discussion you can find me next to my poster.

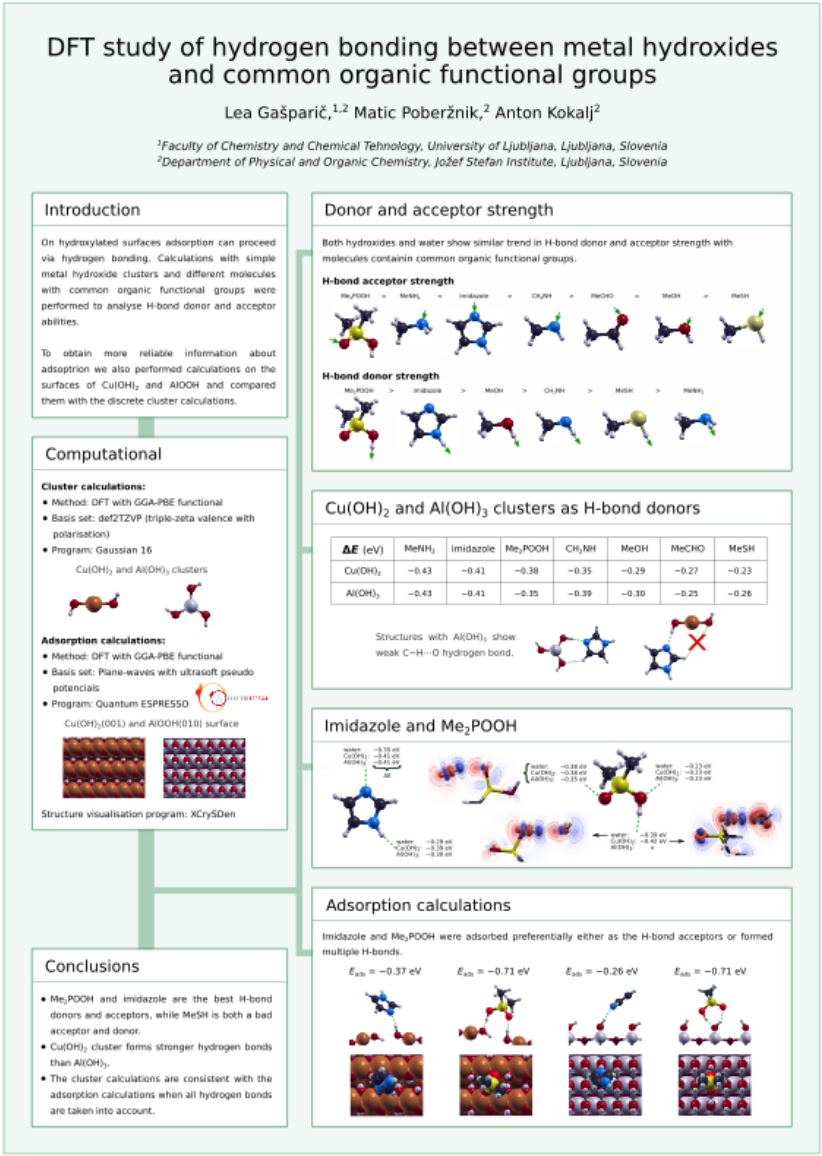

DFT study of hydrogen bonding between metal hydroxides and common organic functional groups

Lea Gašparič,[1,2] Matic Poberžnik,[2] Anton Kokalj[2]

[1]Faculty of Chemistry and Chemical Tehnology, University of Ljubljana, Ljubljana, Slovenia
[2]Department of Physical and Organic Chemistry, Jožef Stefan Institute, Ljubljana, Slovenia

Introduction

On hydroxylated surfaces adsorption can proceed via hydrogen bonding. Calculations with simple metal hydroxide clusters and different molecules with common organic functional groups were performed to analyse H-bond donor and acceptor abilities.

To obtain more reliable information about adsoptrion we also performed calculations on the surfaces of $Cu(OH)_2$ and AlOOH and compared them with the discrete cluster calculations.

Computational

Cluster calculations:
- Method: DFT with GGA-PBE functional
- Basis set: def2TZVP (triple-zeta valence with polarisation)
- Program: Gaussian 16

$Cu(OH)_2$ and $Al(OH)_3$ clusters

Adsorption calculations:
- Method: DFT with GGA-PBE functional
- Basis set: Plane-waves with ultrasoft pseudo potencials
- Program: Quantum ESPRESSO

$Cu(OH)_2$(001) and AlOOH(010) surface

Structure visualisation program: XCrySDen

Conclusions

- Me_2POOH and imidazole are the best H-bond donors and acceptors, while MeSH is both a bad acceptor and donor.
- $Cu(OH)_2$ cluster forms stronger hydrogen bonds than $Al(OH)_3$.
- The cluster calculations are consistent with the adsorption calculations when all hydrogen bonds are taken into account.

Donor and acceptor strength

Both hydroxides and water show similar trend in H-bond donor and acceptor strength with molecules containin common organic functional groups.

H-bond acceptor strength

H-bond donor strength

$Cu(OH)_2$ and $Al(OH)_3$ clusters as H-bond donors

ΔE (eV)	$MeNH_2$	imidazole	Me_2POOH	CH_3NH	MeOH	MeCHO	MeSH
$Cu(OH)_2$	−0.43	−0.41	−0.38	−0.35	−0.29	−0.27	−0.23
$Al(OH)_3$	−0.43	−0.41	−0.35	−0.39	−0.30	−0.25	−0.26

Structures with $Al(OH)_3$ show weak C−H···O hydrogen bond.

Imidazole and Me_2POOH

Adsorption calculations

Imidazole and Me_2POOH were adsorbed preferentially either as the H-bond acceptors or formed multiple H-bonds.

$E_{ads} = -0.37$ eV $E_{ads} = -0.71$ eV $E_{ads} = -0.26$ eV $E_{ads} = -0.71$ eV

10

Ab-initio Study of Lattice Anhamonicities in Bulk Lonsdaleite: Hexagonal Diamond

Rekha Verma

Indian Institute of Information Technology Allahabad

India

Poster No. 12

Motivation : Exploration of materials for Energy Harvesting Application using Thermoelectricity.

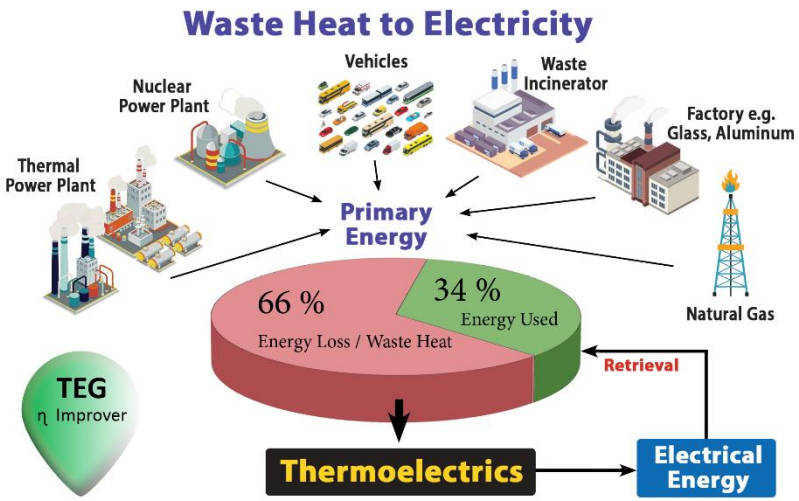

Thermoelectricity :

Conversion of thermal energy (waste heat) into electrical energy using Seebeck effect.

Seebeck Effect : Voltage is induced due to temperature gradient between the two ends of a TE material.

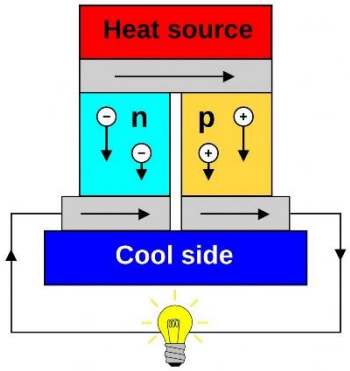

What makes a material to be potential candidate for thermoelectric application?

Thermoelectric (TE) Figure of Merit

$$ZT = \frac{\sigma S_B^2 T}{\kappa_e + \kappa_{ph}}$$

σ : Temperature dependent electrical conductivity

κ_e : Electronic thermal conductivity

κ_{ph} : Phonon thermal conductivity

S_B : Seebeck coefficient

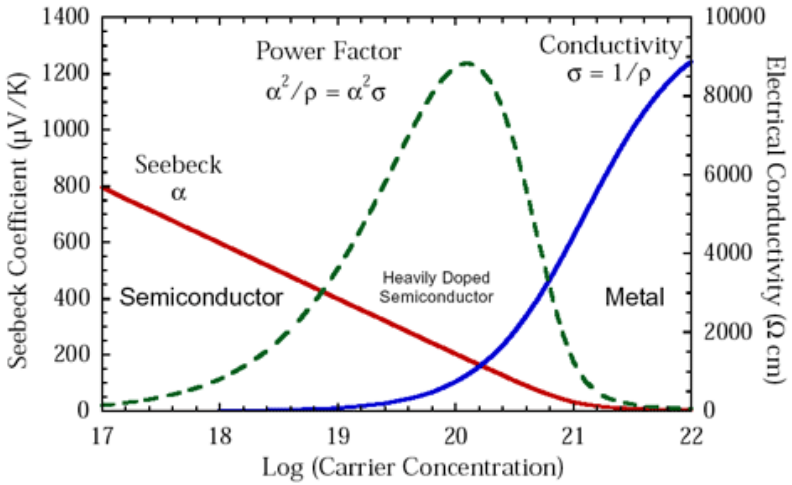

Source: Jeff. Snyder, Northwestern University, USA.

Tune the denominator i.e. the lattice thermal conductivity

How do we do that???

We calculate the thermoelectric transport coefficients i.e., electrical conductivity (σ), Seebeck coefficient (S), Thermal conductivity (κ) by solving Boltzmann transport equation.

Materials under consideration :

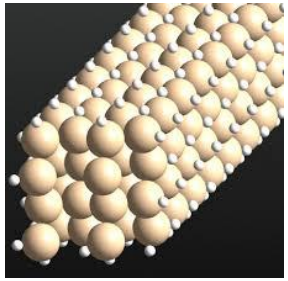

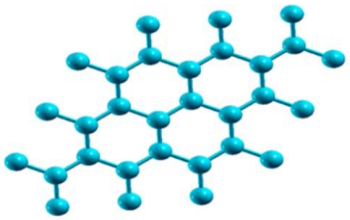

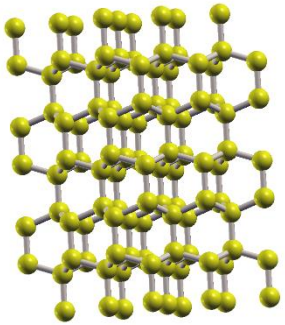

Thank You All

Rekha Verma

Poster No. 12

What does the DFT has to do with the polymer reinforcement?

i.e.

Why am I at DFT school talking about PMMA?

www.graphene.ac.rs

COMPUTATIONAL STUDY OF VIBRATIONAL PROPERTIES OF CHEMICALLY EXFOLIATED TITANIUM CARBIDE MXenes - Ti_3C_2 AND TiC_2

Jelena Pešić, Andrijana Šolajić

Institute of Physics Belgrade, University of Belgrade, Pregrevica 118, 11080 Belgrade, Serbia

Synthesis

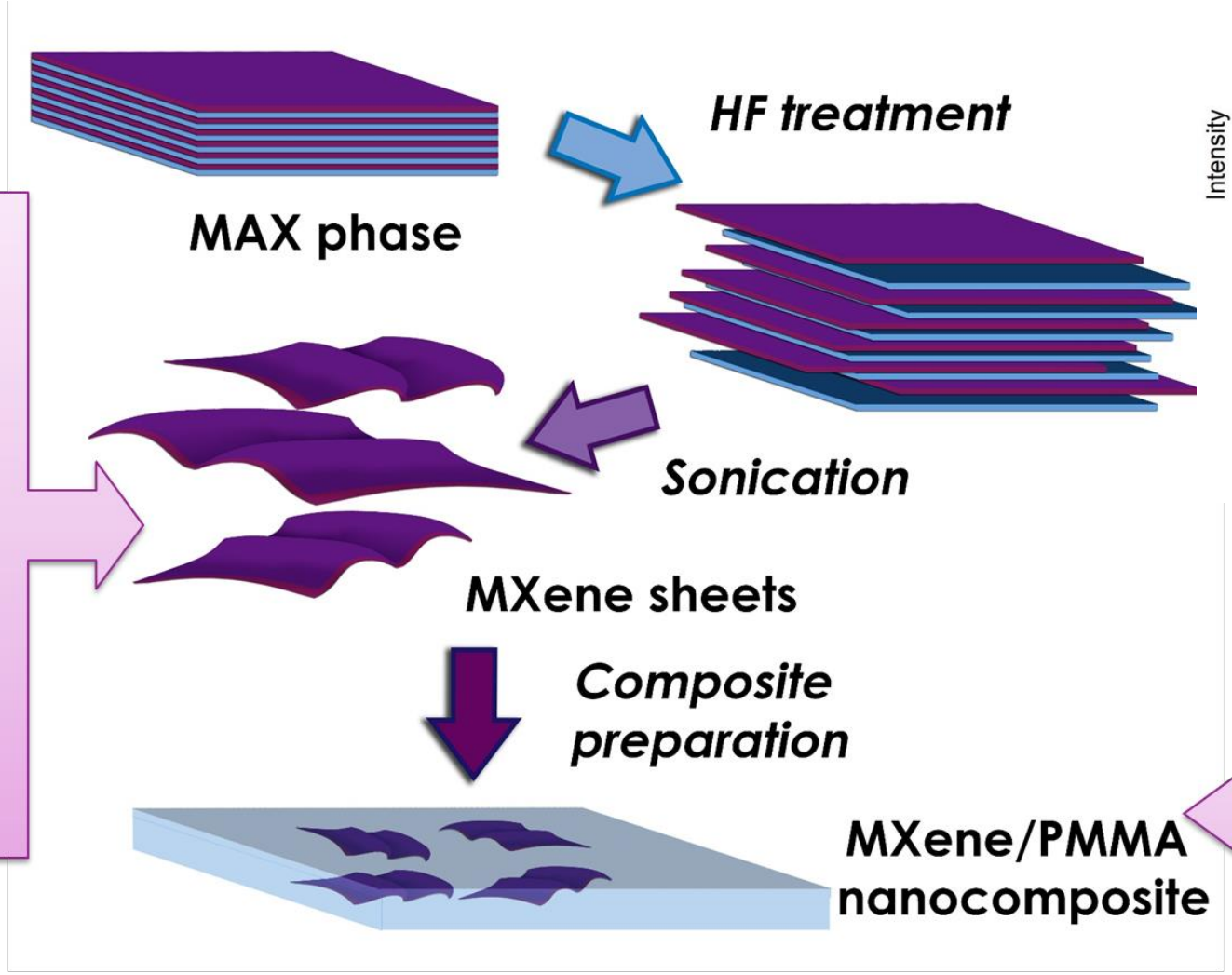

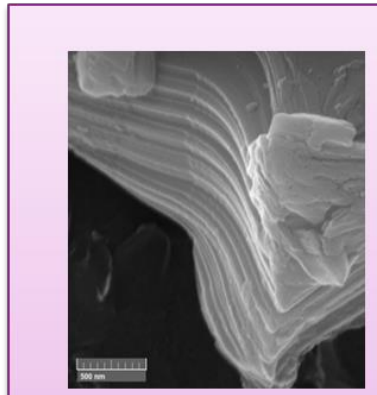

FESEM picture of Mxene film after etching procedure and removal of A layer

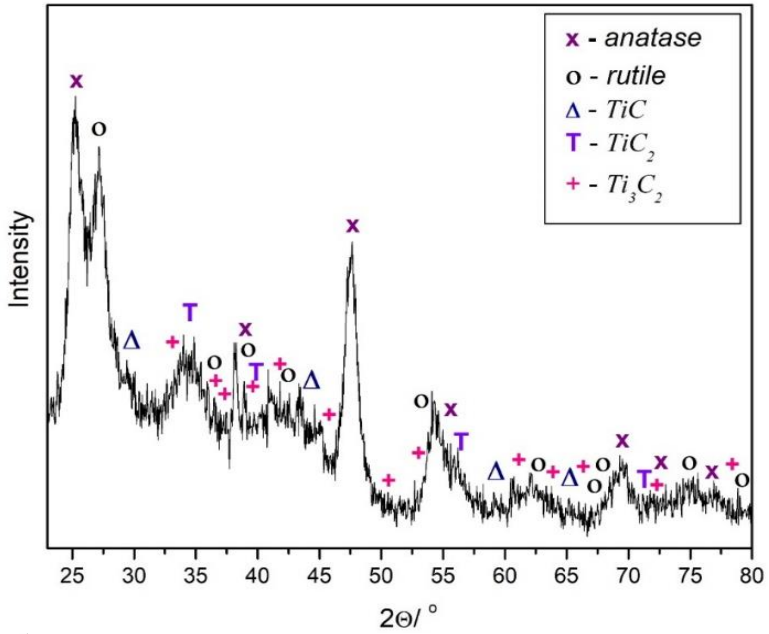

XRD pattern for MXene flakes

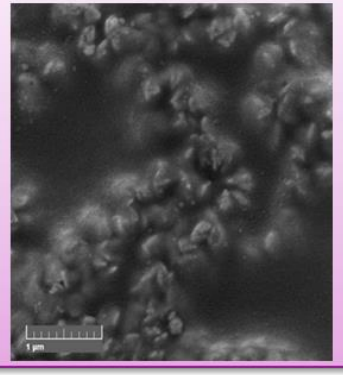

FESEM picture of PMMA/Mxene composite

Optical spectroscopy vs DFT

Raman spectra of MXene flakes after synthesis

DFT calculations

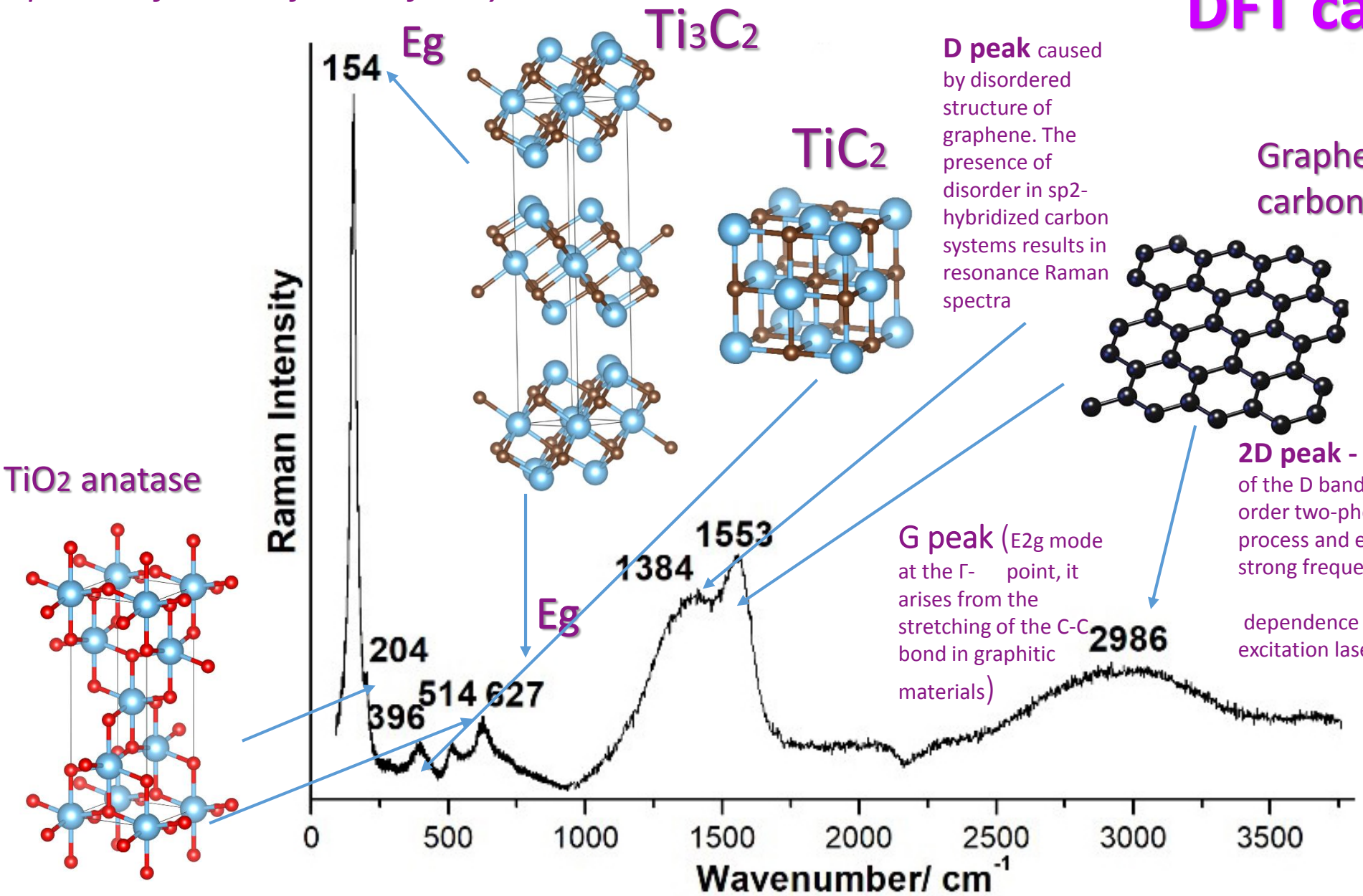

D peak caused by disordered structure of graphene. The presence of disorder in sp2-hybridized carbon systems results in resonance Raman spectra

2D peak - overtone of the D band: second-order two-phonon process and exhibits a strong frequency

dependence on the excitation laser energy

G peak (E2g mode at the Γ- point, it arises from the stretching of the C-C bond in graphitic materials)

Optical spectroscopy vs DFT

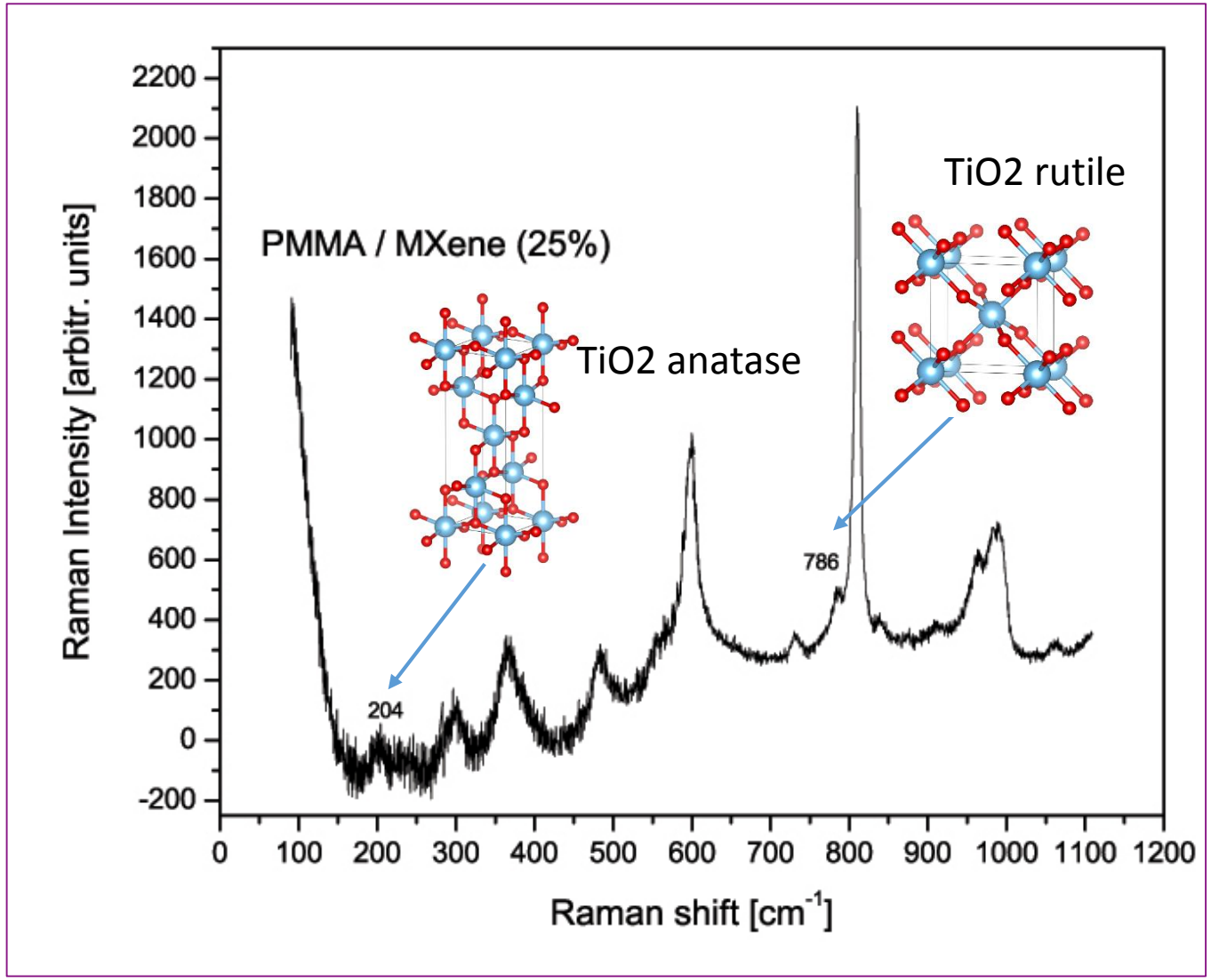

Raman spectra of PMMA/MXene (25%) composite

Optical spectroscopy vs DFT

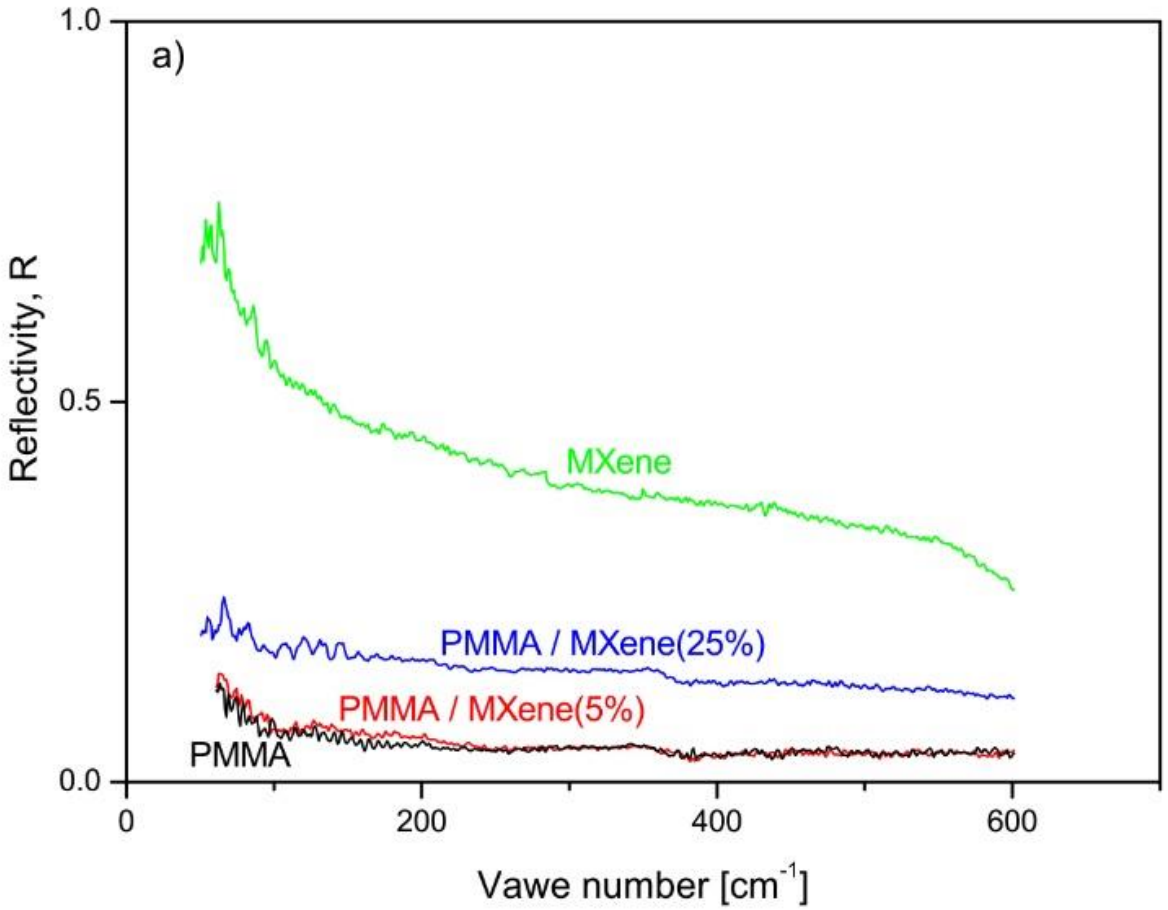

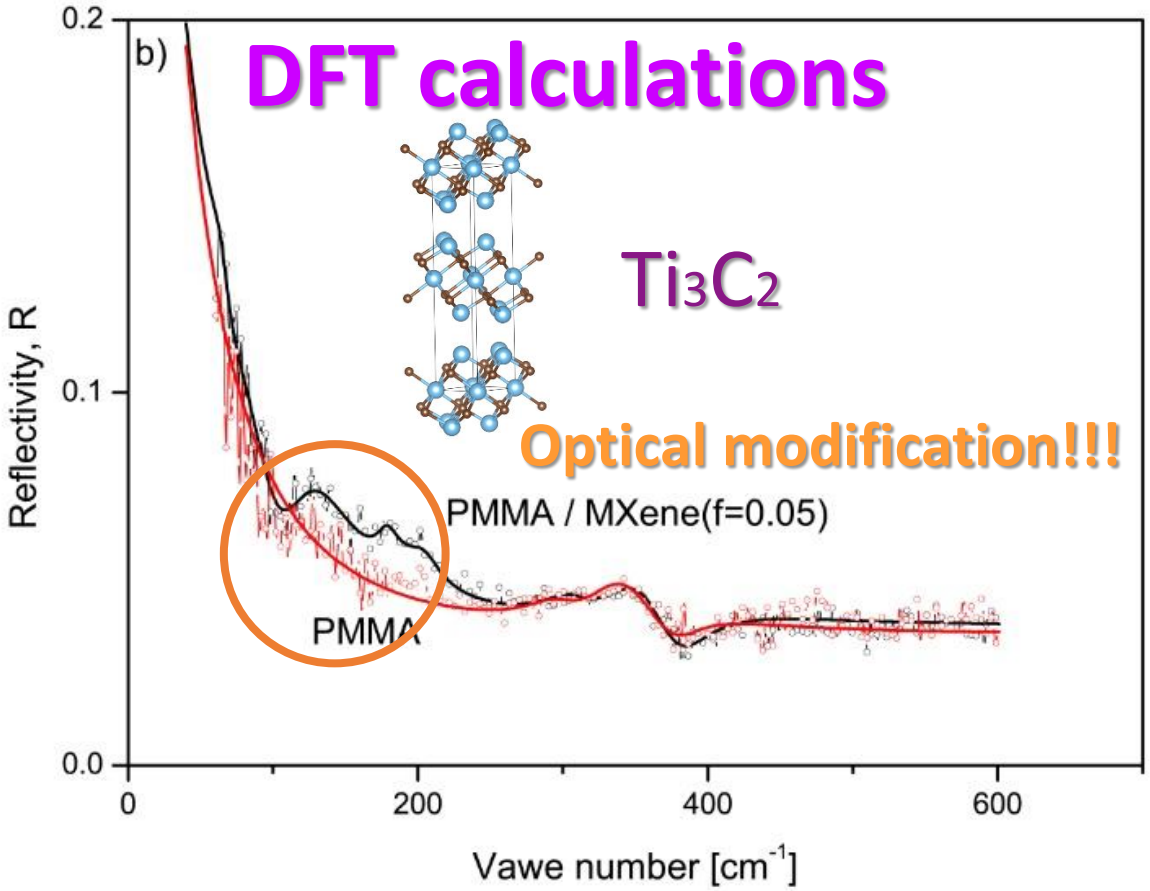

a) Infrared spectra of MXene flakes (green) and composites PMMA/MXene
b) circles represent experimental data and solid lines are fit obtained by Maxwell-Garnet model

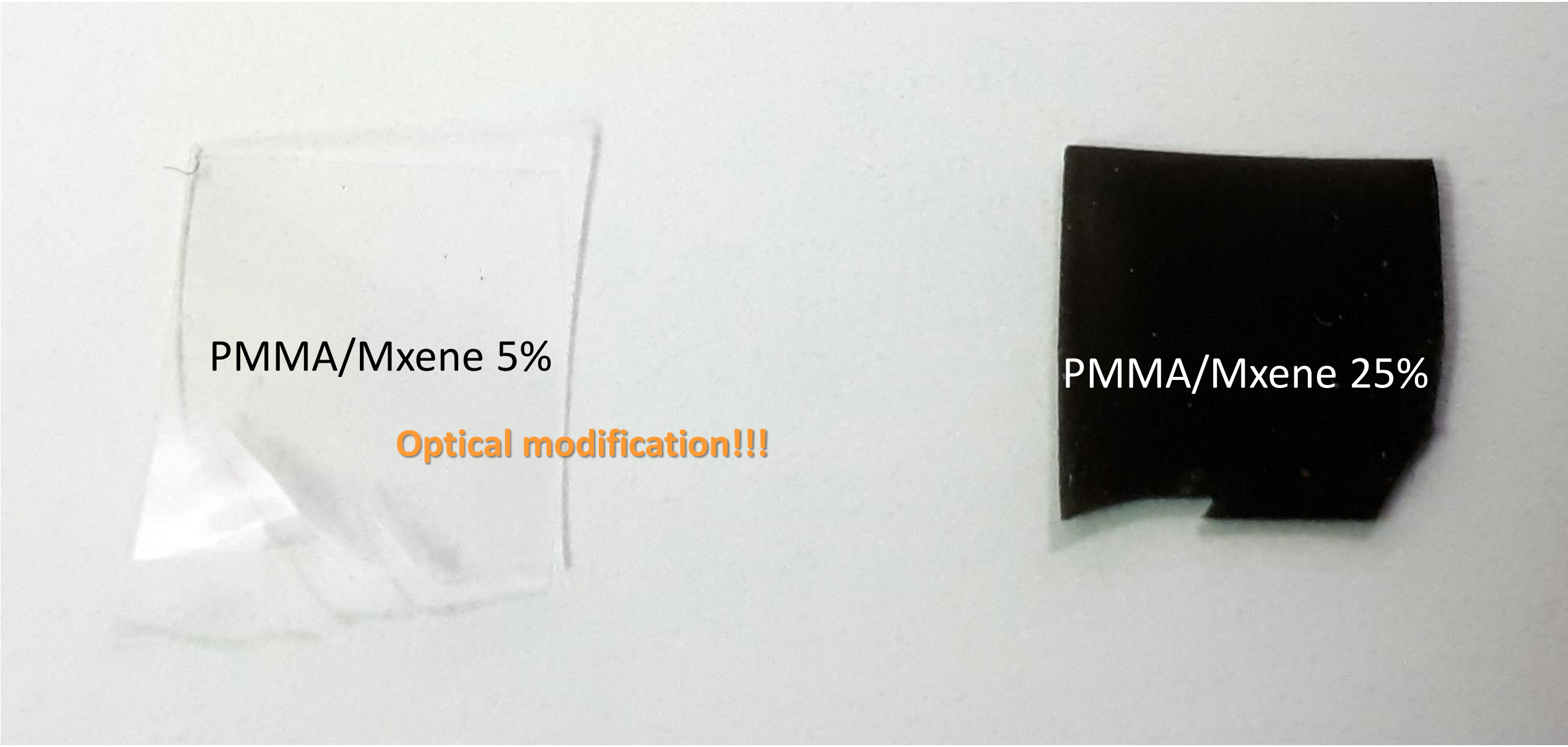
PMMA/Mxene 5%
Optical modification!!!
PMMA/Mxene 25%

Optical spectroscopy **WITH** DFT

Karlsruhe Institute of Technology

Evaluation of elastic characteristics of self-point defects and impurities in beryllium

Thomas Le Crane

IAM, Karlsruhe Institute of Technology, Germany

INSTITUTE OF APPLIED MATERIALS (IAM-AWP), Atomistic Modeling and Validation Group, Department of Metallic Alloys

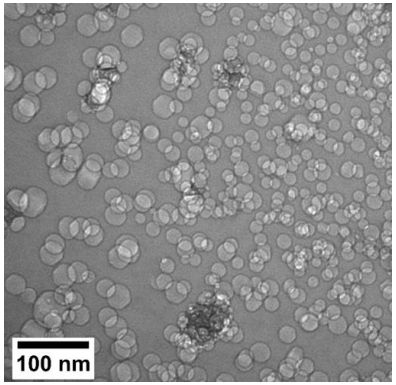

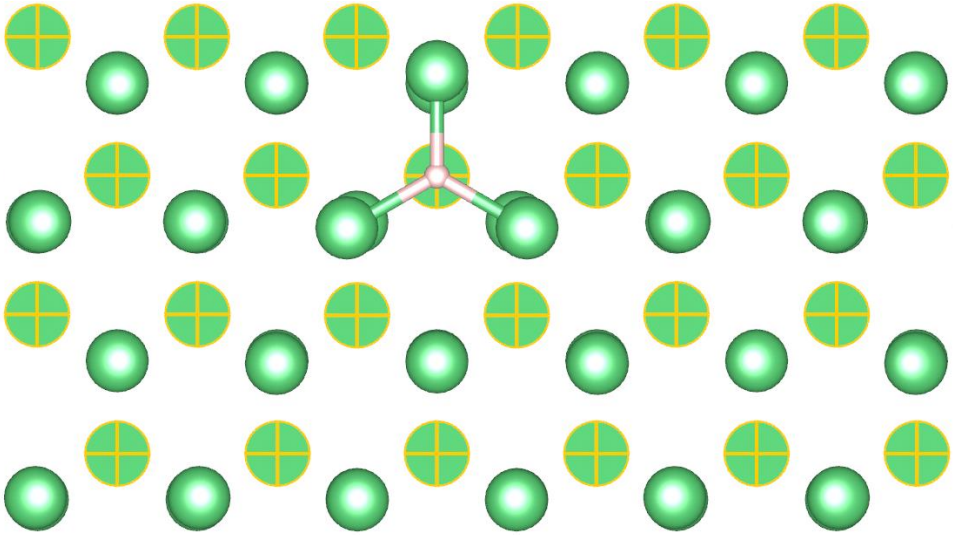

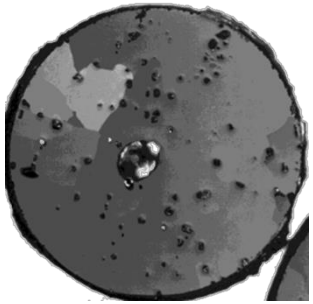

Purpose

First wall

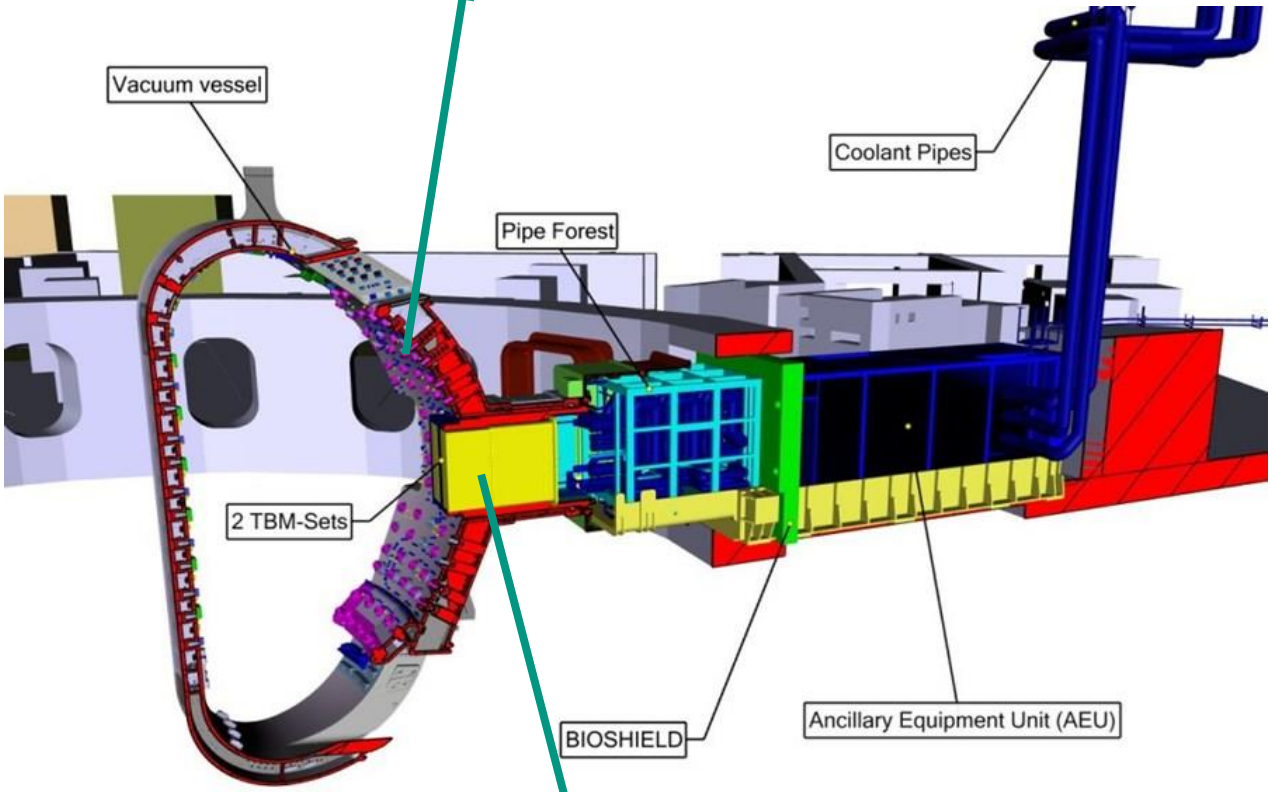

Tritium breeding modules

Motivation

Observations in beryllium parts for fusion :

→ Swelling

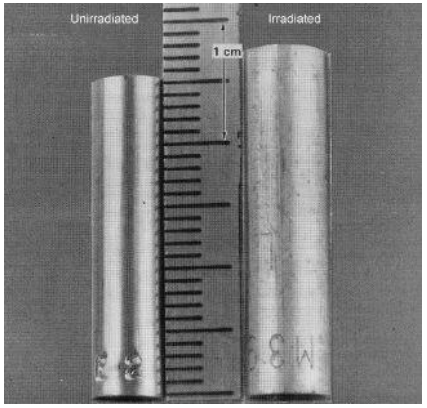

→ Tritium retention

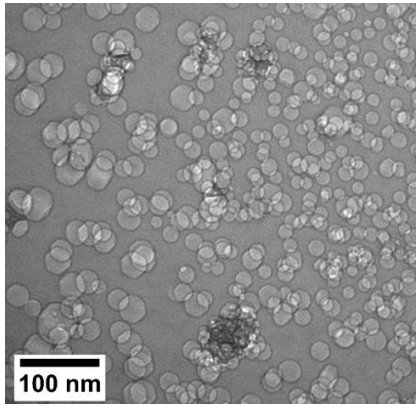

Defects affect the atomic environment → Strain & stress

How do defects move ?

Model

Elastic dipole tensor

What ?

Model for describing point-defects

$$P = \begin{pmatrix} P_{11} & P_{12} & P_{13} \\ P_{12} & P_{22} & P_{23} \\ P_{13} & P_{23} & P_{33} \end{pmatrix}$$

Components in energy unit

$$P_{ij} = -\frac{\partial Ef}{\partial \varepsilon_{ij}}$$

Why ?

Quantification of point-defect's impact

Interaction with strain and stress fields

Defects activation volumes

Defects sink strength

Computation

Beryllium's structure

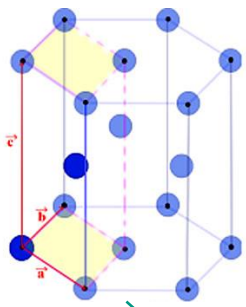

VASP

Top view and deformations

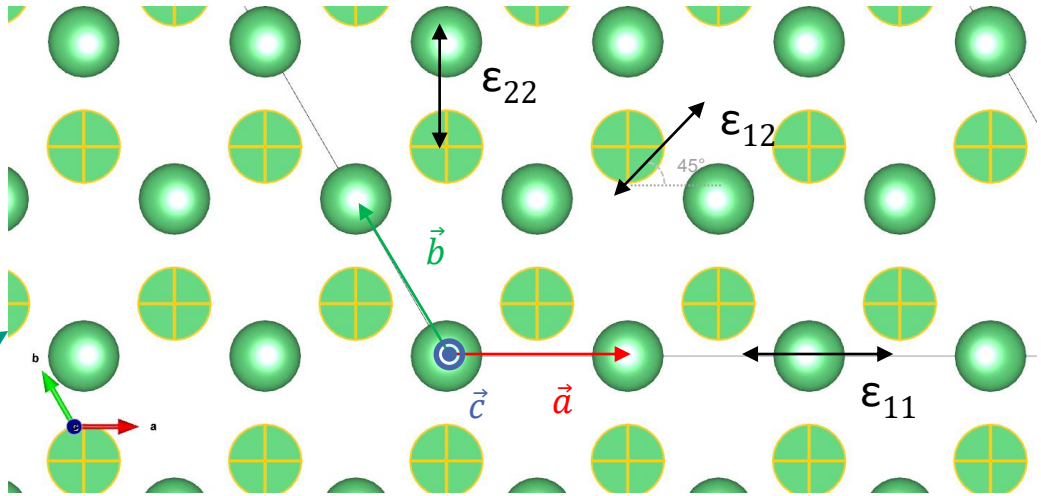

Objective : elastic dipole tensor for point-defects in stable positions.

$$P_{ij} = -\frac{\partial Ef}{\partial \varepsilon_{ij}}$$

Elastic dipole tensor at stable positions

– Calculations

Let's consider the example of Be self-interstitial

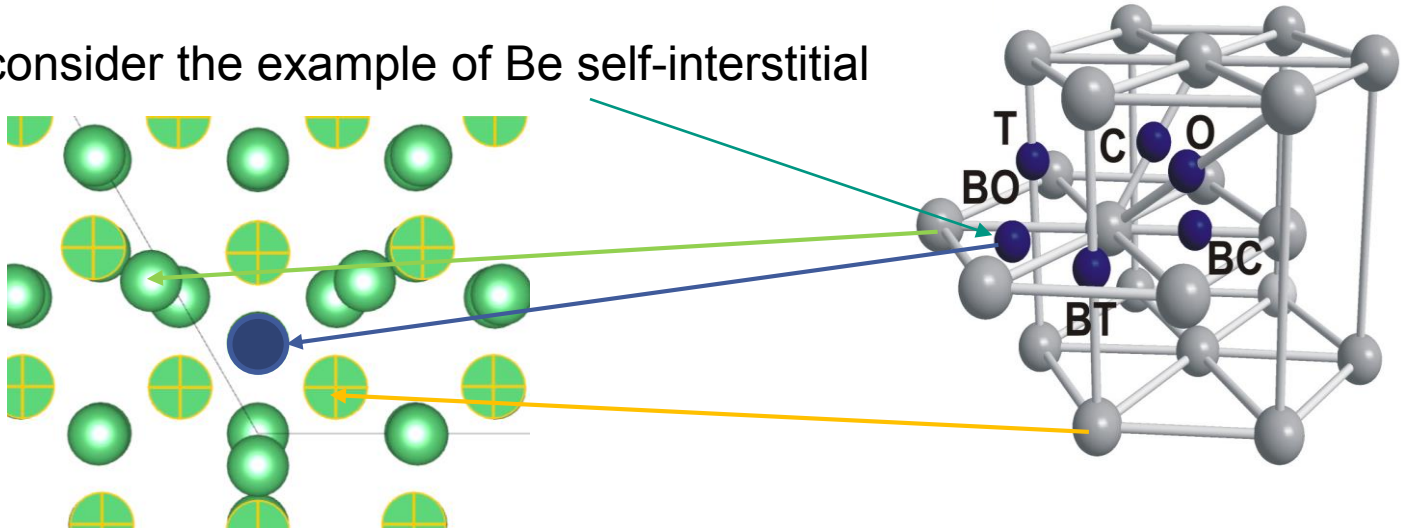

Self-interstitial				
Strain	Formation energy	Defective bulk	Perfect bulk	Potentials
-0,003	4,397407	-476,557	-477,226	-3,7284
-0,002	4,380637	-476,579	-477,231	-3,7284
-0,001	4,363797	-476,598	-477,234	-3,7284
0	4,346887	-476,616	-477,235	-3,7284
0,001	4,329877	-476,632	-477,234	-3,7284
0,002	4,312837	-476,646	-477,231	-3,7284
0,003	4,295707	-476,658	-477,225	-3,7284

Self-interstitial formation energy as a function of strain 11

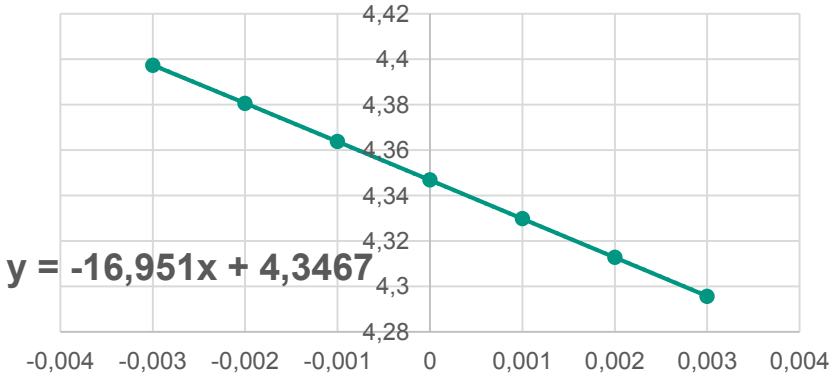

Thank you and now, more on the poster !

BIS(AMINO ACID) FUMARAMIDES AS SMALL MOLECULAR WEIGHT GELATORS: X-RAY DIFFRACTION AND CALCULATION of NMR PROPERTIES

Berislav Perić [a], Tomislav Gregorić [b] and Leo Frkanec [b]

[a] Laboratory for Solid State and Complex Compounds Chemistry and
[b] Laboratory of Supramolecular Chemistry,
Ruđer Bošković Institute, Bijenička 54, 10000 Zagreb, Croatia

Bis(amino acid)oxalamide gelators

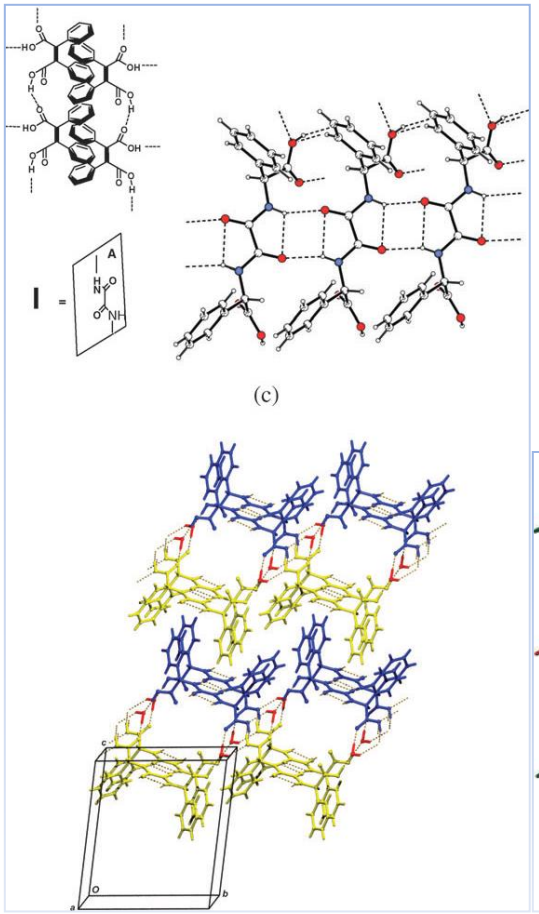

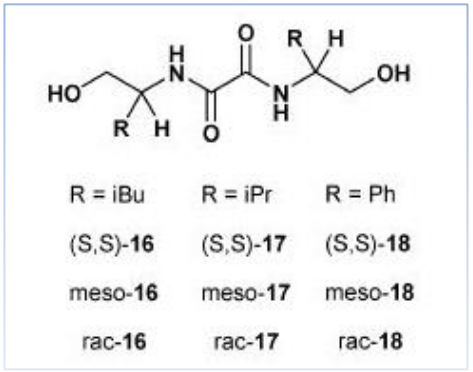

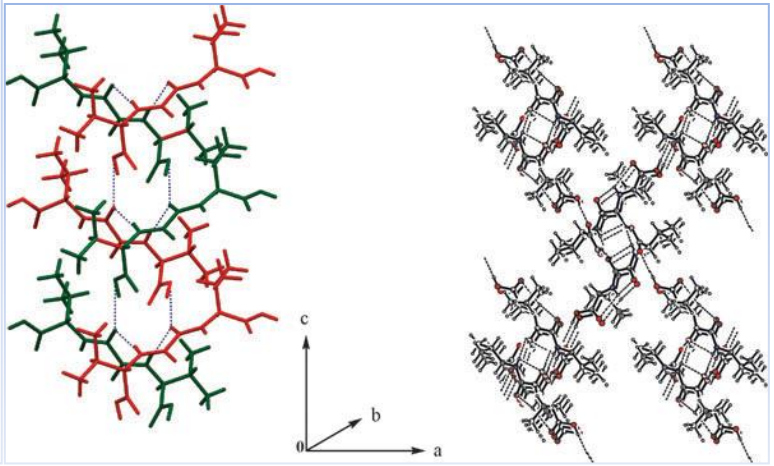

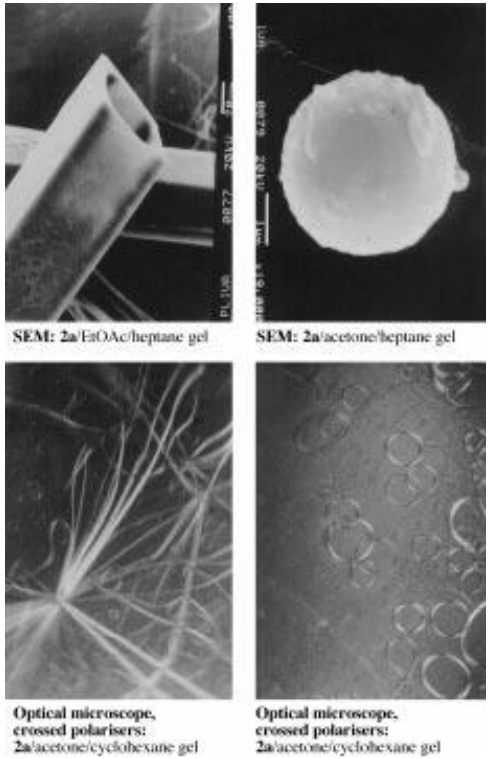

J. Makarević, M. Jokić, B. Perić, V. Tomišić, B. Kojić-Prodić, and M. Žinić, *Chem. Eur. J.*, **7**, (2001), 3328-3341.

B. Kojić-Prodić , B. Perić, Z. Štefanić , A. Meden, J. Makarević , M. Jokić and M. Žinić , *Acta Cryst.* **B60**, (2004), 60, 90.

Proposed scheme for „NMR-crystallography" structural analysis of small molecular gelators

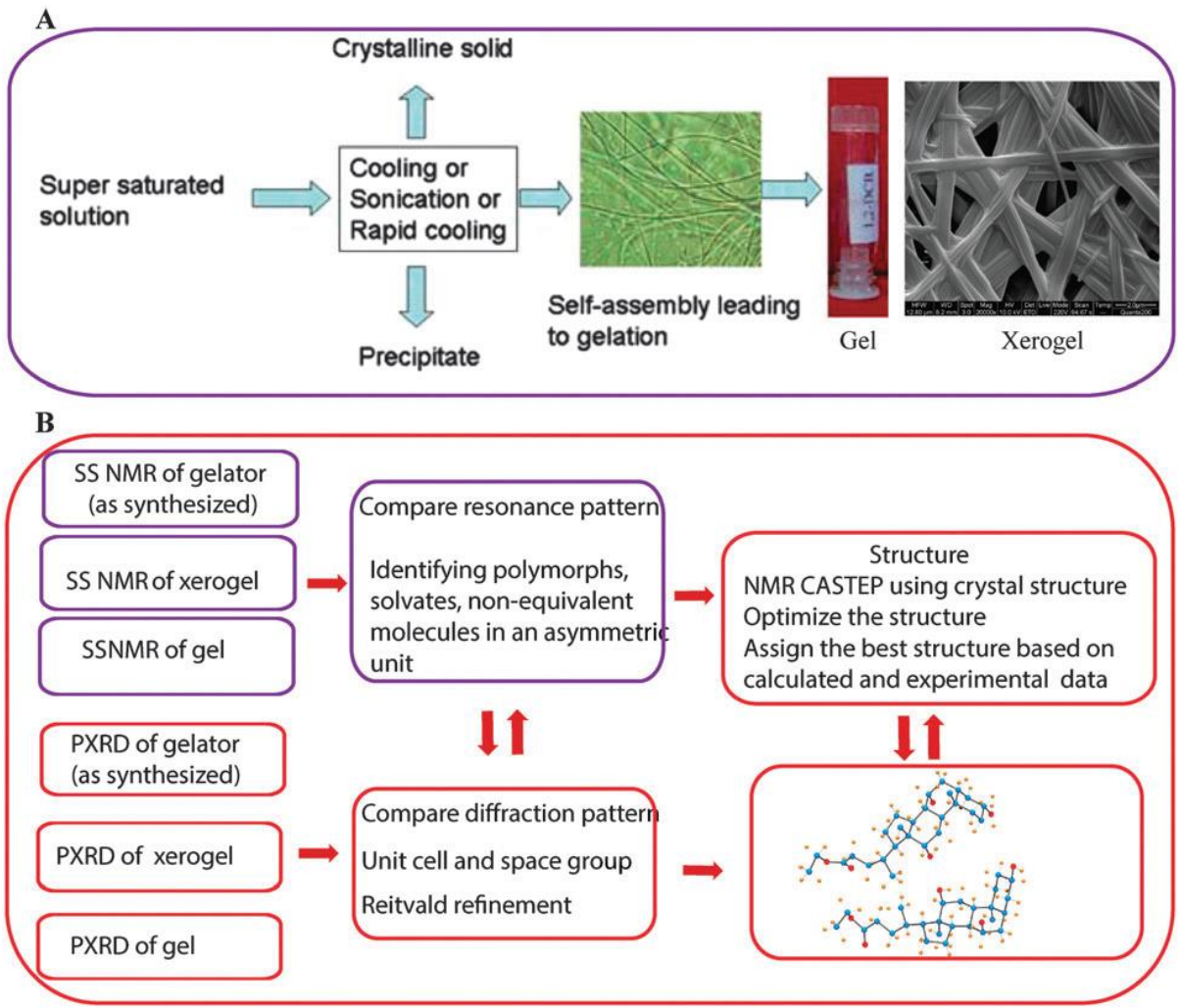

Nonappa and E. Kolehmainen, *Soft Matter*, **12**, (2016), 6015-6026.

BIS(AMINO ACID) FUMARAMIDES

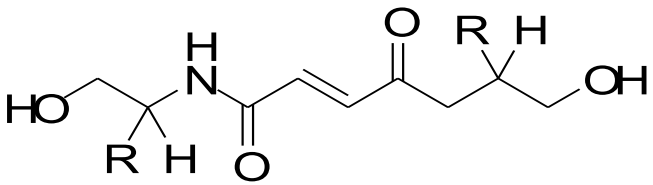

	1				2			
Solvent	**Fum-diLeu-OH**	**Fum-diLeu-OMe**	**Fum-diLeu-NH_2**	**Fum-diLeu-OVinyl**	**Fum-diVal-OH**	**Fum-diVal-OMe**	**Fum-diVal-NH_2**	**Fum-diVal-OVinyl**
H_2O	cryst.	cryst.	cryst.	ns	0.4	ns.	ns	ns.
H_2O/DMSO	0.9+0.37	cryst..	3.65+1.1	ng	0.2+0.03	cryst.	0+1.1	6.2+s5.3
H_2O/DMF	0.45+0.25	cryst.	1.8+1.1^{++}	0.44+0.48	ng.$^{+}$	cryst.	0+8.0	cryst.
EtOH	0.2+0.01*	sol.	cryst.	sol.	sol.	cryst.	ns	cryst.
±2-octanol	sol.	sol.	ns.	sol.	sol.	sol.	ns	cryst.
THF	0.1+0.01*	sol.	ng*$^{++}$	0.26	sol.	cryst.	ns	sol.
dioxane	2.3+0.08*	sol.	0.05+0.05*	sol.	sol.	cryst.	ns	sol.
acetone	0.3+0.01*	cryst.	ns.	0.1+1.3UZ	sol.	cryst..	ns	cryst.
EtOAc	1.4+0.09*	cryst.	ns.	0.2+1.2UZ	2.2+2.0**	sol.	ns	cryst.
CH_2Cl_2	1.0+0.02*	sol.	ng*$^{+}$	ng+	9.0+0.05*	ng. **$^{+++}$	ns	sol.
CH_3CN	0.25+0.01*	cryst.	ns.	cryst.	sol.	ng.$^{++}$	ns	cryst.
toluene	2.75+0.01*	cryst..	ng*$^{++}$	0.2	sol.*	1.8	ns	1.6

sol.= soluble, cryst. = crystal, ng= not gel, ns=not soluble; UZ= ultrasonication, *=DMSO; **=hexane; $^{+}$=gel in solvent;$^{++}$=gel and fibrous aggregates;$^{+++}$= fibrous aggregates

Numbers represent maximal volume of solvent (mL) immobilized by 10 mg of gelator.

BIS(AMINO ACID) FUMARAMIDES

1

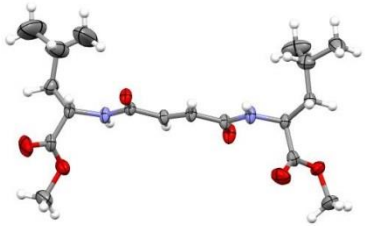

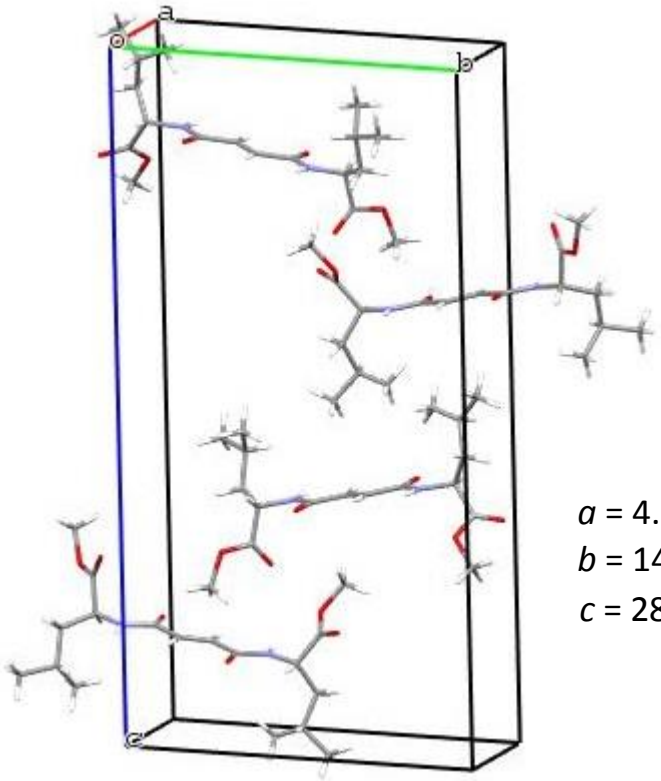

a = 4.9701(2) Å
b = 14.7298(4) Å
c = 28.278(2) Å

2

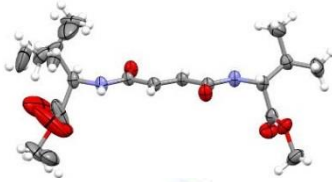

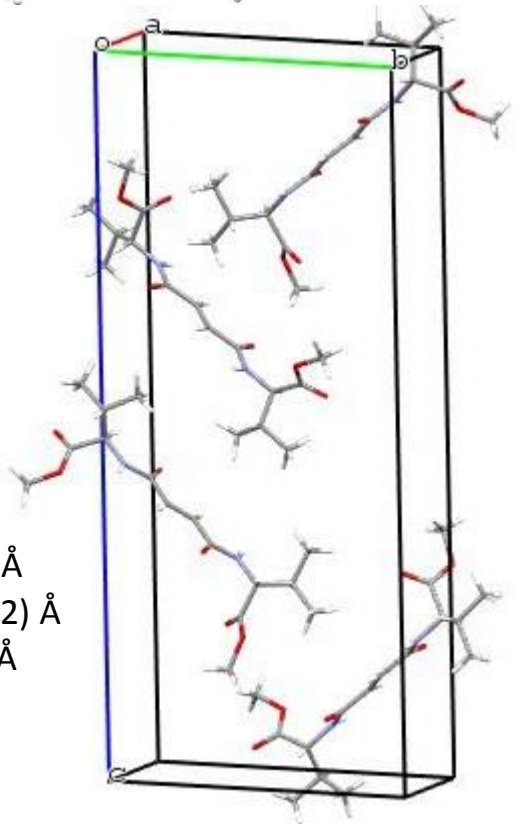

a = 4.9093(3) Å
b = 13.1211(12) Å
c = 30.031(3) Å

(one disorder component, 0.7 occupancy)

space group: $P2_12_12_1$

GEOMETRY OPTIMIZED STRUCTURES AND ^{13}C NMR SHIELDINGS (QUANTUM ESPRESSO)

1

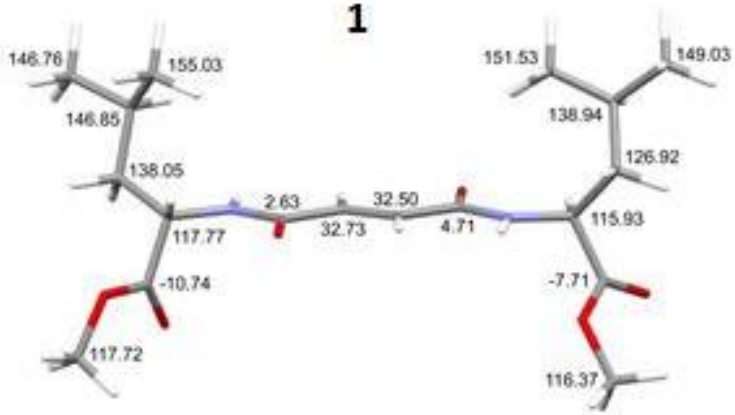

„Binding energy" = -1893.4920426327 Ry

2

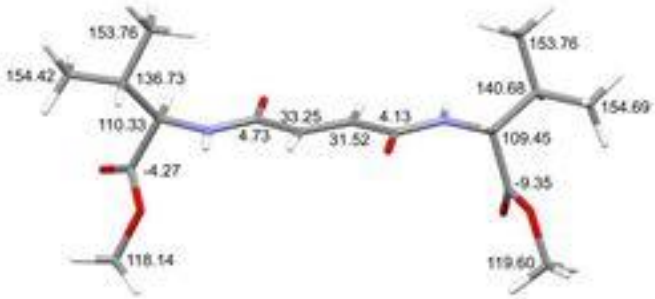

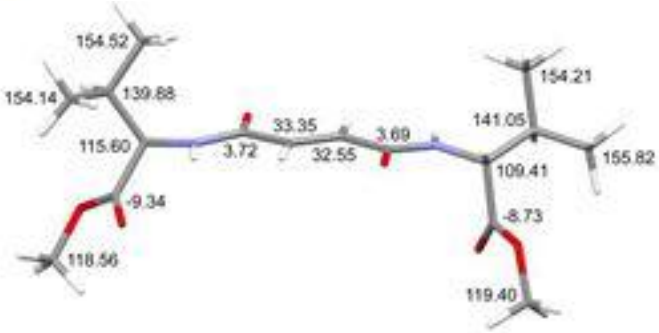

model **A**
occupancy 0.7
„Binding energy" = -1783.0502966905 Ry

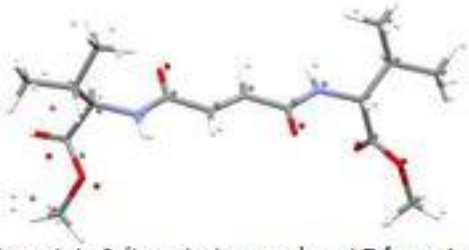

model **B**
occupancy 0.3
„Binding energy" = -1783.0287855331 Ry
≈ 0.0215 Ry (28.2388 *kJ/mol*) above model **A**

superposition of models **A** (bonded atoms) and **B** (**non-bonded atoms**)

Thanks:

Leo Frkanec

Tomislav Gregorić

Zoran Štefanić (X-ray data)

HrZZ, project number 2018-01-6910 - SUPeRNANO

Non-oxidative catalytic dehydrogenation of propane and butane over Cr_2O_3: a DFT study

Matej Huš, Drejc Kopač, Blaž Likozar

Department of Catalysis and Chemical Reaction Engineering
Kemijski inštitut

Ljubljana, 18. 9. 2019

KEMIJSKI INŠTITUT

Motivation

- *Demand for alkenes, such as propylene or butadiene, is rising.*
- *Traditional methods are insufficient:*
  - steam cracking
  - fluid catalytic cracking
- *Thus, catalytic dehydrogenation is becoming more and more important:*
  - $C_3H_8 \rightarrow C_3H_6 + H_2$
  - $C_4H_{10} \rightarrow C_4H_6 + 2\ H_2$
- *Two industrial processes:*
  - *Pt/Sn catalysts*
  - *CrO_x catalysts*

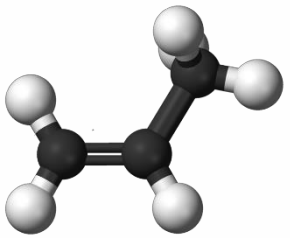

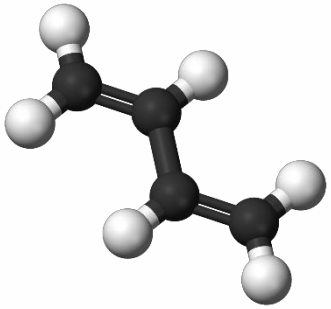

Catalyst model

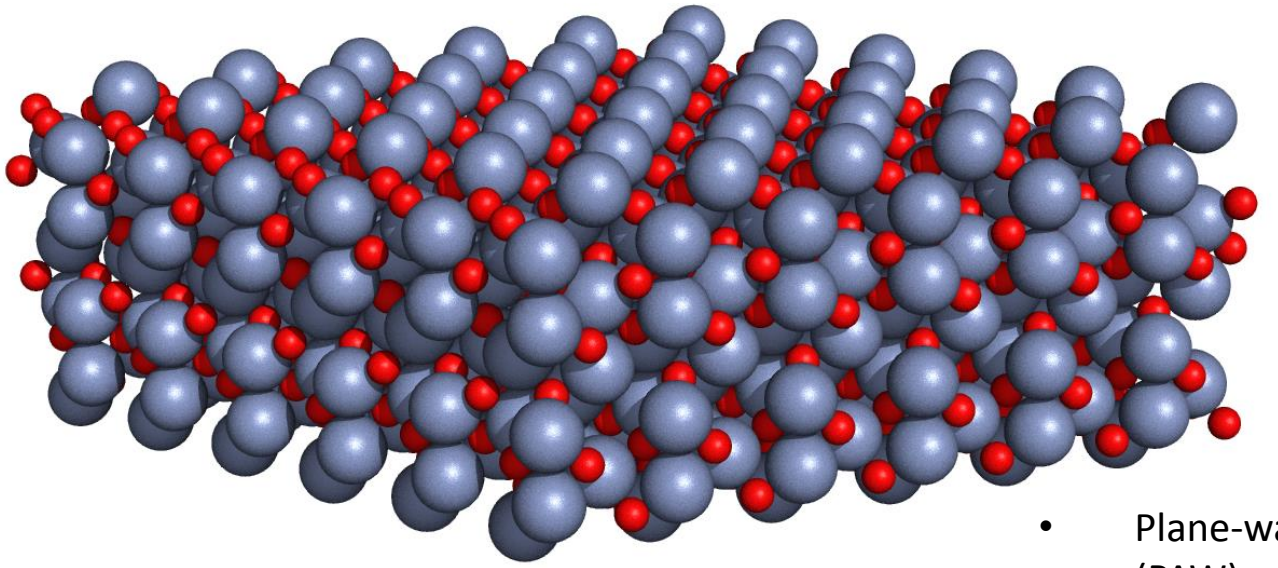

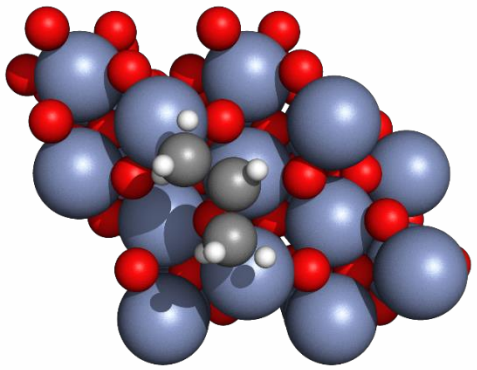

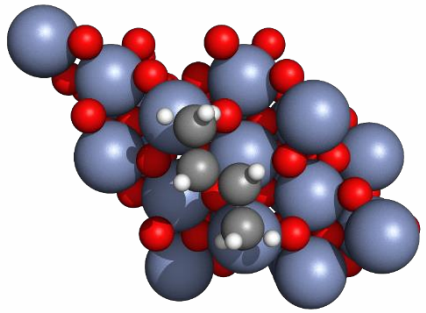

- A slab of Cr_2O_3 (0001)
- 6 layers Cr and 6 layers of O
- Cr-terminated surface

- Plane-wave DFT+U, electron-ion interaction: Projected augmented wave (PAW).
- Perdew-Wang 91 exchange correlation.
- Strong correlation: Hubbard U parameter for Cr, determined from literature.
- Energy cutoff: 500 eV, gamma calculations (large supercell).
- The van der Waals correction: Grimme D3; standard dipole corrections.

Reaction mechanism - propane

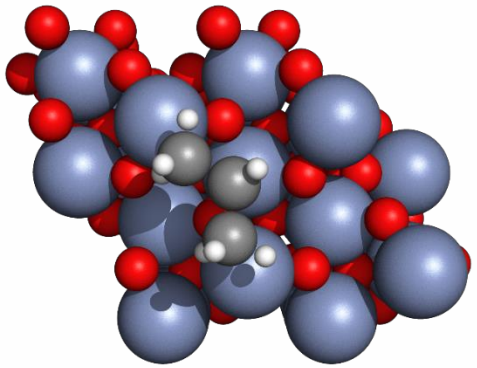

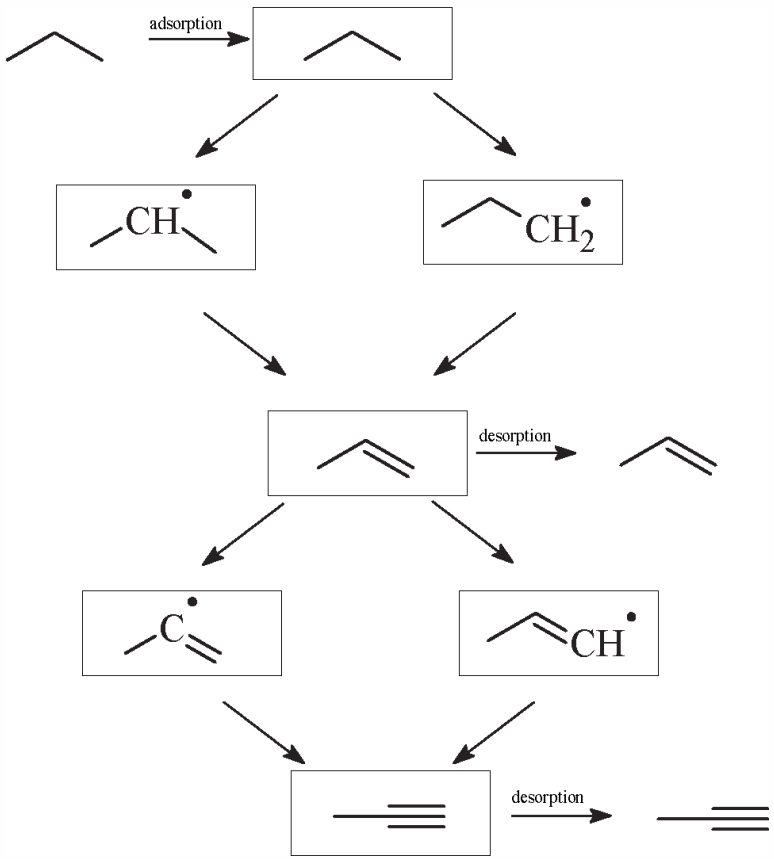

Species	E_{ads}
Propane	-0.27 eV
Prop-1-ene	-0.35 eV
Prop-1-yne	-0.51 eV

Reaction mechanism - butane

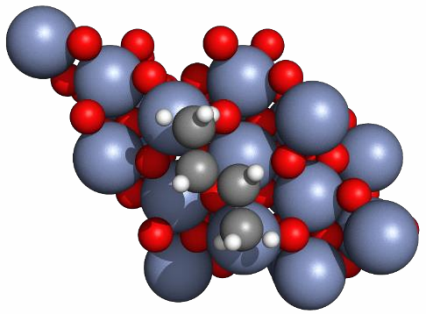

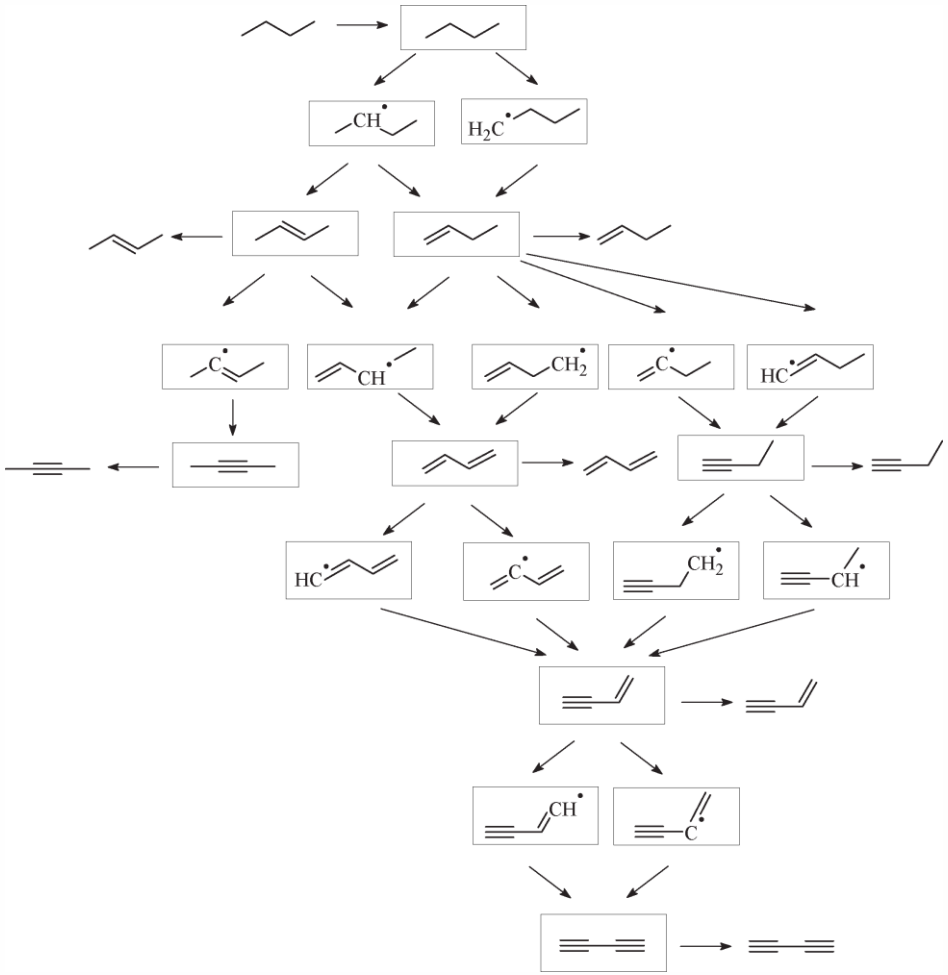

Species	E_{ads}
Butane	-0.28 eV
But-1-ene	-0.39 eV
But-2-ene	-0.40 eV
But-1-yne	-0.51 eV
But-2-yne	-0.50 eV
Butadiene	-0.45 eV
Butadiyne	-0.30 eV
Butynene	-0.35 eV

QUANTUMESPRESSO

Summer School on Advanced Materials and Molecular Modelling

Lateral interactions between electronegative adatoms on metallic surfaces: a high-throughput computational study

Matic Poberžnik and Anton Kokalj

Department of Physical and Organic Chemistry,
Jožef Stefan Institute, Ljubljana

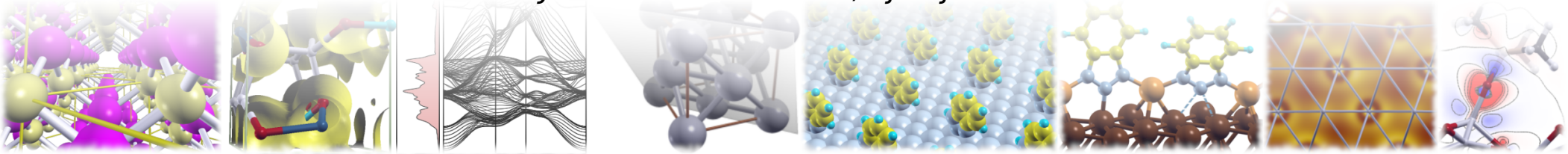

Typical behaviour

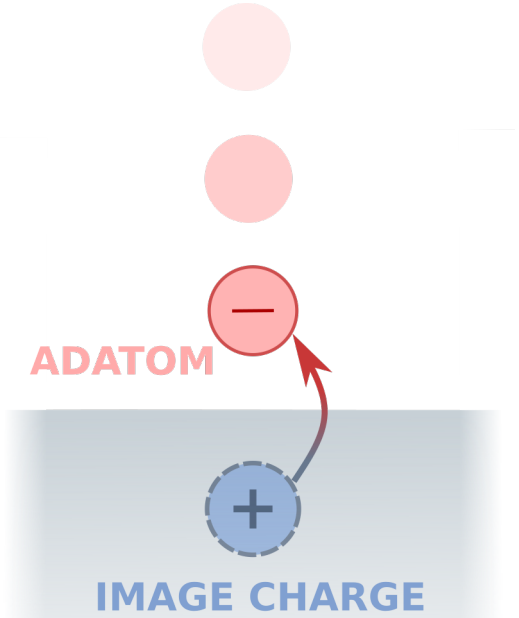

Adatom becomes negatively charged!

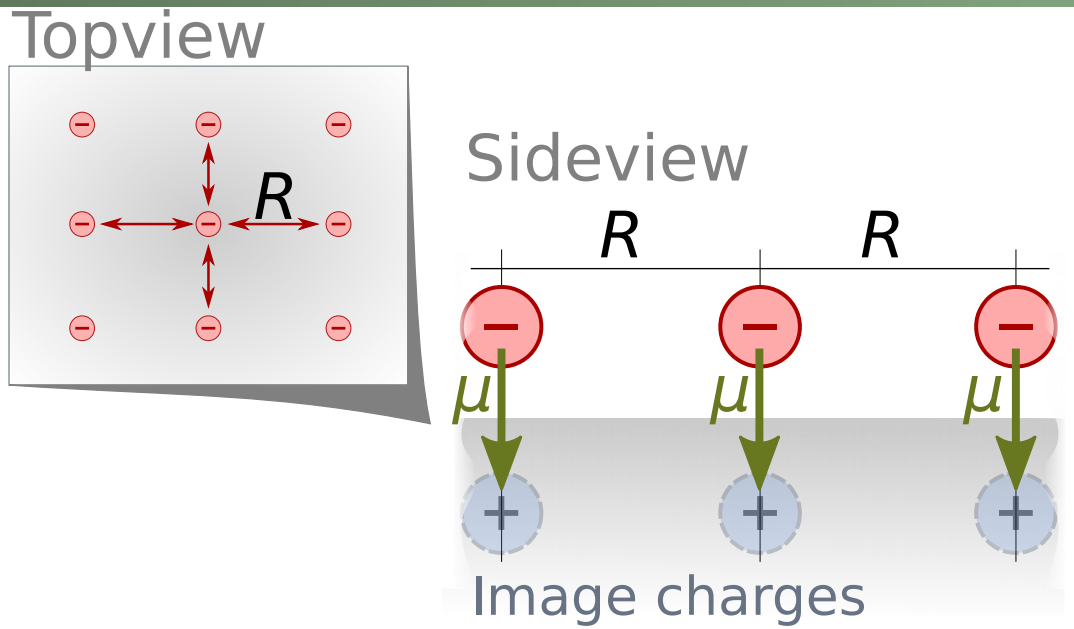

$$E_{\text{rep}} \approx \frac{\mu^2}{R^3} \mathcal{S}_{\text{lattice}} \propto \mu^2 \Theta^{\frac{3}{2}} \mathcal{S}_{\text{lattice}}$$

Typical behaviour

Repulsive dipole-dipole interactions between adatom-image charge pairs expected!

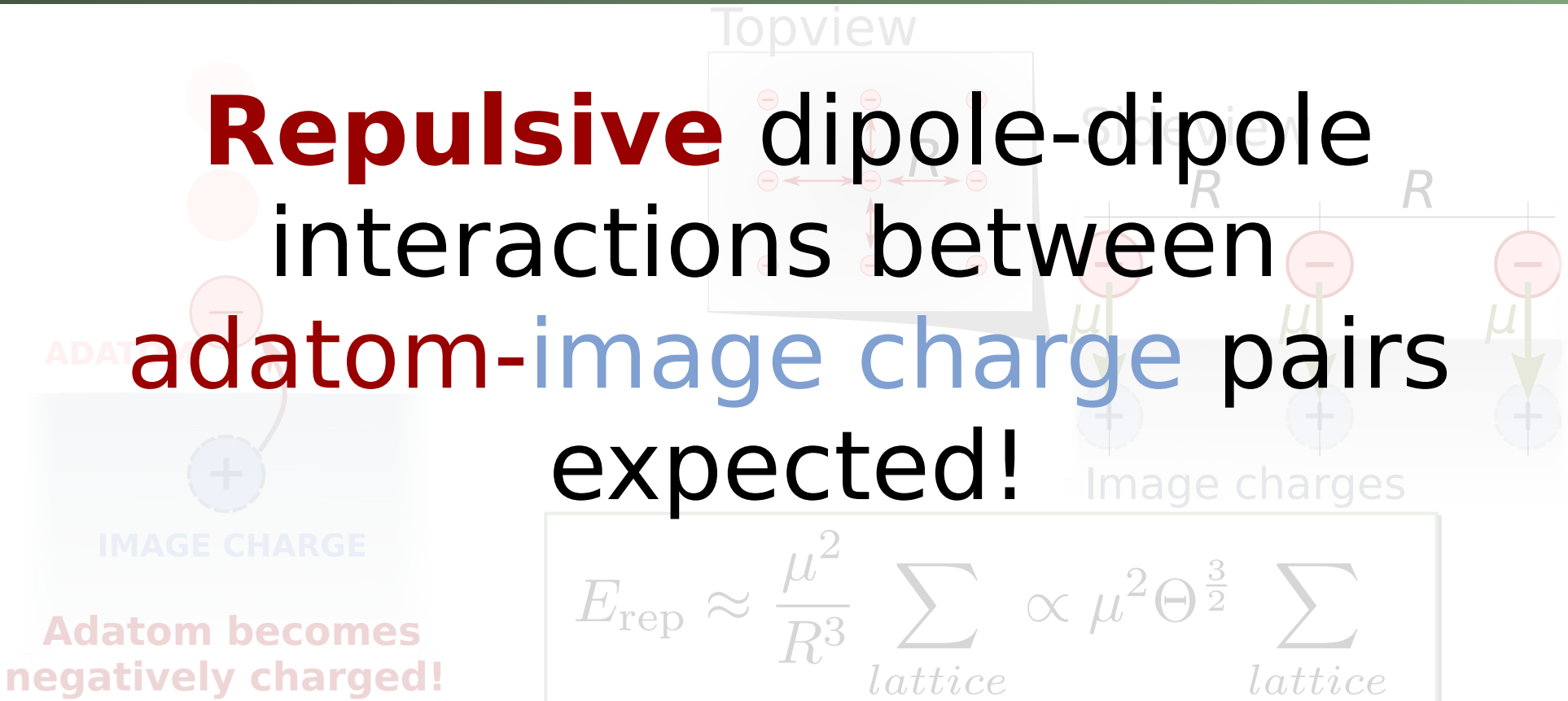

$$E_{\text{rep}} \approx \frac{\mu^2}{R^3} \sum_{lattice} \propto \mu^2 \Theta^{\frac{3}{2}} \sum_{lattice}$$

Typical behaviour

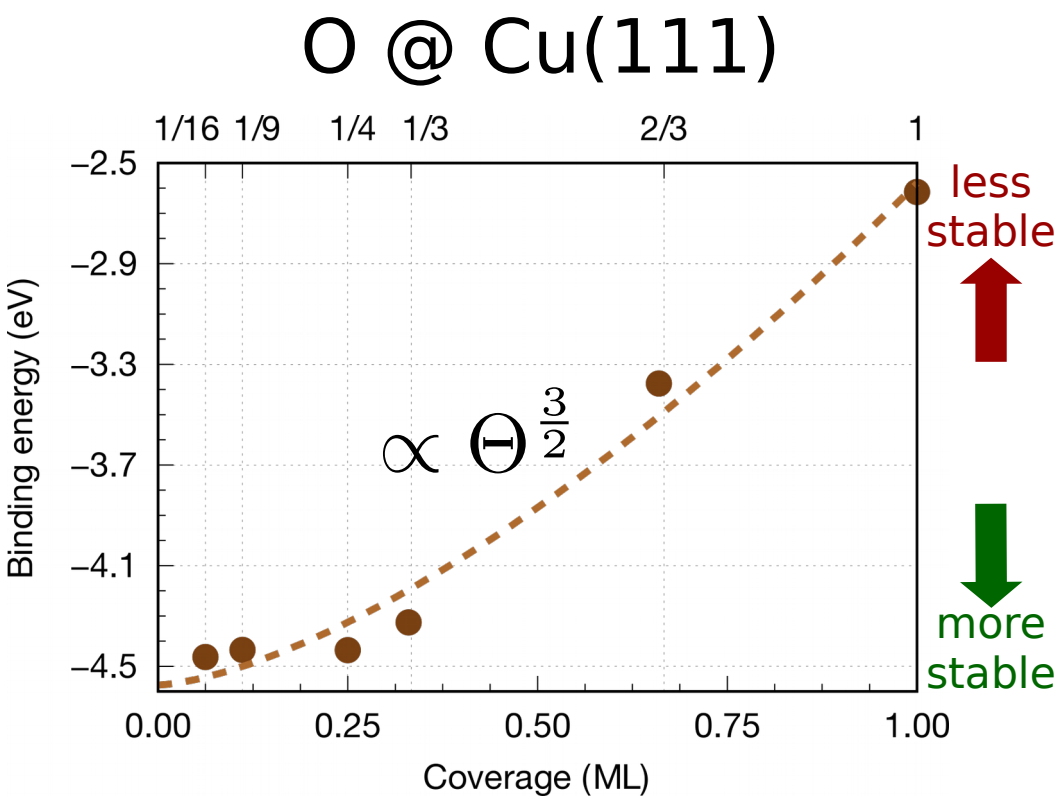

$$E_{\text{rep}} \approx \frac{\mu^2}{R^3}\mathcal{S}_{\text{lattice}} \propto \mu^2 \Theta^{\frac{3}{2}} \mathcal{S}_{\text{lattice}}$$

Coverage

On Cu(111):
Repulsive interactions lead to **lower stability** of **high** coverage oxygen overlayers !

Atypical behaviour: O@Al(111)

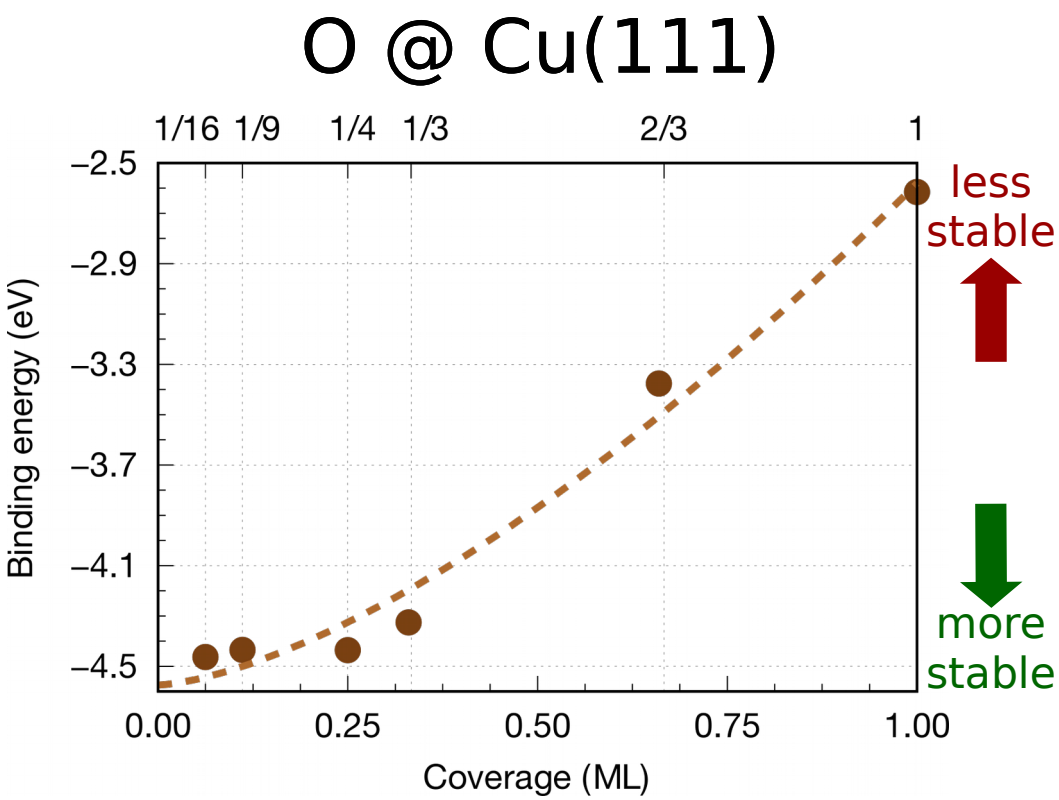

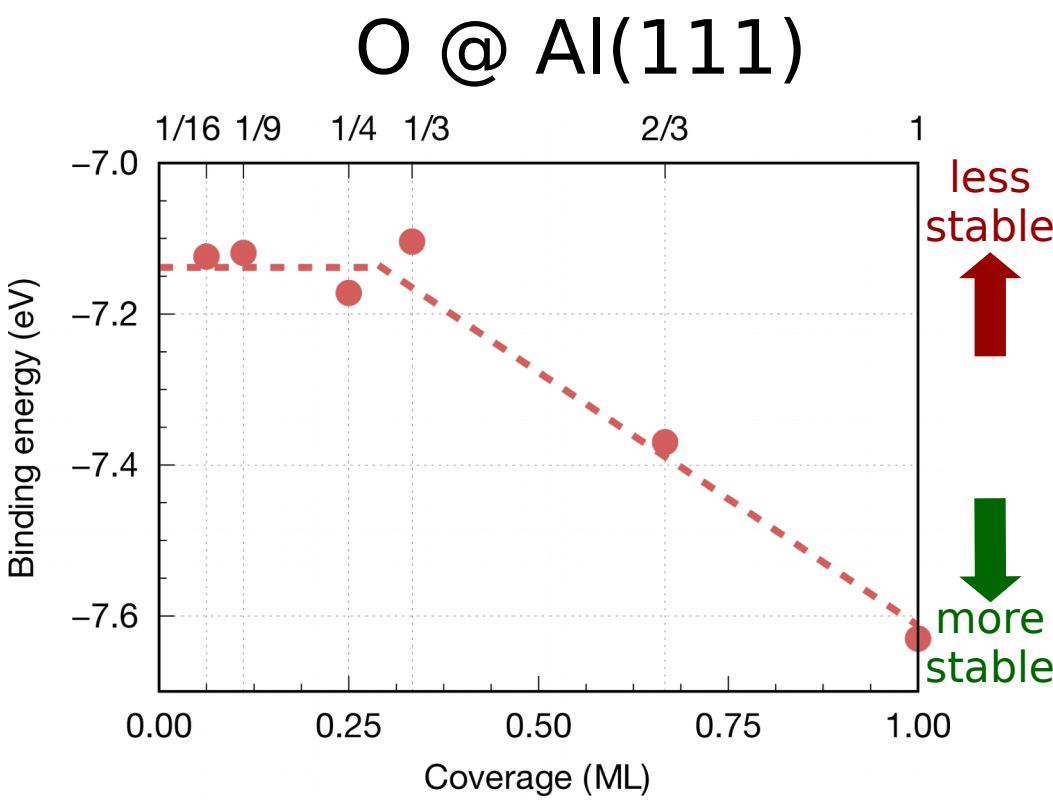

M. Poberžnik, A. Kokalj, *J. Phys. Chem. C*, **2016**, 120

Atypical behaviour: O@Al(111)

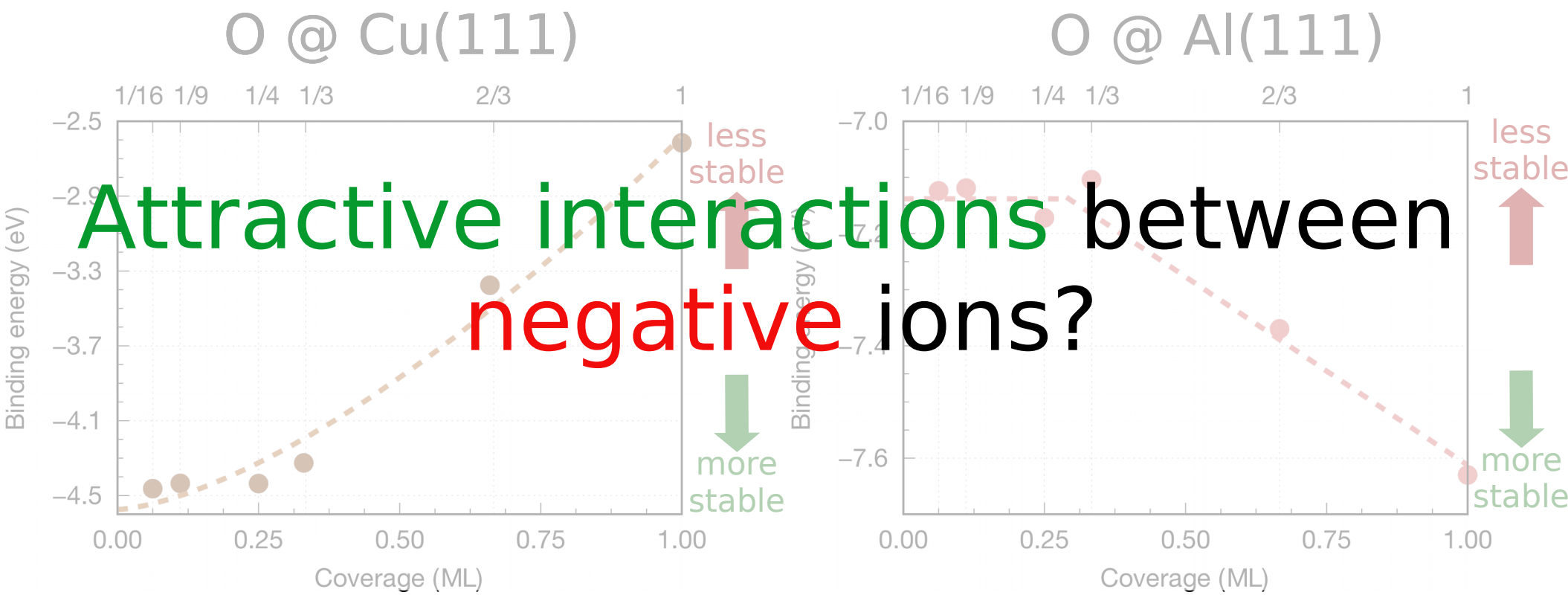

Attractive interactions between negative ions?

DOS @ Fermi energy

States near the Fermi energy **“vanish”** with increasing coverage, indicating **ionic bonding**!

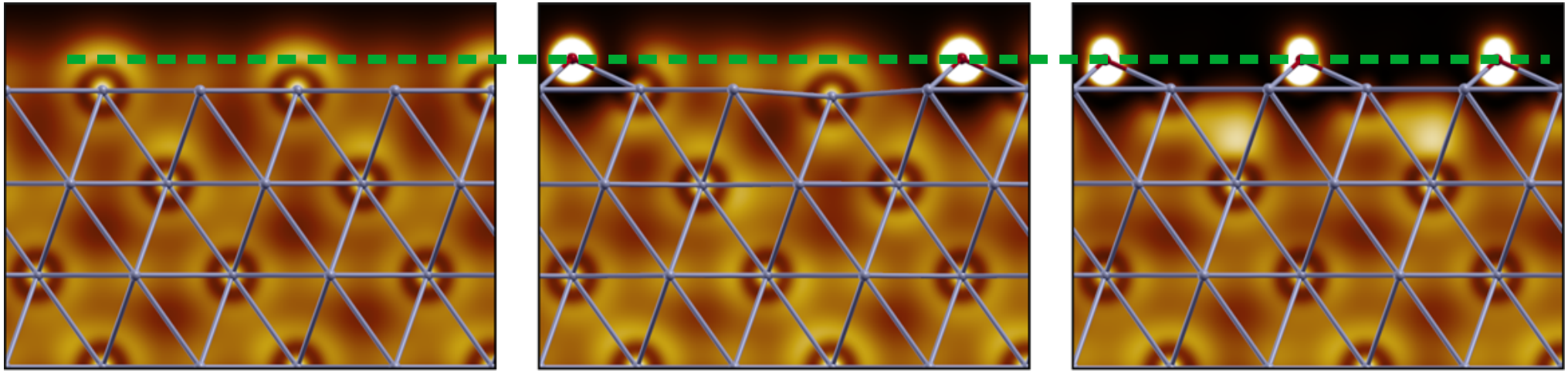

M. Poberžnik, A. Kokalj, *J. Phys. Chem. C*, **2016**, 120

Ionic model

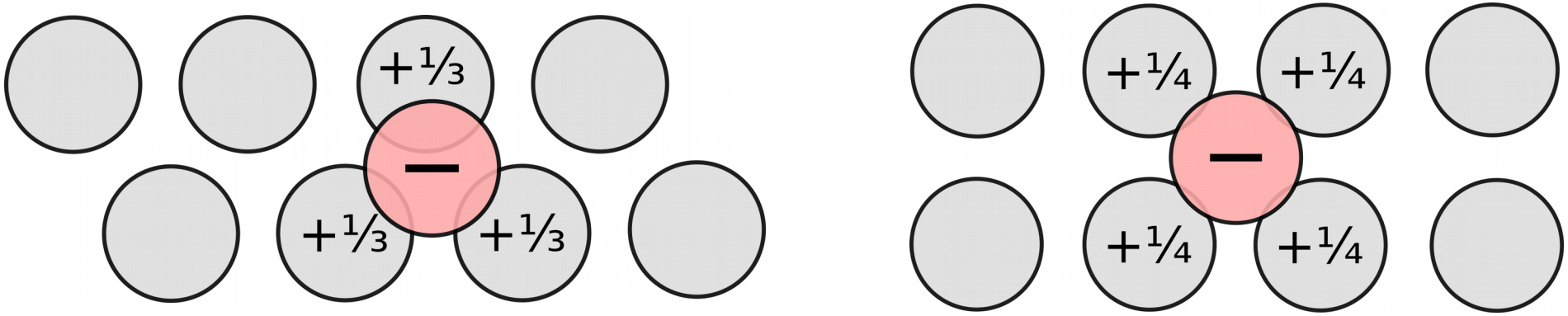

$$E = \mathcal{N} \sum_{i \neq j}^{\infty} \frac{q_i q_j}{|\mathbf{R}_i - \mathbf{R}_j|}$$

O^{fcc} @ Al(111)

ionic model

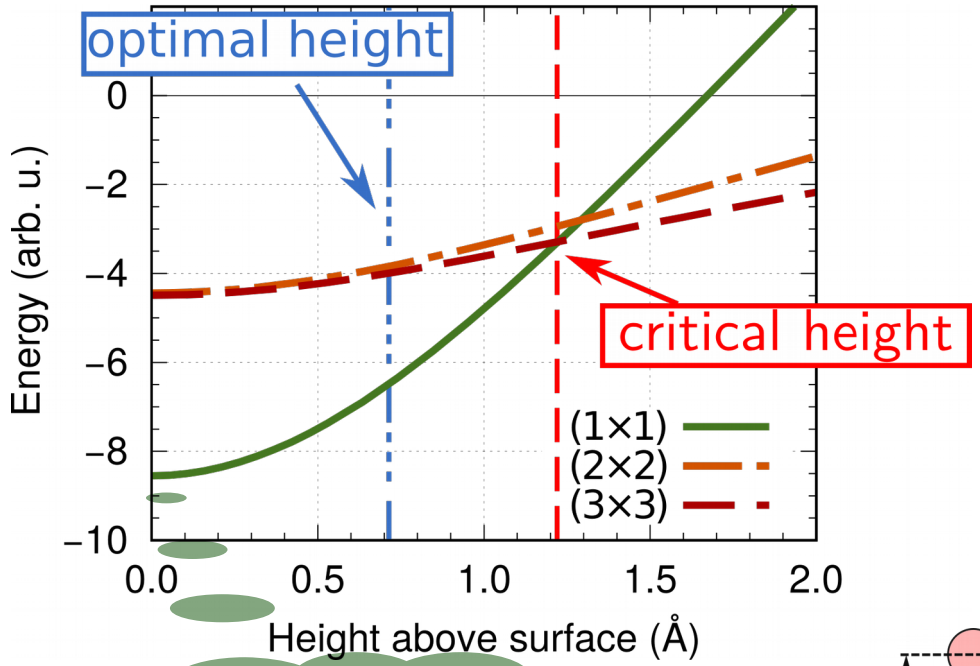

DFT

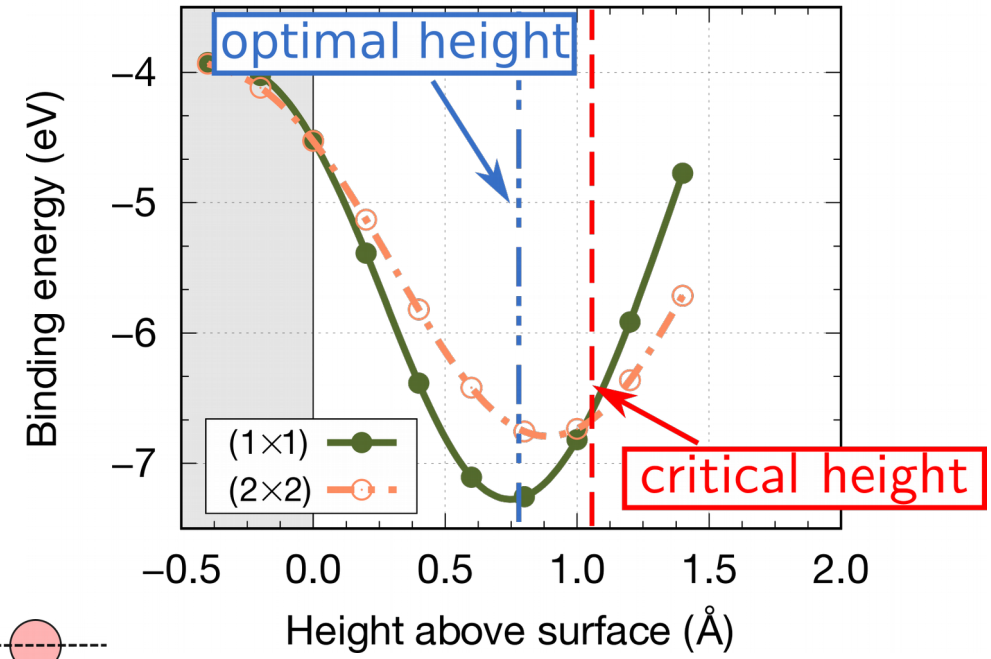

Short range repulsion neglected!

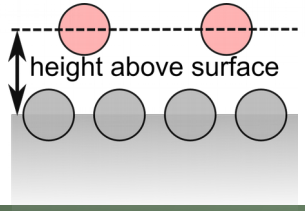

M. Poberžnik, A. Kokalj, *J. Phys. Chem. C*, **2016**, 120

Nothing specific about Al and O

- ionic bonding
- atom close to the surface
  - (large lattice parameter, below critical height)

Nothing specific about Al and O

- Ionic (localized) bonding
- atom close to the surface
  (large lattice parameter)

Other adsorbates and metals?

Adsorbates & Metals

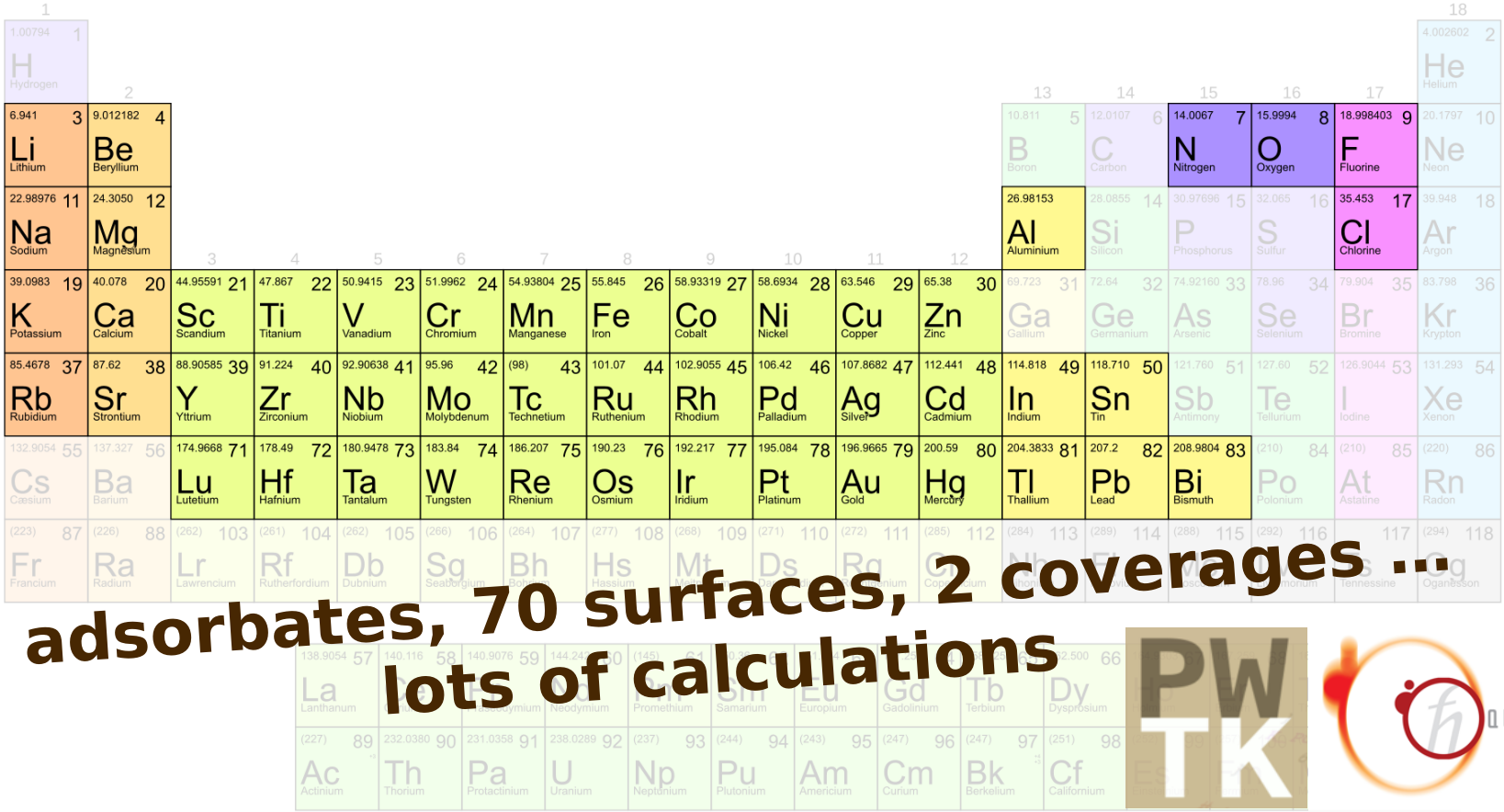

4 adsorbates, 70 surfaces, 2 coverages ...

lots of calculations

PWTK

QUANTUMESPRESSO

Results

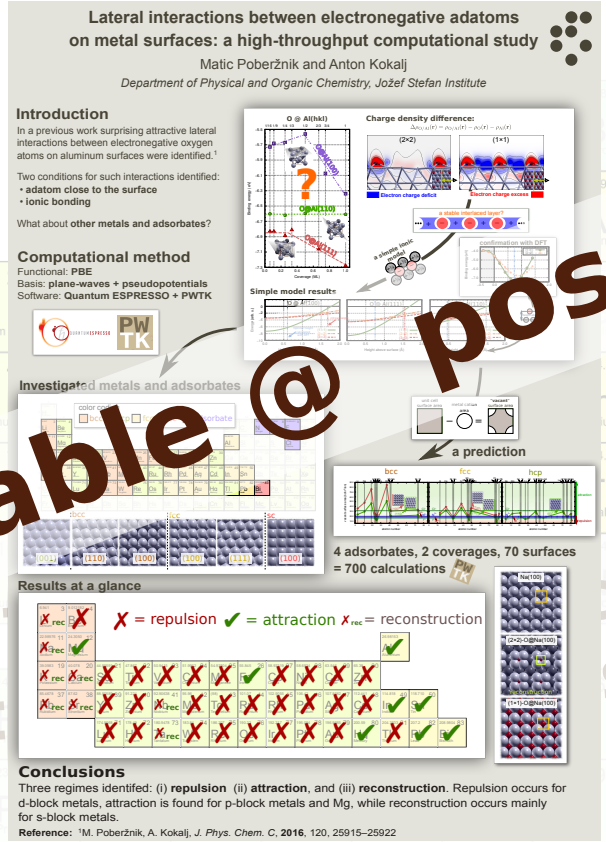

available @ poster 22!

SIMULATING NV CENTERS

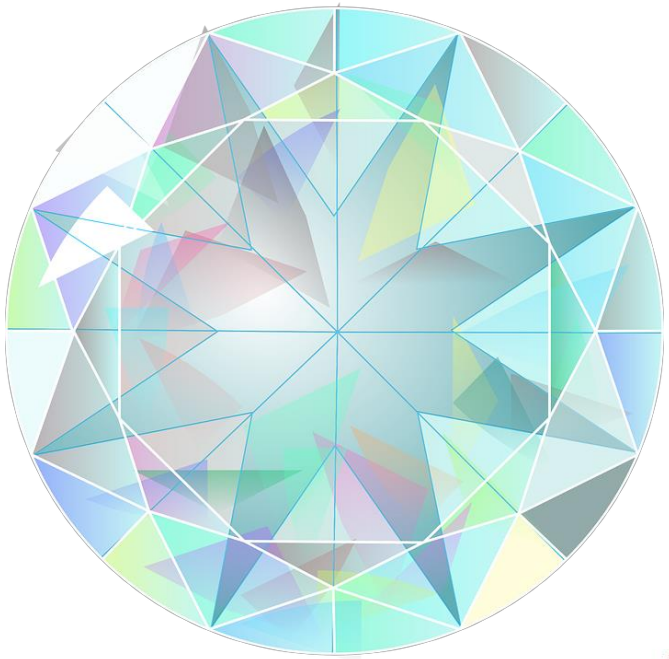

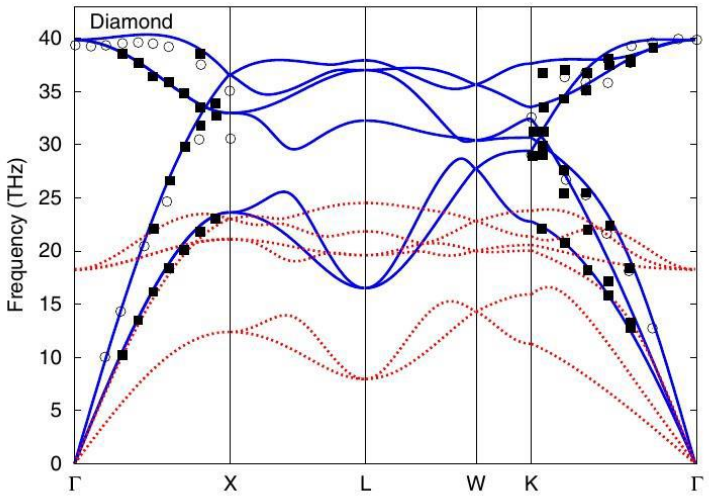

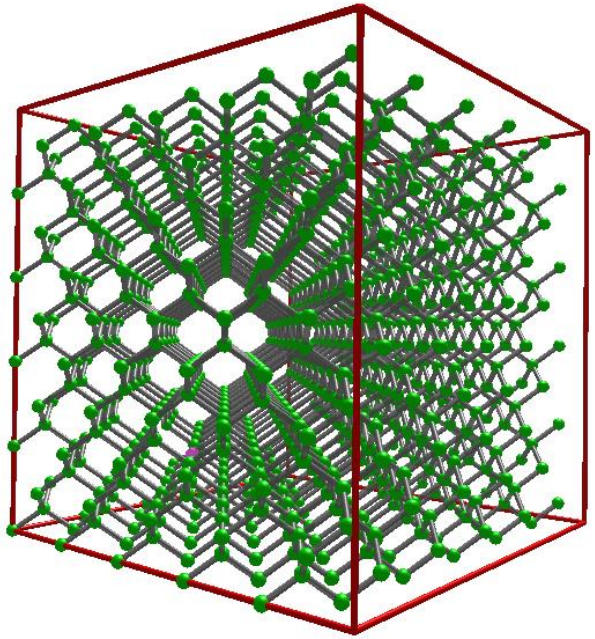

CHIVES

CODE FOR HIGHLY EXCITED VALENCE ELECTRON SYSTEMS

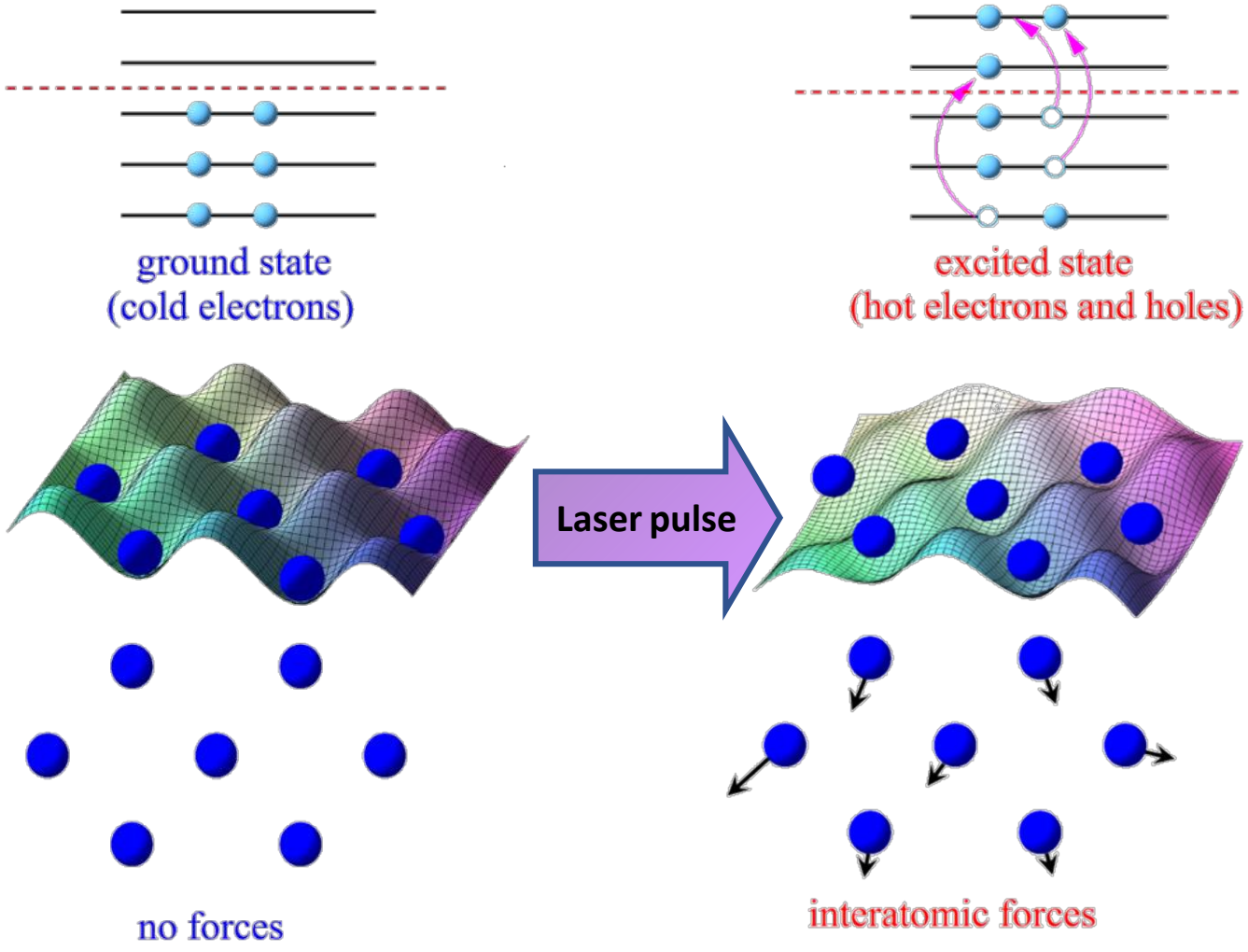

H																	He
Li	Be											B	C	N	O	F	Ne
Na	Mg											Al	Si	P	S	Cl	Ar
K	Ca	Sc	Ti	V	Cr	Mn	Fe	Co	Ni	Cu	Zn	Ga	Ge	As	Se	Br	Kr
Rb	Sr									Ag	Cd	In	Sn	Sb	Te	I	Xe

CODE FOR HIGHLY EXCITED VALENCE ELECTRON SYSTEMS

CHIVES – Simulating laser excitations

Tobias Zier, Marie Kempkes and Martin E. Garcia
Theoretische Physik, Universität Kassel, Kassel, Germany

Intense femtosecond-laser pulses can induce ultrafast structural phenomena in solids by creating a highly non-equilibrium state, which is characterized by high temperature electrons (~ 10 000 K) and near room temperature ions. In order to compute and simulate these laser-induced structural phenomena we developed an electronic-temperature-dependent density-functional-theory Code for Highly excited Valence Electron Systems, short CHIVES. Basically, the hybrid parallel implementation (MPI + OpenMP) of most of the subroutines used in CHIVES and the use of a norm-conserving basis set for the valence electrons enables us to perform ab initio molecular dynamics simulations with supercells containing up to 1440 atoms in bulk and/or thin film geometry. Besides technical details of CHIVES, we present preliminary results on the influence of vacancies on laser-induced ultrafast structural phenomena in diamond like nonthermal melting. Additionally, we would like to discuss the possibility to create or modify NV centers in diamond by femtosecond-laser pulses.

Theory

For $T_{el} = 0$ K

- Using Born-Oppenheimer approximation a solid system can be described by an electronic part

$$(\hat{T}_e + V_{ee}' + V_{el}) \cdot \phi = \epsilon \cdot \phi$$

and an ionic part

$$\left[\hat{T}_I + \underbrace{\epsilon + V_{II}}_{\text{= potential energy surface (PES)}}\right] \cdot \chi = E' \cdot \chi$$

- Resources to solve the electronic part using wavefunctions increase exponentially. For systems of several hundreds of electrons it's more practical to use the electronic density → Density functional theory (DFT)

$$\left[\left[-\frac{\hbar^2}{2m}\nabla^2 + V(\vec{r}) + V_H[n(\vec{r})] + V_{XC}[n(\vec{r})]\right] \cdot \Psi_i(\vec{r}) = \epsilon_i \cdot \Psi_i(\vec{r})\right]$$

For $T_{el} > 0$ K

- For excited systems the Helmholts free energy is used

$$F_{el}(\{\vec{R}_i\}, t) = \sum_{i,\vec{k}} n_{i,\vec{k}} \cdot \epsilon_i(\vec{k}) + V_{II}(\{\vec{R}_i\}) - T_{el}(t) \cdot S_{el}(t)$$

which depends on the entropy

$$S_{el}(t) = -k_B \sum_{i,\vec{k}} \left[n(\epsilon_i(\vec{k}), t) \cdot \log(n(\epsilon_i(\vec{k}), t)) + (1 - n(\epsilon_i(\vec{k}), t)) \cdot \log(1 - n(\epsilon_i(\vec{k}), t))\right]$$

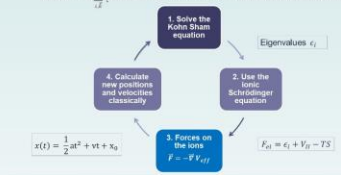

CHIVES (Code for Highly excited Valence Electron Systems)

- In detail, CHIVES has the following features:

- Convenient input from a control file using keywords + input values
- Appropriate default values are assumed, when a keyword is not specified
- Separate electronic and ionic temperatures
- No enforced structural symmetries, e.g., solids, thin films, open boundaries
- 1, 2, 4, or 8 **k**-points for the Inclusion of all partially occupied states (there are many at high electronic temperatures)
- Gaussian basis sets including s, p, and d states
- Analytical, norm-conserving pseudopotentials [1]
- Local density approximation
- Order(N) methods [2] for exchange, correlation, and Hartree potential;
- Pulay-Kerker mixing
- Verlet algorithm to simulate the molecular dynamics
- Possibility of structural relaxation using Fast Inertial Relaxation Engine [3]
- Efficient initialization of the self-consistent cycle using charge density extrapolation from previous time steps
- Enabled to perform on graphic cards
- Hybrid MPI/OPENMP parallel
- Massively parallel (MPI) implementation of the **k**-points
- OPENMP parallelized computation of Hamiltonian matrix elements, electronic charge density, and density matrix
- Efficient diagonalization using optimized OPENMP parallel LAPACK subroutines

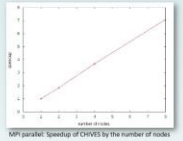

MPI parallel: Speedup of CHIVES by the number of nodes

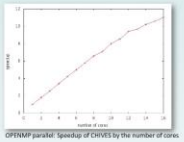

OPENMP parallel: Speedup of CHIVES by the number of cores

Physical picture

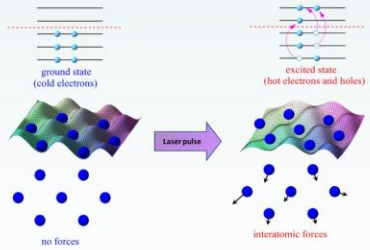

Illustration of the microscopic physical picture used to analyze laser-induced structural changes.

Before the action of the laser pulse the solid is in thermodynamic equilibrium. At low temperature, electrons fill the states up to the Fermi level. The atoms are at the equilibrium positions of the ground state potential energy surface.

The laser pulse changes the electronic occupations. This leads to rapid changes in the potential energy landscape. As a consequence, the lattice becomes unstable and forces appear on the atoms, driving a structural change.

Vacancies in diamond

- Used supercell with 1000 atoms (left), supercell with 999 atoms, including a NV-center (right)

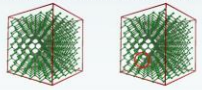

- Phonon band structures of diamond

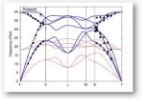

- Phonon frequencies of the ground state (blue)
- Laser irradiated state, where 10% of the valence electrons are excited (red)
- In good accordance with experimental data (black squares [4], white dots [5])

- (111) structure factor intensity for one thermalization run (left) and walltime for the first 50 steps of the thermalization (right)

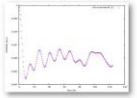

- Andersen thermostat
- 1000 atoms
- T_{el} = 0.00095 Ha ≙ 300 K
- Gaussian distributed velocities

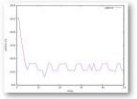

References
[1] C. Hartwigsen, S. Goedecker, and J. Hutter, Relativistic separable dual-space Gaussian pseudopotentials from H to Rn, Phys. Rev. B 58, 3641 (1998).
[2] S. Goedecker, O(N) methods for electronic structure calculations, Rev. Mod. Phys. 71,1085 (1999).
[3] E. Bitzek, P. Koskinen, F. Gähler, M. Moseler, and P. Gumbsch, Structural relaxation made simple, Phys. Rev. Lett. 97, 170201 (2006).
[4] Phys. Rev. 158, 805 (1967)
[5] Phys. Rev. Lett. 80, 5572 (1998)

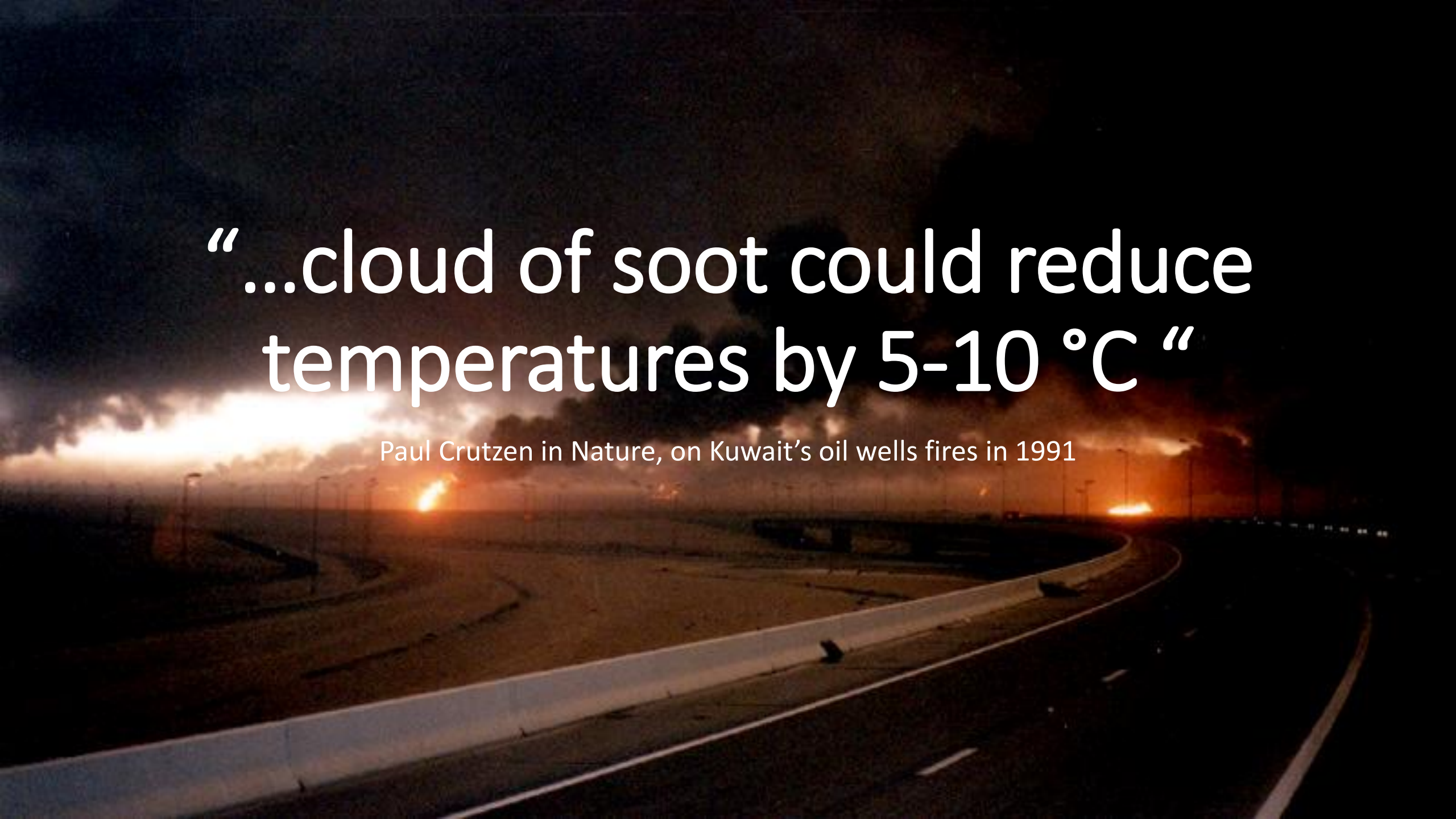

“…cloud of soot could reduce temperatures by 5-10 °C “

Paul Crutzen in Nature, on Kuwait’s oil wells fires in 1991

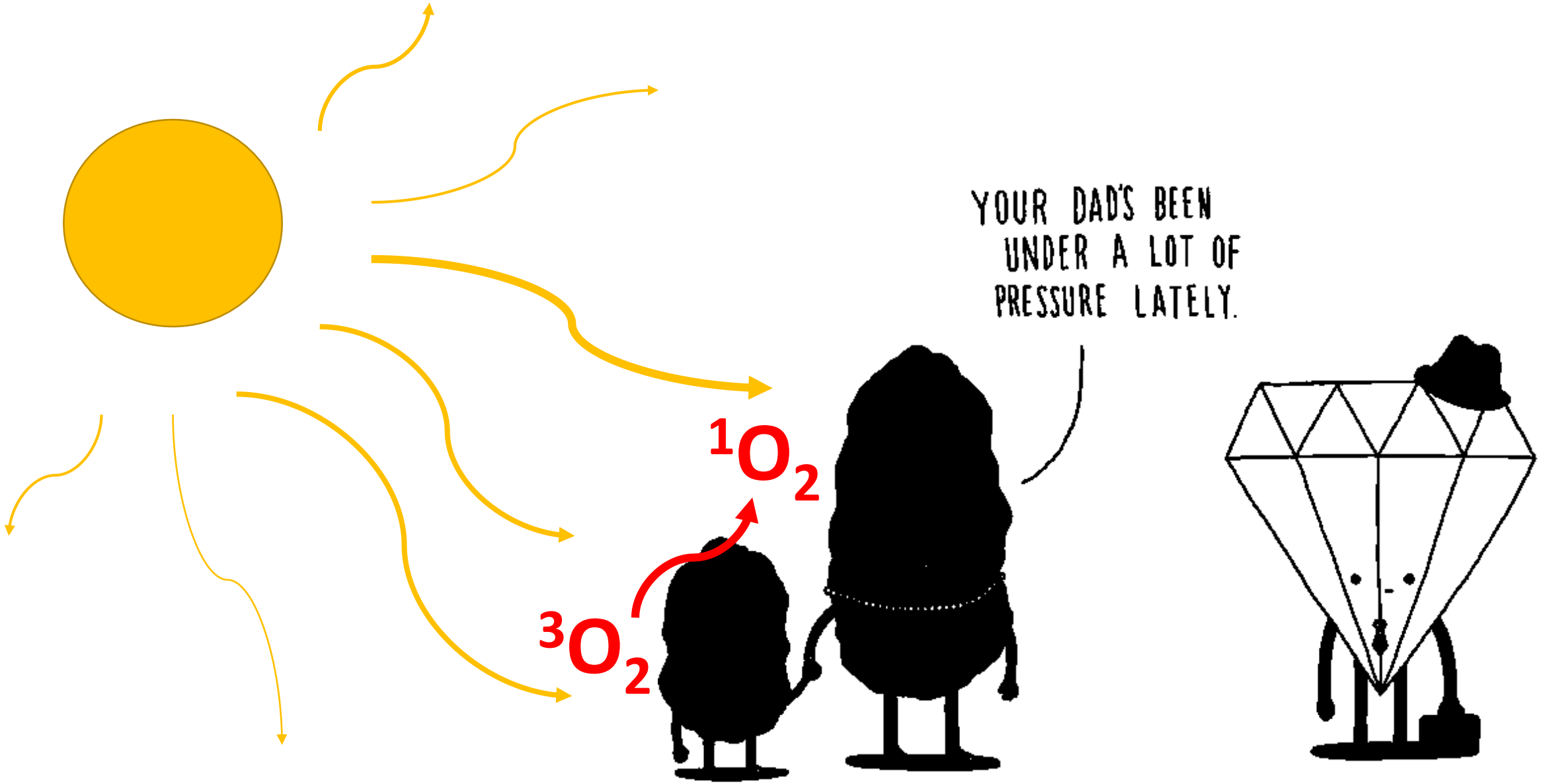
YOUR DAD'S BEEN UNDER A LOT OF PRESSURE LATELY.
$^1O_2$
$^3O_2$

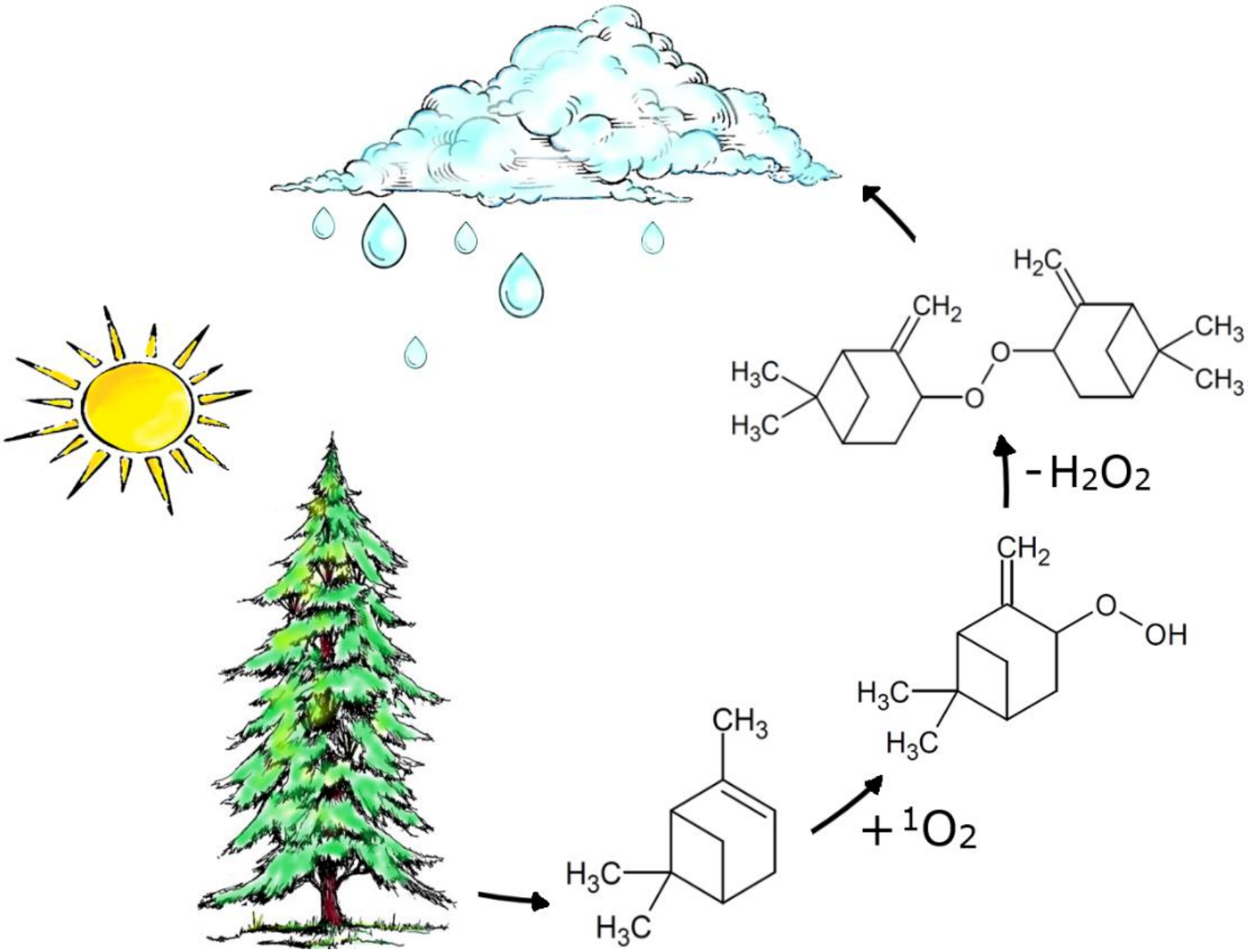
H_2C
CH_2
CH_3
CH_3
H_3C
H_3C
O
O
$-H_2O_2$
CH_2
O
OH
H_3C
H_3C
CH_3
H_3C
H_3C
$+ {}^1O_2$

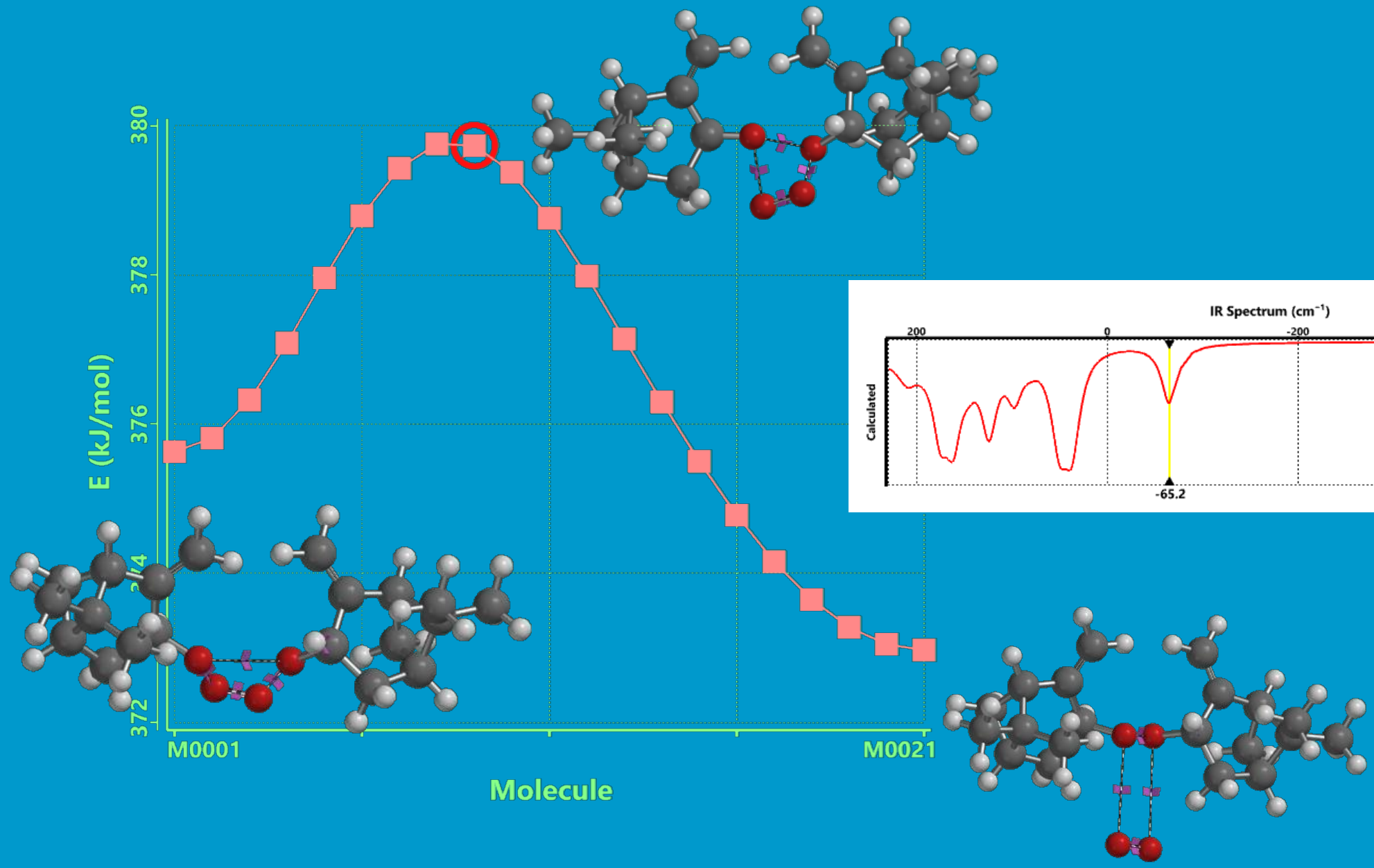
E (kJ/mol)
380
378
376
374
372
M0001
M0021
Molecule

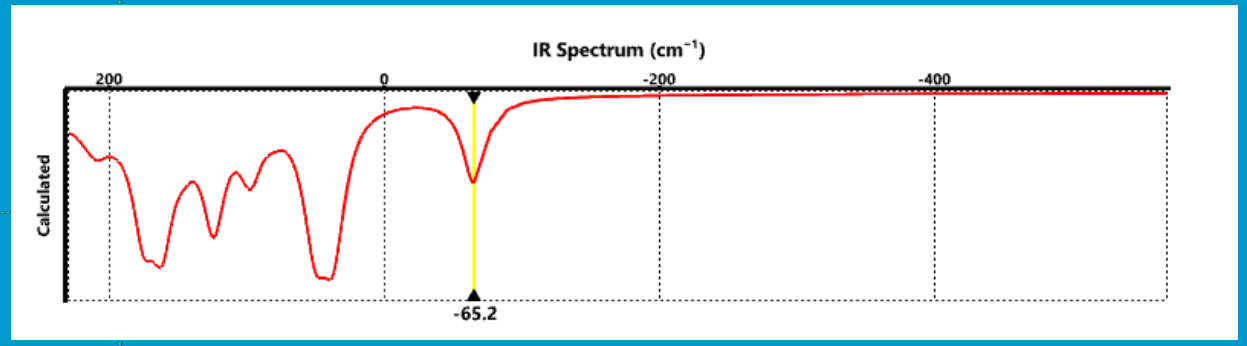
IR Spectrum (cm⁻¹)
200
0
-200
-400
Calculated
-65.2

QUANTUMESPRESSO

September 15–20, 2019
Ljubljana, Slovenia

Summer School on Advanced Materials and Molecular Modelling

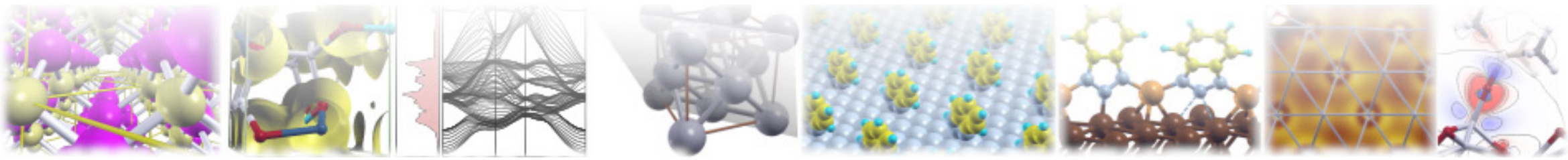

LET'S CONTINUE IN THE LOBBY DOWNSTAIRS.

QUANTUM ESPRESSO FOUNDATION

MAX DRIVING THE EXASCALE TRANSITION

Jožef Stefan Institute
Ljubljana, Slovenija

cecam
Centre Européen de Calcul Atomique et Moléculaire

EUROTECH
Imagine. Build. Succeed.